NASA-CR-66313

TECHNICAL REPORT

SURI No.1620.1245-60

ON THE DYNAMIC STABILITY OF ECCENTRICALLY REINFORCED CIRCULAR CYLINDRICAL SHELLS

BY

WERNER K. DIETZ

Sponsor: National Aeronautics and Space Administration (NASA)

NASA Grant No. NsG-~~637~~627 (S/A No.1)

Period : September 1, 1965 - January 31, 1967.

Project Director: R.M. Evan-Iwanowski

SYRACUSE UNIVERSITY RESEARCH INSTITUTE
Department of Mechanical & Aerospace Engineering
APPLIED MECHANICS LABORATORY

TECHNICAL REPORT

SURI-No.1620.1245-60

ON THE DYNAMIC STABILITY OF ECCENTRICALLY REINFORCED CIRCULAR CYLINDRICAL SHELLS

BY

WERNER K. DIETZ

Sponsor: National Aeronautics and Space Administration (NASA)
NASA Grant No. NsG-627-62 (S/A No.1)

Period : September 1, 1965 - January 31, 1967.

Project Director: R.M. Evan-Iwanowski

SYRACUSE UNIVERSITY RESEARCH INSTITUTE
Department of Mechanical & Aerospace Engineering
APPLIED MECHANICS LABORATORY

ABSTRACT

An analytical investigation of dynamic buckling of eccentrically reinforced circular cylindrical shells is carried out. The stringer and ring stiffeners are assumed to be closely-spaced, and general instability is investigated by an "equivalent shell" approach in that the reinforcement effects are smeared-out over their spacing distances.

A new set of field equations (equilibrium and compatibility) is derived on the basis of large deflection theory. Initial imperfections and rotatory inertia are included. A radial displacement assumption is made on the basis of expected buckling patterns (checkerboard and diamond) which satisfies clamped boundary conditions on an average over the circumference. The initial imperfections are assumed in spatial harmony with the total displacements. A stress function is determined that satisfies the compatibility equation.

The theory is applied to a clamped reinforced shell which is loaded axially by a controlled rate of endshortening of the form $V = V_0 e^{\gamma t}$. Dynamic equilibrium is satisfied in the sense of Bubnov-Galerkin which leads to a system of two second order differential equations of the third degree in the checkerboard and diamond buckling pattern amplitudes.

These differential equations are solved numerically for a particular shell for which static test results have been reported. It is shown that a fourth order Runge-Kutta method leads to paradoxial results due to instability of the numerical method.

A combined Runge-Kutta Predictor-Corrector method resolves these paradoxes.

For "static" rates of endshortening, $\gamma = 0$, and imperfections of the order of manufacturing tolerances, it is shown that the predicted buckling load is in good agreement with the reported static value.

The effects on the dynamic buckling load of rotatory inertia, magnitude of V_o, size and direction of initial imperfections, and time constant $\frac{1}{\gamma}$ are given for a limited parameter range.

An eighth order linear Donnell-type static buckling differential equation is derived also and then applied to the shell under consideration. For mode numbers corresponding to those reported in the tests, good agreement exists between predicted and measured buckling loads.

The concept of stiffener location effectiveness is introduced within the scope of linear classical theory and the assumption of equal mode numbers for both reinforcement locations.

A stiffener location effectiveness optimization chart for the particular shell clearly reveals that the increase in the buckling load due to external stiffener location depends on the mode numbers.

PREFACE

Design advantages of using eccentrically reinforced circular cylindrical shells have been predicted [32] and experimentally verified [34] for shells which are subjected to static axial loads.

It is the purpose of this dissertation to extend this scope to include dynamic axial loads.

The dynamic buckling loads of a clamped reinforced circular cylindrical shell, loaded axially by a controlled rate of endshortening of the form $V = V_o e^{\gamma t}$, are determined numerically. Geometry and material parameters are used that correspond to a particular shell for which static test results are available [34].

The effects on the dynamic buckling load of rotatory inertia, magnitude of V_o, size and direction of initial imperfections, and time constant $\frac{1}{\gamma}$ are given for this particular shell within a limited range of parameters.

I. TABLE OF CONTENTS

II INDEX TO FIGURES

III INDEX TO TABLES

IV LIST OF SYMBOLS

A cross sectional area of column, see p.69, also total composite shell cross section, see p.84, Table(VI-1)

A_S cross sectional area of stringer

A_R cross sectional area of ring

Ai Airy function symbol

A_{11}; A_{12}; A_{13}; A_{22} flexibility coefficients of composite shell, see summary p.153; with superscript (0) for quasi-orthotropic shell, see p.43.

a_{12}; a_{22} flexibility coefficient ratios, defined p.54

a sinusoidal buckling half wavelength in axial direction, p.15

B subscript for buckling variables

B_1.....B_7 coefficients of differential equation (A-4), defined on pp.147-148; with superscript (C) for column, with superscript (0) for zero imperfections

Bi Airy function symbol

b sinusoidal buckling half wavelength in circumferential direction, p.15

C_1.....C_9 coefficients of differential equation (A-14), defined on pp.150-152, with superscript (0) for zero imperfections

D; D_ν; D_G; D_S; D_R; D_{GS}; D_{GR}; D_{MS}; D_{MR}; D_{MGS}; D_{MGR}; D_1; D_2; D_{11}; D_{12}; D_{22} flexural rigidities, see summary on p.154

d stringer spacing, see p.15

e endshortening, defined on p.64

$\bar{e}$ average endshortening, defined on p.66

E; E_S ; E_R Young's moduli of monocoque shell, stringer and ring

F_1; F_2 right hand sides of differential equations (VI-2), p.87

F_x ; F_y Force acting on stringer in x-direction, respectively on ring in y-direction

$\mathcal{F}$ function of y, see p.60

F_{Sb} force eccentricity coefficient for stringer

F_{Rb} force eccentricity coefficient for ring

f stress function for zero imperfections

f_1 time-dependent amplitude of the checkerboard buckling pattern

f_o amplitude of the initial imperfection checkerboard pattern

f_P static stress function, referring to prebuckling

f_B static stress function, referring to buckling

G ; G_S ; G_R shear moduli of monocoque shell, stringer and ring

g_1 time-dependent amplitude of diamond buckling pattern

g_o amplitude of the initial imperfection diamond buckling pattern.

H dynamic equilibrium expression used in Galerkin's integral, defined on p.68

h monocoque shell thickness, also time-step size

i dummy variable, used on p.33, indicating particular location

I area moment of inertia of column, see pp.69 and 70

I_{SO} area moment of inertia of the stringer cross section with respect to the local y-axis

I_{SC} area moment of inertia of the stringer cross section with respect to an axis parallel to the y-axis through the centroid of the stringer cross section

I_{RO} area moment of inertia of the ring cross section with respect to the local x-axis

I_{RC} area moment of inertia of the ring cross section with respect to an axis parallel to the x-axis through the centroid of the ring cross section

$I_{\bar{m}}$ composite mass moment of inertia per unit length, defined on p.27; with superscript (0) for the quasi-orthotropic shell, see p.43

K; K_v; K_G; K_P; K_S; K_R; K_{MS}; K_{MR} extensional stiffnesses, see summary on p.153

k_1; k_2 .....k_{10} coefficients in stress function differential equation, defined on p.54 and 55

k_1; k_2; k_3 Runge-Kutta parameters, see p.88

L length of composite cylindrical shell

$\mathcal{L}_{11}$; $\mathcal{L}_{12}$; $\mathcal{L}_{22}$; $\mathcal{L}_{8}$; $\mathcal{L}_{8}^{(m)}$ linear operators, defined on pp.122-124

ℓ ring spacing, see p.15

ℓ_1; ℓ_2; ℓ_3 Runge-Kutta parameters, defined on p.88

M_x; M_y; M_{xy}; M_{yx}; $\bar{M}_{xy}$ moments per unit length of the composite shell; with superscript (S) for stringer; with superscript (R) for ring

$M^{(S)}$; $M_t^{(S)}$; $M_t^{(R)}$ bending and twisting moments of stringer and ring

$\mathcal{M}_x$; $\mathcal{M}_y$ Surface moments of the composite shell, see p.24

$\bar{m}$ smeared-out mass per unit area of composite shell

m number of sinusoidal buckling half wavelengths in the axial direction

(m) superscript, referring to monocoque shell

N_x; N_y; N_{xy}; N_{yx} stress resultants of the composite shell; with superscript (S) for stringer, with (R) for ring

N_{xA} applied compressive load per unit circumference in the axial direction

$\bar{N}_{xo}$; $\bar{N}_{yo}$ compressive average stress resultants, where subscript o refers to being independent of x and y

$\bar{N}_{oxMAX}$ maximum of $\bar{N}_{ox}(t)$ curve

$\bar{N}_{oxc}$ critical dynamic axial buckling load, defined as the lowest of all $\bar{N}_{oxMAX}$

N_{xP}; N_{yP}; N_{xyP} static prebuckling stress resultants, where the first two quantities refer to compressive stresses

N_{ox} static compressive stress resultant, independent of x and y

N_{oxc} critical static axial buckling load, minimized with respect to m and n

n number of sinusoidal full buckling wavelengths in the circumferential direction

n_S; n_R number of equally spaced stringers and rings

P subscript to denote prebuckling variables

P_{max} maximum total buckling load

p external lateral pressure

partial differentiation: denoted by comma, followed by independent variable with respect to which the differentiation applies

Q_1; Q_2; Q_3 coefficients, defined on p.79

Q_x; Q_y shear stress resultants, with superscript (m) for monocoque shell, see pp.12 and 24

R radius of middle surface of monocoque cylindrical shell

R_1; R_2; R_3; R_4 constants defined on p.80

r_g radius of gyration of column, see p.70

S_{11}; S_{12}; S_{13}; S_{14}; S_{22} eccentricity parameters, see pp.30 and 31; also in summary p.153

s Laplace transform variable; quantities with bar denote transformed variables

T kinetic energy; with superscripts (m), (S) and (R), for monocoque shell, stringer and ring.

t time

t_{f_1}; t_{g_1} upper time limits for asymptotic expansions, see p.82

U strain energy

U_1.....U_6 coefficients, see p.75, with superscript (0) for constant rate of endshortening

u tangential displacement of the middle surface in the axial direction, also used as $f_1(t)=u(z)$, see p.78

V time varying rate of endshortening

V_o magnitude of rate of endshortening

V_{11}; V_{12}; V_{21}; V_{22}; V_{31}; V_{32}; V_{41}; V_{42}; V_5; V_6 coefficients, defined on p.76

$V_1^{(0)}$.....$V_6^{(0)}$ coefficients for constant rate of endshortening, see p.77

v tangential displacement of middle surface in circumferential direction

W external work

w lateral displacement of middle surface, positive toward the inside; also net lateral displacement

$w_{(1)}$ total lateral displacement of the middle surface

$w_{(0)}$ initial imperfection displacement of the midsurface

X surface force per unit area in axial direction, see p.24

x coordinate in axial direction, see p.12; also indicating time in numerical work, see p.87

Y surface force per unit area in circumferential direction

y coordinate in circumferential direction, see p.12; also identical with f_1, see p.87

Z surface force per unit area in lateral direction

z coordinate in lateral direction, positive inward, see p.12; also identical with g_1, see p.87; furthermore used in time transformation (V-31), see p.78

$\bar{z}_S$; $\bar{z}_R$ centroidal coordinates of stringer and ring cross sections, positive inward from middle surface

z_o constant, defined on p.80

α axial buckling wave parameter, defined on p.51

β circumferential buckling wave parameter, see p.51

γ exponential decay coefficient, reciprocal of time constant

γ_{xy} shear strain of middle surface

γ_{xyT} shear strain at some distance z from the midsurface

δ variational symbol

Δ determinant, defined on p.72

ϵ_x; ϵ_y middle surface strains in the axial and circumferential directions

ζ coordinate from the middle surface in the z-direction where N_{xA} is applied

η stiffener location effectiveness, defined on p.129; also generic variable for z or τ, see p.81;

ϑ buckling aspect ratio, defined on p.89

θ imperfection coupling frequency parameter, defined on p.71, also used as dummy integration variable, pp.79-80

$\lambda_1 \ldots\ldots \lambda_{10}$ coefficients of stress function, defined on p.56

λ_1; λ_2; λ_3; λ_4 initial condition parameters, defined on p.80

Λ generic variable parameter, defined on p.81

$\mu_1 \ldots\ldots \mu_5$ composite shell parameters, see summary p.154, with superscript (m) for monocoque shell

ν Poisson's ratio of monocoque shell

ξ mode parameter, defined on p.126; also dummy integration variable, see p.60

ρ; ρ_S; ρ_R mass densities of monocoque shell, stringer and ring

σ_x; σ_y normal stresses in axial and circumferential directions, with superscripts (m), (S) and (R), referring to monocoque shell, stringer and ring

$\tau_{xy}^{(m)}$; $\tau_{yx}^{(m)}$ shear stresses of the monocoque shell

τ time transformation variable, defined on p.78

Φ stress function with imperfections

ω_1; ω_2 circular frequencies, defined on p.72, with superscript (0) for zero imperfections

Ω mode parameter, defined on p.125

ERRATA

Abstract-page	bottom line:	paradoxical
p.2	line 9:	discrete
p.6	line 13:	Among these,
p.6	line 3 from bottom:	paradoxical
p.8	line 10 from bottom:	paradoxical
p.39	Eqs.(II-30), second line:	$f_{,xy}=0$
p.54	Eq.(IV-7):	$\Phi_{,xxxx} + 2a_{12}\Phi_{,xxyy} + \cdots$
p.77	Eqs.(V-29):	$V_2^{(0)} = \frac{\cdots - \frac{\Omega}{\omega_2}(B_1 C_2 - \cdots}{\cdots\cdots\cdots}$
p.81	line 1:	Equations (V-35)
p.87	line 9 from bottom:	..of the function are required.
p.88	Eqs.(VI-3)	$\ell_2 = h\, F_2\left(x_n + \frac{h}{2};\ y_n + \frac{h}{2}y_n' + \frac{h}{8}k_1;\ \cdots\right)$
p.89	line 2 (title):	Paradoxical Results
p.89	line 6:	paradoxical nature
p.96	line 11:	...of fifth order formulas
p.106	line 1:	$\overline{N}_{ox}(t)$
p.106	line 9 from bottom:	$\overline{N}_{ox}$,also line 4 from bottom
p.106	line 2 from bottom:	..led to clear..
p.106	last line:	paradoxical situation
p.107	line 5 from bottom:	equation (A-3)
p.107	line 4 from bottom:	quantities
p.108	line 4 from bottom:	..underlined in..
p.109	below Table:	*underlined
p.110	below Table:	*underlined
p.110	line 5 from bottom:	underlined values
p.112	line 3 below Table:	**underlined

p.115 below Table: *underlined

p.117 line 3: $\bar{N}_{oxc}$=833 lb/in

p.117 line 2 from bottom: separately

p.122 first typed line: dropped

p.136 line 8: ... for other_ ... (remove comma)

p.140 line 11 from bottom: ..investigate "discrete"..

p.141 Figure (VIII-1) DISCRETE POINTS

p.155 line 6 from bottom: .. computations are executed...

p.156 line 8: divided

p.167 [26] : ... Theory of Elasticity of an...

INTRODUCTION

The literature on shell theory has mushroomed in the past one to one-and-one half decades so that it becomes a major undertaking just to become up-to-date on what has been done. Fortunately, some excellent survey articles [1-11] * exist which make this task considerably easier. Comprehensive bibliographies are available in the works [12-15].

It would be beyond the scope of this dissertation to give a historical survey of the major contributions in shell stability theory. A few remarks are in order, however, to indicate the relative position of this dissertation in regard to the overall field.

Let us restrict ourselves to cylindrical shells and discuss static and dynamic stability investigations separately.

1. Static Stability Investigations.

The large discrepancy between theoretically predicted static axial buckling loads on thin monocoque (unstiffened) cylindrical shells and experimentally measured values has been the topic of research of many people over many years. Large deflection theory, imperfections, and the influence of boundary conditions were found to explain away a good share of this discrepancy [16-22].

Static stability investigations of stiffened cylindrical shells are not numerous by comparison. One of the earliest analyses is given in Flügge's habilitation paper [23]. During the second

---

* Numbers within square brackets refer to the reference list at the end.

World War a program of analytical and experimental investigation was initiated at the Guggenheim Aeronautical Laboratory of the California Institute of Technology [24]. These efforts generated some empirical relations involving a combination of loading conditions.

Let us briefly discuss some concepts peculiar to stiffened shells. When the number of stiffening elements (stringers and rings) is small and therefore their interbay distance at least of the order of the buckling half wavelength, a discreet treatment of the stiffening elements, interacting with the monocoque shell, is necessary. In such cases the skin alone might buckle between the gridwork of stiffeners (interbay buckling or local buckling in the large). One might reduce such problems to those of panel stability with boundary conditions corresponding to stiffeners of varying degrees of fixity. A great deal of design information of this kind is available in the NACA "Handbook of Structural Stability" [25]. This dissertation will not be concerned with problems of this kind.

When the number of stiffeners is large so that their interbay distance is small with respect to the buckling half wavelength, buckling occurs simultaneously for both, skin and stiffeners, and one speaks of general instability. A distributed approach is usually taken in that the stringer- and ring stiffnesses are smeared-out over their interbay distances so that an "equivalent cylindrical shell" is treated analytically.

Two more distinctions become necessary:

- The centroids of the stringers and rings lie on the middle surface of the monocoque cylindrical shell. In this case, the

equivalent shell is analogous to a "quasi-orthotropic" shell with its principal elastic directions along the generators and circles of the shell [26;27;28].

- The above mentioned centroids are off-set from the middle surface. Such structural shells are called eccentrically reinforced shells.

In the papers [23;29;30;31] , static stability analyses are presented using the equivalent shell approach. Small deflection theory is employed, while eccentricity effects are entirely neglected. As early as 1947, Van der Neut [32] demonstrated the importance of eccentricity in determining the buckling strength of stiffened cylindrical shells. Unfortunately, this early report seems to have been largely neglected. It took the pressures of the space race to renew such interests [33-37]. The sign (inward or outward) of the eccentricity of stringers and rings affects the magnitude of the buckling load drastically. This has been verified experimentally [34] to the extent that a particular externally stiffened cylinder under axial compression has been shown to carry over twice the load sustained by its internally stiffened counterpart. Small deflection theory is used in all these reports except in the paper [35]. The use of the small deflection theory for stiffened cylindrical shells is commonly argued on the basis that imperfections are small with respect to the equivalent shell thickness in contrast to the monocoque shell. Experimental evidence is however lacking to support such an assumption. In addition, it was already pointed

out that the imperfections are only part of the story for the monocoque shell.

2. Dynamic Stability Investigations.

Prior to discussing dynamic stability, we might call attention to some papers dealing with lateral vibrations of the monocoque cylindrical shell in small deflection theory [38;39;40], and stiffened cylindrical shells with the same restrictions [36;37;41].

Almost in a class by themselves are the so-called parametric instability problems, discussed by Evan-Iwanowski in the articles [6;7]. They have only recently been attacked, and for the most part, for much simpler structural elements [42]. In these, disturbances (generalized loads) are of the sustained periodic type and instability regions can be determined from the resulting Hill or Mathieu differential equations. As far as cylindrical shells are concerned, information is meager. The papers [43;44] treat the problem of parametric instability of a monocoque cylindrical shell subjected to an axial pulsating load, using small deflection theory. Report [45] gives results for the case of a monocoque cylindrical shell loaded by a constant axial force in combination with a pulsating lateral pressure, restricted to small deflection theory.

As far as nonparametric dynamic stability investigations are concerned, we might speak of those problems involving nonperiodic disturbances either applied laterally or axially.

The former seems to be the easier problem while the latter usually requires the introduction of some kind of imperfection or eccentricity of the axial disturbance. A lateral step pressure is applied to the monocoque cylindrical shell in report [45] using small deflection theory. This paper contains a few Russian references on dynamic stability. The Russians seem to be pioneers in this field. Agamirov and Volmir* [46] have used large deflection theory to treat the monocoque cylindrical shell under a lateral ramp pressure and axial compression. Little details are shown, however, for the latter case. They give credit to Hoff [47;48] for having initiated dynamic buckling with the case of the column. Subsequent domestic variations of Agamirov and Volmir's approach can be found in the reports [50;51;52;53]. The GE-report [51] deals with an experimental investigation of impact of monocoque shells. It also contains a theoretical analysis of the dynamic stability of a monocoque cylindrical shell which is subjected to a constant rate of endshortening in the manner of Hoff's treatment of the column [47]. No comparison between experiments and theory is shown. It appears furthermore that the results defy physical reasoning in that the dynamic buckling loads show no minimum value, but become lower and lower with increasing mode numbers. With the exception of paper [52] which deals with transverse nonlinear vibrations of orthotropic cylindrical shells, all these references are restricted to monocoque cylindrical shells.

---

* His book on flexible plates and shells is now available in a German translation [49].

3. New Features of the Present Topic.

The difficult problem of the dynamic stability of cylindrical shells in axial compression has not been treated adequately in the literature. Of the two references on the monocoque shell known to the author, the first [46] does not provide sufficient details for judgement, while the second [51] leads to results which are doubtful.

The topic of the dynamic stability of eccentrically reinforced cylindrical shells in axial compression fills therefore a gap, not presently covered.

The author feels that this dissertation contains certain new features and makes contributions which should lead to a better understanding of this particular topic. Among theses, one might list:

-Large deflection theory applied to the dynamics of the eccentrically reinforced cylindrical shell.

-Inclusion of initial imperfections in connection with eccentric stiffening.

-Derivation of new dynamic field equations with and without initial imperfections.

-Inclusion of rotatory inertia.

-Clarification of paradoxial results obtained by inadequate numerical integration techniques, such as used in reference [51].

-Determination of the quantitative influence on the dynamic

buckling load of rotatory inertia, rate of endshortening, direction of initial imperfections and time constant of exponentially decaying endshortening for the case of a particular shell.

-Close agreement between predicted and tested buckling load for the case of a particular shell in "static" reduction of the theory.

-Derivation of a linear classical eighth order Donnell-type differential equation for static buckling of an eccentrically reinforced cylindrical shell.

-Evaluation of the concept of stiffener location effectiveness with a simple graphical "optimization chart" for a particular shell.

4.Organization and Preview.

The main body of this dissertation is divided into eight chapters. Chapters I and II develop the governing equations from basic principles and certain assumptions. This effort culminates in a set of new field equations which form the basis of the rest of the development.

Chapter III extends these field equations to include initial imperfections.

In Chapter IV, a radial displacement assumption is made from which a stress function is obtained that satisfies the compatibility equation. The initial imperfection displacement is assumed to be in "spatial harmony" with the total displacement.

Boundary and closure conditions are discussed in detail. Chapter V takes up the problem of a clamped eccentrically reinforced cylindrical shell subjected to a controlled rate of endshortening. The average stress resultant at the ends is derived in terms of the buckling pattern amplitudes. The Bubnov-Galerkin method is applied in order to satisfy the dynamic equilibrium equation with the derived stress function and the assumed radial displacement. There results a pair of simultaneous second order differential equations of the third degree in the buckling pattern amplitudes. The remainder of the chapter concentrates on these important equations and demonstrates physical insight through the consideration of simplified cases, whose solutions are also included.

In Chapter VI, numerical methods are discussed briefly and then applied to the practical problem of a stringer shell which Card [34] tested statically. It is clearly demonstrated that the application of the Runge-Kutta method over the full range leads to paradoxial results. A combined Runge-Kutta Predictor-Corrector method resolves these paradoxes and leads to results which are in agreement with physical intuition. The critical dynamic buckling load is defined and a criterion is given for selecting it. The remainder discusses the effects of various factors on the critical dynamic buckling load.

In Chapter VII, the static buckling equations are derived in order to present a more complete picture of the topic of the eccentrically reinforced cylindrical shell. Prior to this derivation, the static reduction of the dynamic theory is de-

monstrated for Card's shell and close agreement is shown between predicted and measured buckling load. A linear Donnell-type eighth order differential equation is derived for static buckling. It is then applied to Card's shell also and a comparison is made between theory and test. The problem of selecting the proper mode numbers is discussed. Finally, the concept of stiffener location effectiveness is introduced. Under the assumption of equal mode numbers for externally and internally stiffened shell, an analytic expression is given for the stiffener location effectiveness. A relatively simple graphical "optimization chart" is presented for Card's shell.

Chapter VIII presents a summary, gives conclusions and indicates future work needed on this complex topic.

CHAPTER I : FORMULATION OF THE DYNAMIC EQUILIBRIUM EQUATIONS FOR THE ECCENTRICALLY REINFORCED CYLINDRICAL SHELL.

1. Stress Resultants and Moments for the Shallow Monocoque Cylindrical Shell.

The plane stress-strain relations of the engineering theory of elasticity are assumed to be valid for the monocoque shell. Denoting these stresses with superscript (m), they are stated as,

$$\left.\begin{aligned} \sigma_x^{(m)} &= \frac{E}{1-\nu^2}\left(\varepsilon_{xT} + \nu\,\varepsilon_{yT}\right) \\ \sigma_y^{(m)} &= \frac{E}{1-\nu^2}\left(\varepsilon_{yT} + \nu\,\varepsilon_{xT}\right) \\ \tau_{xy}^{(m)} &= G\,\gamma_{xyT} \end{aligned}\right\} \qquad \text{(I-1)}$$

where the usual symbols are used, and where the subscript T on the strains refers to the total strain at any height in the thickness direction z.

The strains in the middle surface are written without subscript. It is assumed that straight lines normal to the middle surface remain straight, unstretched and normal to the middle surface after deformation. The total strains are then related to the midsurface strains by,

$$\left.\begin{aligned} \varepsilon_{xT} &= \varepsilon_x - z\,w_{,xx} \\ \varepsilon_{yT} &= \varepsilon_y - z\,w_{,yy} \\ \gamma_{xyT} &= \gamma_{xy} - 2z\,w_{,xy} \end{aligned}\right\} \qquad \text{(I-2)}$$

where $w_{,xx}$, $w_{,yy}$, and $w_{,xy}$ are the approximate changes in curvature and twist of the midsurface, and the usual comma notation for partial differentiation has been employed. Figure (I-1), shown below, illustrates the chosen coordinate system, the stresses and displacements in regard to a monocoque shell segment of thickness h, and middle surface radius R.

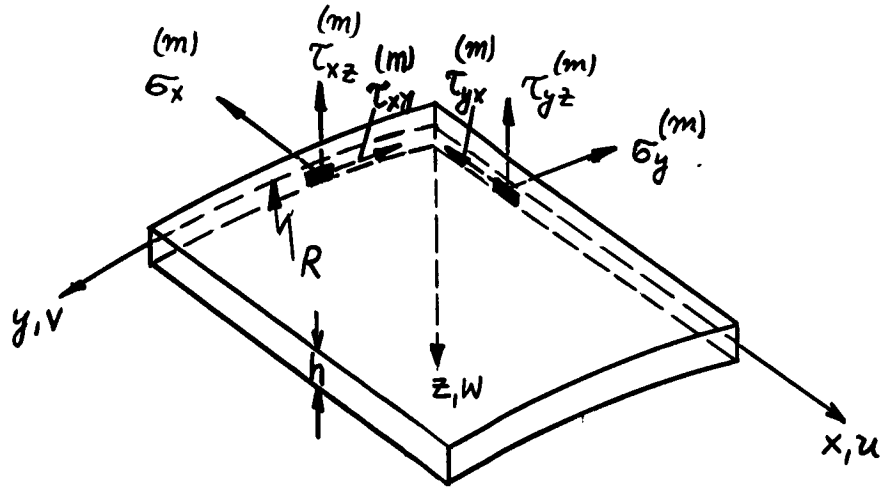

Figure (I-1) : Coordinate System, Stresses and Displacements on a Monocoque Shell Segment.

The monocoque cylindrical shell is assumed to be shallow ($\frac{|z|}{R} < \frac{h}{R} << 1$) such that the stress resultants, moments and shear forces can be approximated by,

$$N_x^{(m)} = \int_{-\frac{h}{2}}^{\frac{h}{2}} \sigma_x^{(m)}\, dz \qquad N_y^{(m)} = \int_{-\frac{h}{2}}^{\frac{h}{2}} \sigma_y^{(m)}\, dz \qquad \text{(I-3)}$$

$$
\begin{aligned}
N_{xy}^{(m)} &= \int_{-\frac{h}{2}}^{\frac{h}{2}} \tau_{xy}^{(m)}\, dz & N_{yx}^{(m)} &= \int_{-\frac{h}{2}}^{\frac{h}{2}} \tau_{yx}^{(m)}\, dz \\
Q_x^{(m)} &= \int_{-\frac{h}{2}}^{\frac{h}{2}} \tau_{xz}^{(m)}\, dz & Q_y^{(m)} &= \int_{-\frac{h}{2}}^{\frac{h}{2}} \tau_{yz}\, dz \\
M_x^{(m)} &= \int_{-\frac{h}{2}}^{\frac{h}{2}} \sigma_x^{(m)}\, z\, dz & M_y^{(m)} &= \int_{-\frac{h}{2}}^{\frac{h}{2}} \sigma_y^{(m)}\, z\, dz \\
M_{xy}^{(m)} &= -\int_{-\frac{h}{2}}^{\frac{h}{2}} \tau_{xy}^{(m)}\, z\, dz & M_{yx}^{(m)} &= \int_{-\frac{h}{2}}^{\frac{h}{2}} \tau_{yx}\, z\, dz
\end{aligned}
\qquad \approx \qquad (I\text{-}3)
$$

where the superscript (m) refers again to the monocoque shell, and the convention adopted is shown in Figure (I-2) below:

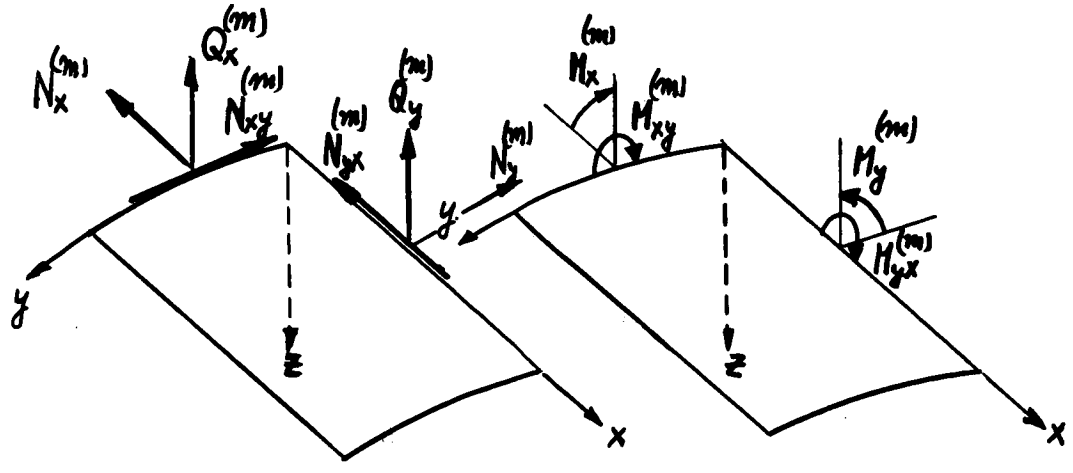

Figure (I-2) : Middle Surface Stress Resultants, Shear Forces and Moments on a Monocoque Shell Segment.

Introducing equations (I-2) into (I-1), the stress resultants and moments can be evaluated by integrating expressions (I-3), which yields the result;

$$\left.\begin{aligned} N_x^{(m)} &= K\varepsilon_x + K_\nu \varepsilon_y \\ N_y^{(m)} &= K\varepsilon_y + K_\nu \varepsilon_x \\ N_{xy}^{(m)} &= K_G \gamma_{xy} \\ M_x^{(m)} &= -(D w_{,xx} + D_\nu w_{,yy}) \\ M_y^{(m)} &= -(D w_{,yy} + D_\nu w_{,xx}) \\ M_{xy}^{(m)} &= -M_{yx}^{(m)} = D_G w_{,xy} \end{aligned}\right\} \qquad \text{(I-4)}$$

where use has been made of certain stiffness and rigidity parameters which are defined as:

$$\left.\begin{aligned} K &= \frac{Eh}{1-\nu^2} \qquad K_\nu = \frac{\nu Eh}{1-\nu^2} \qquad K_G = \frac{Eh}{2(1+\nu)} = Gh \\ D &= \frac{Eh^3}{12(1-\nu^2)} \qquad D_\nu = \frac{\nu Eh^3}{12(1-\nu^2)} \qquad D_G = \frac{Eh^3}{12(1+\nu)} = \frac{Gh^3}{6} \end{aligned}\right\} \qquad \text{(I-5)}$$

The stress resultants and moments of the monocoque cylindrical shell can be cast into the following matrix form:

$$\begin{Bmatrix} N_x \\ N_y \\ N_{xy} \\ M_x \\ M_y \\ M_{xy} \end{Bmatrix}^{(m)} = \begin{pmatrix} K & K_\nu & 0 & 0 & 0 & 0 \\ K_\nu & K & 0 & 0 & 0 & 0 \\ 0 & 0 & K_6 & 0 & 0 & 0 \\ 0 & 0 & 0 & -D & -D_\nu & 0 \\ 0 & 0 & 0 & -D_\nu & -D & 0 \\ 0 & 0 & 0 & 0 & 0 & D_6 \end{pmatrix} \begin{Bmatrix} \varepsilon_x \\ \varepsilon_y \\ \gamma_{xy} \\ w_{,xx} \\ w_{,yy} \\ w_{,xy} \end{Bmatrix} \quad \text{(I-6)}$$

2. Stress Resultants and Moments for the Eccentrically Reinforced Shallow Cylindrical Shell.

The monocoque cylindrical shell is assumed to be stiffened by an orthogonal net of stringers and rings, parallel to the x- and y-coordinates, the centroids of their respective cross sectional areas being off-set from the middle surface.

A typical reinforced shell segment is shown in Figure (I-3) below:

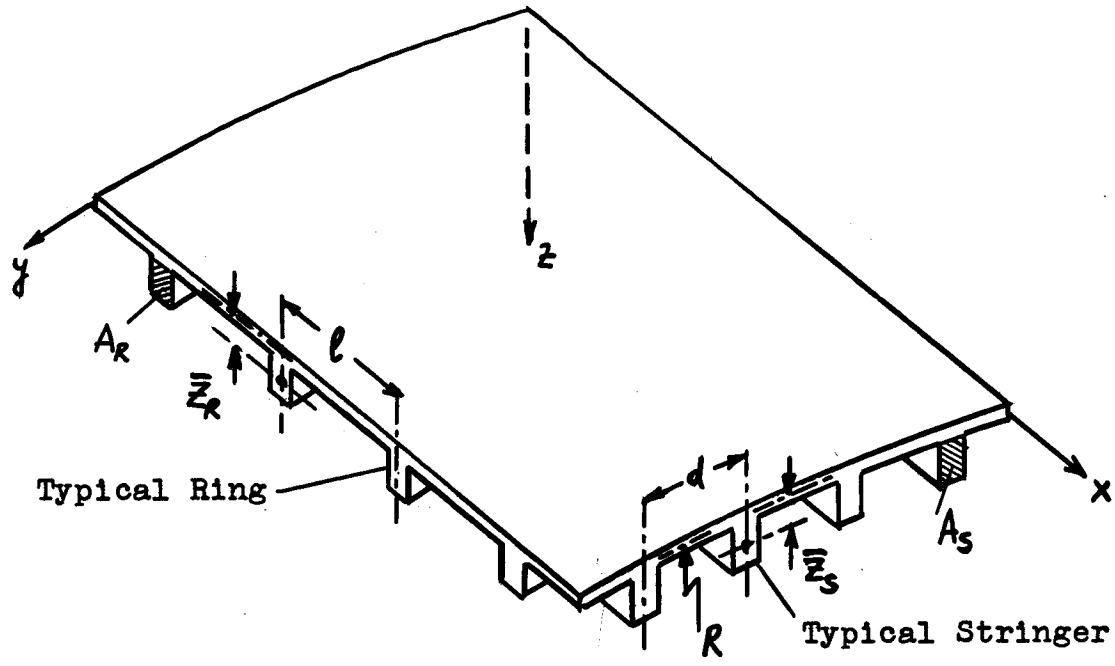

Figure (I-3) : Typical Eccentrically Reinforced Cylindrical Shell Element.

The distances between stringers, d, and rings, ℓ, are assumed small with respect to the buckling half wavelength since we are interested in the general stability of the reinforced shell. This condition may be stated as follows:

$$\left.\begin{aligned} d < b &= \frac{2\pi R}{2n} \\ \ell < a &= \frac{L}{m} \end{aligned}\right\} \qquad \text{(I-7)}$$

where a and b are the buckling half wavelengths in the axial and circumferential directions, while m and 2n are the number of half waves in these directions, L being the length of the

reinforced shell.

It is assumed that the stringers and rings can be treated as beams. On account of the shell being shallow, the rings can be treated as straight beams. For rectangular cross section rings of moderate height, it is common practice to treat a ring as a straight beam in pure bending when the radius of curvature-to height ratio exceeds about ten.

The condition of continuity of the strains must be satisfied at the interfaces between monocoque shell, stringer, and ring.

The stresses are given by,

$$\left.\begin{aligned} \sigma_x^{(S)} &= E_S \varepsilon_x - E_S z\, w_{,xx} \\ \sigma_y^{(R)} &= E_R \varepsilon_y - E_R z\, w_{,yy} \end{aligned}\right\} \qquad \text{(I-8)}$$

where the super- and subscripts S and R refer to stringer and ring.

When the materials are different for the monocoque shell, stringer, and ring, there is a stress discontinuity at the respective interfaces.

a) <u>The Contribution of Stringers and Rings to the Stress Resultants</u>.

The force, acting in the x-direction on a stringer cross section, can be obtained by integrating the first equation

of (I-8) over the cross sectional stringer area A_S. Similarly, integrating the second equation over the ring cross sectional area A_R, leads to the force on the ring cross section in the y-direction. The result becomes,

$$F_x = E_S A_S \varepsilon_x - E_S w_{,xx} \int_{A_S} z\, dA_S = E_S A_S \varepsilon_x - E_S A_S \bar{z}_S w_{,xx}$$

$$F_y = E_R A_R \varepsilon_y - E_R w_{,yy} \int_{A_R} z\, dA_R = E_R A_R \varepsilon_y - E_R A_R \bar{z}_R w_{,yy}$$

where $\bar{z}_S$ and $\bar{z}_R$ are the centroidal distances from the middle surface. In the above integration it was tacitly assumed that the strains and curvature changes of the mid-surface can be considered constant. This is justified on the basis that the region of the cross sectional areas covers only a fraction of the stiffener distances, the latter being small with respect to the buckling half wavelengths.

In order to arrive at a composite stress resultant due to stringers and rings, let us smear-out both force contributions over their stiffener spacings, e.g.

$$\left.\begin{aligned} N_x^{(S)} &= \frac{E_S A_S}{d} \varepsilon_x - \frac{E_S A_S \bar{z}_S}{d} w_{,xx} \\ N_y^{(R)} &= \frac{E_R A_R}{\ell} \varepsilon_y - \frac{E_R A_R \bar{z}_R}{\ell} w_{,yy} \end{aligned}\right\} \qquad \text{(I-9)}$$

Any contribution to the shear stress resultant due to stringers and rings is assumed negligible.

b) The Contribution of Stringers and Rings to the Moments.

Let us take moments of the forces due to the stresses of equations (I-8) about the local coordinate axes of the middle surface. With due regard to the sign convention adopted in Figure (I-2), we obtain:

$$M^{(S)} = \int_{A_S} (E_S \varepsilon_x z - E_S w_{,xx} z^2)\, dA_S = E_S A_S \bar{z}_S \varepsilon_x - E_S I_{SO} w_{,xx}$$

where I_{SO} is the area moment of inertia of the stringer cross section with respect to the local y-axis of the middle surface.

Smearing-out this moment contribution over the stringer spacing d, the stringer component of the composite moment per unit length is obtained. Similar considerations apply to the ring. We thus arrive at the following expressions:

$$\left.\begin{aligned} M_x^{(S)} &= \frac{E_S A_S \bar{z}_S}{d} \varepsilon_x - \frac{E_S I_{SO}}{d} w_{,xx} \\ M_y^{(R)} &= \frac{E_R A_R \bar{z}_R}{\ell} \varepsilon_y - \frac{E_R I_{RO}}{\ell} w_{,yy} \end{aligned}\right\} \qquad \text{(I-10)}$$

Twisting of the stringer and ring occurs due to the twisting curvature change $w_{,xy}$ of the midsurface. Neglecting any possible rigidization due to the junction of the stiffeners and assuming free warping, the contributions to the twisting moment of the stringer and ring can be written as,

$$M_t^{(S)} = G_S J_S \, w_{,xy}$$
$$M_t^{(R)} = -G_R J_R \, w_{,xy}$$

where J_S and J_R are the torsion constants of the stringer and ring cross sections and use has been made of our adopted sign convention.

Smearing-out these twisting moment contributions over the stiffener spacings, we obtain:

$$\left.\begin{aligned} M_{xy}^{(S)} &= \frac{G_S J_S}{d} \, w_{,xy} \\ M_{yx}^{(R)} &= -\frac{G_R J_R}{\ell} \, w_{,xy} \end{aligned}\right\} \qquad \text{(I-11)}$$

c) <u>The Composite Stress Resultants and Moments of the Eccentrically Reinforced Circular Cylindrical Shell</u>.

By adding corresponding stress resultants and moments from equations (I-4), (I-8), (I-10), and (I-11), composite stress resultants and moments are obtained. These refer to the middle surface of the monocoque shell and can be written as:

$$\left.\begin{aligned} N_x &= N_x^{(m)} + N_x^{(S)} = K\varepsilon_x + K_\nu \varepsilon_y + \frac{E_S A_S}{d}\varepsilon_x - \frac{E_S A_S \bar{z}_S}{d} w_{,xx} \\ N_y &= N_y^{(m)} + N_y^{(R)} = K\varepsilon_y + K_\nu \varepsilon_x + \frac{E_R A_R}{\ell}\varepsilon_y - \frac{E_R A_R \bar{z}_R}{\ell} w_{,yy} \\ N_{xy} &= N_{yx} = N_{xy}^{(m)} = N_{yx}^{(m)} = K_G \gamma_{xy} \end{aligned}\right\} \qquad \text{(I-12)}$$

$$
\begin{aligned}
M_x &= M_x^{(m)} + M_x^{(s)} = -D w_{,xx} - D_\nu w_{,yy} + \frac{E_s A_s \bar{z}_s}{d}\varepsilon_x - \frac{E_s I_{s0}}{d} w_{,xx} \\
M_y &= M_y^{(m)} + M_y^{(R)} = -D w_{,yy} - D_\nu w_{,xx} + \frac{E_R A_R \bar{z}_R}{\ell}\varepsilon_y - \frac{E_R I_{R0}}{\ell} w_{,yy} \\
M_{xy} &= M_{xy}^{(m)} + M_{xy}^{(s)} = D_G w_{,xy} + \frac{G_s J_s}{d} w_{,xy} \\
M_{yx} &= M_{yx}^{(m)} + M_{yx}^{(R)} = -D_G w_{,xy} - \frac{G_R J_R}{\ell} w_{,xy}
\end{aligned}
\qquad \text{(I-12)}
$$

Since the stress resultants and moments are related to the middle surface strains and curvature changes, it seems only natural to lump corresponding coefficients. This leads to the following definitions of parameters:

$$
\begin{aligned}
K_s &= \frac{E_s A_s}{d} & F_{sb} &= \frac{E_s A_s}{d}\bar{z}_s \\
K_R &= \frac{E_R A_R}{\ell} & F_{Rb} &= \frac{E_R A_R}{\ell}\bar{z}_R \\
K_{MS} &= K + K_s = \frac{Eh}{1-\nu^2} + \frac{E_s A_s}{d} \\
K_{MR} &= K + K_R = \frac{Eh}{1-\nu^2} + \frac{E_R A_R}{\ell} \\
D_s &= \frac{E_s I_{s0}}{d} = \frac{E_s}{d}(I_{sc} + \bar{z}_s^2 A_s) \\
D_R &= \frac{E_R I_{R0}}{\ell} = \frac{E_R}{\ell}(I_{Rc} + \bar{z}_R^2 A_R) \\
D_{GS} &= \frac{G_s J_s}{d} & D_{GR} &= \frac{G_R J_R}{\ell} \\
D_{MS} &= D + D_s = \frac{Eh^3}{12(1-\nu^2)} + \frac{E_s}{d}(I_{sc} + \bar{z}_s^2 A_s) \\
D_{MR} &= D + D_R = \frac{Eh^3}{12(1-\nu^2)} + \frac{E_R}{\ell}(I_{Rc} + \bar{z}_R^2 A_R)
\end{aligned}
\qquad \text{(I-13)}
$$

$$\left.\begin{aligned} D_{MGS} &= D_G + D_{GS} = \frac{Gh^3}{6} + \frac{G_S J_S}{d} \\ D_{MGR} &= D_G + D_{GR} = \frac{Gh^3}{6} + \frac{G_R J_R}{\ell} \end{aligned}\right\} \qquad \text{(I-13)}$$

The K's are extensional stiffness parameters, the D's are flexural rigidity parameters and the F's are eccentricity force coefficients. The latter are "signed" quantities, taken positive for internal stiffeners. I_{SC} and I_{RC} are the area moments of inertia with respect to parallel centroidal axes for stringer and ring.

Rewriting equations (I-12) with these parameters, yields:

$$\left.\begin{aligned} N_x &= K_{MS}\,\varepsilon_x + K_\nu\,\varepsilon_y - F_{Sb}\,w_{,xx} \\ N_y &= K_\nu\,\varepsilon_x + K_{MR}\,\varepsilon_y - F_{Rb}\,w_{,yy} \\ N_{xy} &= N_{yx} = K_G\,\gamma_{xy} \\ M_x &= F_{Sb}\,\varepsilon_x - D_{MS}\,w_{,xx} - D_\nu\,w_{,yy} \\ M_y &= F_{Rb}\,\varepsilon_y - D_\nu\,w_{,xx} - D_{MR}\,w_{,yy} \\ M_{xy} &= D_{MGS}\,w_{,xy} \\ M_{yx} &= -D_{MGR}\,w_{,xy} \end{aligned}\right\} \qquad \text{(I-14)}$$

It must be noted that the twisting moments M_{xy} and M_{yx} are no longer of equal magnitude. D_{GS} and D_{GR} are generally not equal. If we wish to cast (I-14) into a matrix equation,

similar to (I-6), we can define,

$$\bar{M}_{xy} = \frac{1}{2}(M_{xy} - M_{yx}) = \frac{1}{2}(D_{HGS} + D_{HGR})W_{,xy}$$
$$= [D_G + \frac{1}{2}(D_{GS} + D_{GR})]W_{,xy}$$

and introduce:

$$D_1 = D_G + \frac{1}{2}(D_{GS} + D_{GR}) \qquad \text{(I-15)}$$

$\overline{M_{xy}}$ can be interpreted physically as an effective twisting moment for which the differences of torsional stiffnesses of stringers and rings are averaged out.

The stress resultants and moments of the eccentrically reinforced circular cylindrical shell can now be written in the following matrix form:

$$\begin{Bmatrix} N_x \\ N_y \\ N_{xy} \\ M_x \\ M_y \\ \bar{M}_{xy} \end{Bmatrix} = \begin{pmatrix} K_{HS} & K_\nu & 0 & -\bar{F}_{Sb} & 0 & 0 \\ K_\nu & K_{HR} & 0 & 0 & -F_{Rb} & 0 \\ 0 & 0 & K_G & 0 & 0 & 0 \\ F_{Sb} & 0 & 0 & -D_{HS} & -D_\nu & 0 \\ 0 & F_{Rb} & 0 & -D_\nu & -D_{HR} & 0 \\ 0 & 0 & 0 & 0 & 0 & D_1 \end{pmatrix} \begin{Bmatrix} \varepsilon_x \\ \varepsilon_y \\ \gamma_{xy} \\ W_{,xx} \\ W_{,yy} \\ W_{,xy} \end{Bmatrix} \qquad \text{(I-16)}$$

In contrast to the matrix of equation (I-6) for the monocoque shell, the above matrix is no longer symmetric.

3. Stress Resultants and Moments in Terms of Displacements.

Considering the radial displacements to be large in comparison with the tangential (middle surface) displacements u and v, the strain-displacement relations are given by:

$$\left.\begin{aligned} \varepsilon_x &= u_{,x} + \tfrac{1}{2} w_{,x}^2 \\ \varepsilon_y &= v_{,y} + \tfrac{1}{2} w_{,y}^2 - \frac{w}{R} \\ \gamma_{xy} &= u_{,y} + v_{,x} + w_{,x} w_{,y} \end{aligned}\right\} \qquad \text{(I-17)}$$

The above strains are not independent of each other. They must satisfy the compatibility equation for large deflections, given by:

$$\varepsilon_{x,yy} + \varepsilon_{y,xx} - \gamma_{xy,xy} = w_{,xy}^2 - w_{,xx} w_{,yy} - \frac{w_{,xx}}{R} \qquad \text{(I-18)}$$

With the help of the strain-displacement relations, the stress resultants and moments for the eccentrically reinforced shell then become:

$$\left.\begin{aligned} N_x &= K_{MS}\left(u_{,x} + \tfrac{1}{2} w_{,x}^2\right) + K_\nu\left(v_{,y} + \tfrac{1}{2} w_{,y}^2 - \frac{w}{R}\right) - F_{Sb} w_{,xx} \\ N_y &= K_\nu\left(u_{,x} + \tfrac{1}{2} w_{,x}^2\right) + K_{MR}\left(v_{,y} + \tfrac{1}{2} w_{,y}^2 - \frac{w}{R}\right) - F_{Rb} w_{,yy} \\ N_{xy} &= N_{yx} = K_G\left(u_{,y} + v_{,x} + w_{,x} w_{,y}\right) \\ M_x &= F_{Sb}\left(u_{,x} + \tfrac{1}{2} w_{,x}^2\right) - D_{MS} w_{,xx} - D_\nu w_{,yy} \\ M_y &= F_{Rb}\left(v_{,y} + \tfrac{1}{2} w_{,y}^2 - \frac{w}{R}\right) - D_\nu w_{,xx} - D_{MR} w_{,yy} \end{aligned}\right\} \qquad \text{(I-19)}$$

$$\left.\begin{aligned} M_{xy} &= D_{HGS}\, w_{,xy} \\ M_{yx} &= -D_{HGR}\, w_{,xy} \end{aligned}\right\} \qquad \text{(I-19)}$$

4. The Dynamic Equilibrium Equations.

Let us formulate the dynamic equilibrium equations on the basis of the smeared-out eccentrically reinforced shell element of the middle surface. Figure (I-4) below illustrates such an element.

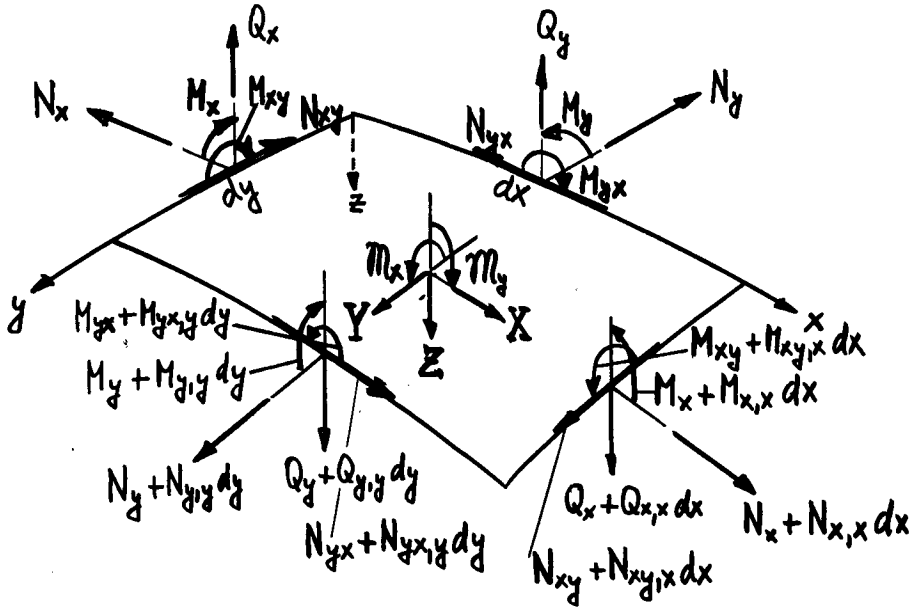

Figure (I-4): Composite Stress Resultants and Moments of the Smeared-out Stiffened Middle Surface Shell Element.

In addition to the composite stress resultants and moments, the components X, Y, and Z of the surface force must be included. The latter consist of possible traction acting in the middle surface, pressure normal to the surface, and d'Alembert forces per unit area due to displacement accele-

rations. For force equilibrium in the z-direction, components due to the change in direction of the tangential forces are taken into account, since the deflected element must be considered for stability analysis.

Force equilibrium in the three coordinate directions can be written as:

$$\left.\begin{aligned} N_{x,x} + N_{yx,y} + X &= 0 \\ N_{y,y} + N_{xy,x} + Y &= 0 \\ N_x w_{,xx} + 2N_{xy} w_{,xy} + N_y w_{,yy} + \frac{N_y}{R} & \\ + (N_{x,x} + N_{yx,y}) w_{,x} + (N_{y,y} + N_{xy,x}) w_{,y} & \\ + Q_{x,x} + Q_{y,y} + Z &= 0 \end{aligned}\right\} \qquad \text{(I-20)}$$

Dynamic moment equilibrium equations are formulated about the x- and y-axes, while moment equilibrium about the z-axis is identically satisfied. In order to account for d'Alembert, or other surface moments, let us introduce m_x as the composite moment per unit area about the x-axis, measured positive in the increasing direction of $w_{,y}$. Similarly, m_y is the composite moment per unit area about the y-axis, taken positive in the increasing direction of $w_{,x}$. The two remaining moment equilibrium equations then become:

$$\left.\begin{aligned} M_{y,y} - M_{xy,x} - Q_y - m_x &= 0 \\ M_{x,x} + M_{yx,y} - Q_x - m_y &= 0 \end{aligned}\right\} \qquad \text{(I-21)}$$

Differentiating the first equation partially with respect to y, the second with respect to x, and introducing the result into equations(I-20), eliminates the shear forces. Thus, there remains:

$$\left.\begin{aligned} N_{x,x} + N_{yx,y} + X &= 0 \\ N_{y,y} + N_{xy,x} + Y &= 0 \\ N_x w_{,xx} + 2N_{xy} w_{,xy} + \frac{N_y}{R} + (N_{x,x} + N_{yx,y}) w_{,x} & \\ + (N_{y,y} + N_{xy,x}) w_{,y} + M_{x,xx} + M_{yx,xy} & \\ + M_{y,yy} - M_{xy,xy} - m_{y,x} - m_{x,y} + Z &= 0 \end{aligned}\right\} \quad \text{(I-22)}$$

5. Consideration of Inertia Terms and External Pressure.

Assuming no midsurface tractions, X and Y are just the d'Alembert forces per unit area. In addition to the external lateral pressure p, Z also includes the d'Alembert force per unit area. In order to calculate the latter, we need the smeared-out mass per unit area of the composite shell, which can be stated as:

$$\bar{m} = \rho h + \rho_s \frac{A_s}{d} + \rho_R \frac{A_R}{\ell} \qquad \text{(I-23)}$$

where $\bar{m}$ is the smeared-out mass per unit area and the ρ's refer to the mass densities of the monocoque shell, stringer and ring.

X, Y, and Z can now be written as:

$$\left.\begin{aligned} X &= -\bar{m}\, u_{,tt} \\ Y &= -\bar{m}\, v_{,tt} \\ Z &= p - \bar{m}\, w_{,tt} \end{aligned}\right\} \qquad \text{(I-24)}$$

Let us assume that no traction forces are acting on the inner and outer composite lateral shell surface. $\mathcal{M}_x$ and $\mathcal{M}_y$ involve then only the d'Alembert moments taken about the x- and y-axes. In calculating the composite mass moments of inertia, we assume again that the contribution of the stiffeners can be smeared-out over their spacing distance. $\mathcal{M}_x$ and $\mathcal{M}_y$ then become:

$$\mathcal{M}_x = -\left(\rho\frac{h^3}{12} + \frac{\rho_R I_{R0}}{\ell} + \frac{\rho_S I_{S0}}{d}\right) w_{,ytt}$$

$$\mathcal{M}_y = -\left(\rho\frac{h^3}{12} + \frac{\rho_S I_{S0}}{d} + \frac{\rho_R I_{R0}}{\ell}\right) w_{,xtt}$$

Introducing the centroidal area moments of inertia, these expressions are modified to:

$$\left.\begin{aligned} \mathcal{M}_x &= -\left(\rho\frac{h^3}{12} + \rho_R\frac{I_{RC} + A_R\bar{z}_R^2}{\ell} + \rho_S\frac{I_{SC} + A_S\bar{z}_S^2}{d}\right) w_{,ytt} \\ \mathcal{M}_y &= -\left(\rho\frac{h^3}{12} + \rho_S\frac{I_{SC} + A_S\bar{z}_S^2}{d} + \rho_R\frac{I_{RC} + A_R\bar{z}_R^2}{\ell}\right) w_{,xtt} \end{aligned}\right\} \qquad \text{(I-25)}$$

Defining a composite mass moment of inertia per unit length,

$$I_{\bar{m}} = \rho\frac{h^3}{12} + \rho_S\frac{I_{SC} + A_S\bar{z}_S^2}{d} + \rho_R\frac{I_{RC} + A_R\bar{z}_R^2}{\ell} \qquad \text{(I-26)}$$

the above equations can be written as:

$$\left.\begin{aligned} m_x &= -I_{\bar{m}} w_{,ytt} \\ m_y &= -I_{\bar{m}} w_{,xtt} \end{aligned}\right\} \qquad \text{(I-27)}$$

In the sequel, the tangential inertia forces will be neglected. This is common practice in shell dynamics. In essence, such a simplification amounts to assuming that a disturbance propagates with infinite velocity in the axial and circumferential directions. The axial and circumferential directions are much "stiffer" elastically than the lateral direction so that its natural frequencies are much higher than those corresponding to the lateral direction. Thus, the problem of wave propagation in the eccentrically reinforced cylindrical shell will not be considered. It is therefore assumed that,

$$\chi \approx \gamma \approx 0 \qquad \text{(I-28)}$$

CHAPTER II : DERIVATION OF THE FIELD EQUATIONS.

1. The Dynamic Equilibrium Equations for Negligible Tangential Inertia.

For vanishing X and Y, the first two equations of (I-22) eliminate the two terms in parentheses of the third expression of (I-22). Utilizing the third equation of (I-24), and (I-27), the dynamic equilibrium equations can be written as:

$$\left.\begin{aligned} N_{x,x} + N_{yx,y} &= 0 \\ N_{y,y} + N_{xy,x} &= 0 \\ N_x w_{,xx} + 2N_{xy} w_{,xy} + N_y w_{,yy} + \frac{N_z}{R} & \\ + M_{x,xx} + M_{yx,xy} + M_{y,yy} - M_{xy,xy} + p &= \bar{m} w_{,tt} \\ & - I_{\bar{m}}(w_{,xxtt} + w_{,yytt}) \end{aligned}\right\} \quad \text{(II-1)}$$

2. The Use of a Stress Function.

Let us introduce a stress function f(x,y,t), defined such that the first two equations of (II-1) are identically satisfied, e.g.

$$\left.\begin{aligned} N_x &= f_{,yy} \\ N_y &= f_{,xx} \\ N_{xy} &= -f_{,xy} \end{aligned}\right\} \quad \text{(II-2)}$$

On using equations (II-2) and (I-19), the remaining equilibrium equation can be manipulated into the form,

$$-\left(D_{HS}\, w_{,xxxx} + 2D_2\, w_{,xxyy} + D_{HR}\, w_{,yyyy}\right) + f_{,yy}\, w_{,xx} - 2f_{,xy}\, w_{,xy} + f_{,xx}\, w_{,yy} + \frac{f_{,xx}}{R} + F_{Sb}\left(u_{,xxx} + w_{,xx}^2 + w_{,x}\, w_{,xxx}\right) + F_{Rb}\left(v_{,yyy} + w_{,yy}^2 + w_{,y}\, w_{,yyy} - \frac{w_{,yy}}{R}\right) + p = \bar{m}\, w_{,tt} - I_{\bar{m}}\left(w_{,xxtt} + w_{,yytt}\right) \qquad \text{(II-3)}$$

where the additional flexural rigidity parameter D_2 is defined by:

$$D_2 = D_1 + \tfrac{1}{2}\left(D_{HGR} + D_{HGS}\right) \qquad \text{(II-4)}$$

The tangential terms containing u and v in equation (II-3) can be eliminated with the help of the first two equations of (I-19), where the N's are expressed by the stress function. After some algebra, there results,

$$\left.\begin{aligned} u_{,x} &= -A_{13}\, f_{,xx} + A_{22}\, f_{,yy} + S_{14}\, w_{,xx} - S_{22}\, w_{,yy} - \tfrac{1}{2} w_{,x}^2 \\ v_{,y} &= A_{11}\, f_{,xx} - A_{13}\, f_{,yy} - S_{11}\, w_{,xx} + S_{13}\, w_{,yy} - \tfrac{1}{2} w_{,y}^2 + \frac{w}{R} \end{aligned}\right\} \qquad \text{(II-5)}$$

where the following parameters have been used:

$$\left.\begin{aligned} A_{11} &= \frac{K_{HS}}{K_{HS}K_{HR} - K_V^2} & S_{11} &= F_{Sb}\, A_{13} \\ A_{13} &= \frac{K_V}{K_{HS}K_{HR} - K_V^2} & S_{13} &= F_{Rb}\, A_{11} \\ A_{22} &= \frac{K_{HR}}{K_{HS}K_{HR} - K_V^2} & S_{14} &= F_{Sb}\, A_{22} \\ & & S_{22} &= F_{Rb}\, A_{13} \end{aligned}\right\} \qquad \text{(II-6)}$$

The middle surface strains can be expressed in terms of the stress function by using equations (II-5) and the third of (I-19). This leads to:

$$\left.\begin{aligned} \varepsilon_x &= -A_{13} f_{1xx} + A_{22} f_{1yy} + S_{14} w_{1xx} - S_{22} w_{1yy} \\ \varepsilon_y &= A_{11} f_{1xx} - A_{13} f_{1yy} - S_{11} w_{1xx} + S_{13} w_{1yy} \\ \gamma_{xy} &= -\frac{1}{K_G} f_{1xy} \end{aligned}\right\} \quad \text{(II-7)}$$

The effect of the stiffener eccentricities is represented by the S parameters in the above expressions. Differentiating equations (II-5) appropriately and introducing the result into the remaining equilibrium equation (II-3), yields:

$$\left.\begin{aligned} &-\left[(D_{HS} - F_{Sb} S_{14}) w_{1xxxx} + 2\left(D_2 + \tfrac{1}{2}(F_{Sb} S_{22} + F_{Rb} S_{11})\right) w_{1xxyy}\right. \\ &\left. + (D_{HR} - F_{Rb} S_{13}) w_{1yyyy}\right] - S_{11} f_{1xxxx} + (S_{13} + S_{14}) f_{1xxyy} \\ &- S_{22} f_{1yyyy} + f_{1xx} w_{1yy} - 2 f_{1xy} w_{1xy} + f_{1yy} w_{1xx} \\ &+ \frac{f_{1xx}}{R} + p = \bar{m} w_{1tt} - I_{\bar{m}} (w_{1xxtt} + w_{1yytt}) \end{aligned}\right\} \quad \text{(II-8)}$$

Let us define the following additional parameters:

$$\left.\begin{aligned} D_{11} &= D_{HS} - F_{Sb} S_{14} \\ D_{12} &= D_2 + \tfrac{1}{2}(F_{Sb} S_{22} + F_{Rb} S_{11}) \\ D_{22} &= D_{HR} - F_{Rb} S_{13} \\ S_{12} &= \tfrac{1}{2}(S_{13} + S_{14}) \end{aligned}\right\} \quad \text{(II-9)}$$

The dynamic equilibrium equation of the eccentrically reinforced shell therefore becomes:

$$\left.\begin{aligned} & D_{11} w_{,xxxx} + 2 D_{12} w_{,xxyy} + D_{22} w_{,yyyy} \\ & + S_{11} f_{,xxxx} - 2 S_{12} f_{,xxyy} + S_{22} f_{,yyyy} \\ & - f_{,xx} w_{,yy} + 2 f_{,xy} w_{,xy} - f_{,yy} w_{,xx} \\ & - \frac{f_{,xx}}{R} - p + \bar{m} w_{,tt} - I_{\bar{m}} (w_{,xxtt} + w_{,yytt}) = 0 \end{aligned}\right\} \qquad \text{(II-10)}$$

3. Alternative Derivation of the Dynamic Equilibrium Equation from Hamilton's Principle.

The purpose of this alternative derivation is twofold: First, it offers a check on the previously derived equation; second, it will yield the boundary conditions as a byproduct.

Hamilton's principle can be stated in the form,

$$\delta \int_{t_1}^{t_2} (T - U + W)\, dt = 0 \qquad \text{(II-11)}$$

where T is the kinetic energy, U the strain energy, and W the external work.

The kinetic energy can be split-up into:

$$T = T^{(m)} + T^{(s)} + T^{(R)} \qquad \text{(II-12)}$$

where the superscripted quantities refer to the total kinetic energies of the monocoque shell, the stringers, and the rings. Each of these can be expressed by:

$$T^{(m)} = \frac{1}{2}\rho \int_0^L \int_0^{2\pi R} \int_{-\frac{h}{2}}^{\frac{h}{2}} (u_{T,t}^2 + v_{T,t}^2 + w_{,t}^2)\, dx\, dy\, dz \qquad \text{(II-13)}$$

where the subscript T again refers to the total quantity at any height z.

$$T^{(S)} = \frac{1}{2}\rho_S \sum_{i=1}^{n_S} \int_0^L \int_{A_S} (u_{Ti,t}^2 + v_{Ti,t}^2 + w_{i,t}^2)\, dA_S\, dx \qquad \text{(II-14)}$$

where $n_S = \frac{2\pi R}{d}$ is the number of stringers and i refers to the particular location. Similarly,

$$T^{(R)} = \frac{1}{2}\rho_R \sum_{i=1}^{n_R} \int_0^{2\pi R} \int_{A_R} (u_{Ti,t}^2 + v_{Ti,t}^2 + w_{i,t}^2)\, dA_R\, dy \qquad \text{(II-15)}$$

where $n_R = \frac{L}{\ell}$ is the number of rings.

The total tangential velocities are related to those of the middle surface by:

$$\left.\begin{aligned} u_{T,t} &= u_{,t} - z\, w_{,xt} \\ v_{T,t} &= v_{,t} - z\, w_{,yt} \end{aligned}\right\} \qquad \text{(II-16)}$$

In keeping with the assumption of negligible tangential inertia, we can neglect the middle surface velocity terms $u_{,t}$ and $v_{,t}$ in the further development. As in the previous derivation, the effects of stringers and rings are smeared-out over their respective spacings. This means that the summation is replaced by an integration. With these considerations, the kinetic energy terms can be written as:

$$T^{(m)} = \frac{1}{2}\rho \int_0^{L}\int_0^{2\pi R}\int_{-\frac{h}{2}}^{\frac{h}{2}} [z^2(w_{,xt}^2 + w_{,yt}^2) + w_{,t}^2]\, dx\, dy\, dz$$

$$= \frac{1}{2}\rho \int_0^{L}\int_0^{2\pi R} [\frac{h^3}{12}(w_{,xt}^2 + w_{,yt}^2) + h w_{,t}^2]\, dx\, dy \qquad \text{(II-17)}$$

$$T^{(s)} = \frac{1}{2}\rho_s \frac{1}{d}\int_0^{L}\int_0^{2\pi R}\left\{\int_{A_s} [\bar{z}^2(w_{,xt}^2 + w_{,yt}^2) + w_{,t}^2]\, dA_s\right\} dx\, dy$$

$$= \frac{1}{2}\rho_s \frac{1}{d}\int_0^{L}\int_0^{2\pi R} \{I_{so}(w_{,xt}^2 + w_{,yt}^2) + A_s w_{,t}^2\}\, dx\, dy$$

$$= \frac{1}{2}\rho_s \frac{1}{d}\int_0^{L}\int_0^{2\pi R} [(I_{sc} + \bar{z}_s^2 A_s)(w_{,xt}^2 + w_{,yt}^2) + A_s w_{,t}^2]\, dx\, dy \qquad \text{(II-18)}$$

and similarly,

$$T^{(R)} = \frac{1}{2}\rho_R \frac{1}{\ell}\int_0^{L}\int_0^{2\pi R} [(I_{Rc} + \bar{z}_R^2 A_R)(w_{,xt}^2 + w_{,yt}^2) + A_R w_{,t}^2]\, dx\, dy \qquad \text{(II-19)}$$

The total kinetic energy of equation (II-12) then becomes,

$$T = \frac{1}{2}\int_0^{L}\int_0^{2\pi R}\left\{\left[\rho h + \frac{\rho_s A_s}{d} + \frac{\rho_R A_R}{\ell}\right] w_{,t}^2 + \left[\rho\frac{h^3}{12} + \rho_s\frac{I_{sc} + \bar{z}_s^2 A_s}{d} + \rho_R\frac{I_{Rc} + \bar{z}_R^2 A_R}{\ell}\right](w_{,xt}^2 + w_{,yt}^2)\right\} dx\, dy$$

or, on utilizing expressions (I-23) and (I-26),

$$T = \frac{1}{2}\left\{\int_0^{L}\int_0^{2\pi R} [\bar{m} w_{,t}^2 + I_{\bar{m}}(w_{,xt}^2 + w_{,yt}^2)]\, dx\, dy\right\} \qquad \text{(II-20)}$$

The first variation of T can be written as,

$$\delta\int_{t_1}^{t_2} T\, dt = \int_{t_1}^{t_2}\int_0^{L}\int_0^{2\pi R} [\bar{m} w_{,t}\delta w_{,t} + I_{\bar{m}}(w_{,xt}\delta w_{,xt} + w_{,yt}\delta w_{,yt})]\, dx\, dy\, dt \qquad \text{(II-21)}$$

Integrating the first term by parts once, the second term twice, and omitting some algebra, the following expression results:

$$\delta\int_{t_1}^{t_2} T\,dt = \int_{t_1}^{t_2}\int_0^L\int_0^{2\pi R}\left[-\bar{m}\,w_{,tt} + I_{\bar{m}}\left(w_{,xxtt} + w_{,yytt}\right)\right]\delta w\,dx\,dy\,dt$$

$$+ \int_0^L\int_0^{2\pi R}\left[\bar{m}\,w_{,t}\,\delta w + I_{\bar{m}}\left(w_{,xt}\,\delta w_{,x} + w_{,yt}\,\delta w_{,y}\right)\right]\Big|_{t_1}^{t_2} dx\,dy$$

$$- \left\{\int_{t_1}^{t_2} I_{\bar{m}}\left[\int_0^{2\pi R}\left(w_{,xtt}\,\delta w\right)\Big|_0^L dy + \int_0^L\left(w_{,ytt}\,\delta w\right)\Big|_0^{2\pi R} dx\right] dt\right\}$$

In Hamilton's principle, it is inherently assumed that δw vanishes at t_1 and t_2, so that, as a consequence, $\delta w_{,x}$ and $\delta w_{,y}$ are also zero. The middle term of the above expression can thus be deleted and there remains:

$$\delta\int_{t_1}^{t_2} T\,dt = \int_{t_1}^{t_2}\left\{\int_0^L\int_0^{2\pi R}\left[-\bar{m}\,w_{,tt} + I_{\bar{m}}\left(w_{,xxtt} + w_{,yytt}\right)\right]\delta w\,dx\,dy\right.$$

$$\left. - \int_0^L\left[I_{\bar{m}}\,w_{,ytt}\,\delta w\right]\Big|_0^{2\pi R} dx - \int_0^{2\pi R}\left[I_{\bar{m}}\,w_{,xtt}\,\delta w\right]\Big|_0^L dy\right\} dt \qquad \text{(II-22)}$$

The variation of the second term in equation (II-11) can be written as:

$$-\delta\int_{t_1}^{t_2} U\,dt = \int_{t_1}^{t_2}\left\{\int_0^L\int_0^{2\pi R}\left[-N_x\,\delta\varepsilon_x - N_y\,\delta\varepsilon_y - N_{xy}\,\delta\gamma_{xy} + M_x\,\delta w_{,xx}\right.\right.$$

$$\left.\left. + M_y\,\delta w_{,yy} - M_{xy}\,\delta w_{,xy} + M_{yx}\,\delta w_{,xy}\right] dx\,dy\right\} dt$$

(II-23)

The stress resultants are replaced by the stress function relations (II-2). On using equations (I-14), (II-6), (II-7), and (II-9), the moments can be expressed by:

$$\left.\begin{aligned} M_x &= -S_{11} f_{,xx} + S_{14} f_{,yy} - D_{11} w_{,xx} - (D_\nu + F_{56} S_{22}) w_{,yy} \\ M_y &= S_{13} f_{,xx} - S_{22} f_{,yy} - (D_\nu + F_{R6} S_{11}) w_{,xx} - D_{22} w_{,yy} \\ M_{xy} &= D_{HGS} w_{,xy} \\ M_{yx} &= -D_{HGR} w_{,xy} \end{aligned}\right\} \qquad \text{(II-24)}$$

The variations of the strains are obtained from (I-17) as:

$$\left.\begin{aligned} \delta\varepsilon_x &= \delta u_{,x} + w_{,x}\,\delta w_{,x} \\ \delta\varepsilon_y &= \delta v_{,y} + w_{,y}\,\delta w_{,y} - \frac{\delta w}{R} \\ \delta\gamma_{xy} &= \delta u_{,y} + \delta v_{,x} + w_{,x}\,\delta w_{,y} + w_{,y}\,\delta w_{,x} \end{aligned}\right\} \qquad \text{(II-25)}$$

After substituting for the moments and strain variations, and after considerable algebra, the first variation of the strain energy finally becomes:

$$-\delta\int_{t_1}^{t_2} U\,dt = \int_{t_1}^{t_2}\Bigg\{\int_0^L\int_0^{2\pi R}\Big[-D_{11} w_{,xxxx} - 2D_{12} w_{,xxyy} - D_{22} w_{,yyyy} - S_{11} f_{,xxxx}$$

$$+ 2S_{12} f_{,xxyy} - S_{22} f_{,yyyy} + f_{,xx} w_{,yy} - 2f_{,xy} w_{,xy} + f_{,yy} w_{,xx} + \frac{f_{,xx}}{R}\Big]\delta w\,dx\,dy$$

$$+ \int_0^L \Big[f_{,xy}\,\delta u - f_{,xx}\,\delta v + (f_{,xy} w_{,x} - f_{,xx} w_{,y} + S_{22} f_{,yyy} - S_{13} f_{,xxy} + (D_\nu + F_{R6} S_{11}) w_{,xxy}$$

$$+ D_{22} w_{,yyy})\,\delta w - \frac{(D_{HGS} + D_{HGR})}{2\pi R} w_{,xy}\,\delta w_{,x} + (S_{13} f_{,xx} - S_{22} f_{,yy} - (D_\nu + F_{R6} S_{11}) w_{,xx}$$

$$- D_{22} w_{,yy})\,\delta w_{,y}\Big]\Big|_0\,dx$$

(continued next page)

$$+\int_0^{2\pi R}\Big[-f_{,yy}\,\delta u + f_{,xy}\,\delta v + (f_{,xy}\,w_{,y} - f_{,yy}\,w_{,x} + S_{11}f_{,xxx} - S_{14}f_{,xyy} + (D_\nu + F_{Sb}\,S_{22})\,w_{,xyy} + D_{11}\,w_{,xxx} + (D_{nGS} + D_{nGR})\,w_{,xyy})\,\delta w + (-S_{11}f_{,xx} + S_{14}f_{,yy} - (D_\nu + F_{Sb}S_{22})\,w_{,yy} - D_{11}\,w_{,xx})\,\delta w_{,x}\Big]_0^L dy\Big\}\,dt \tag{II-26}$$

In order to evaluate the first variation of the external work, we must assume a specific loading case. Let us take an eccentrically reinforced shell which is compressed axially by an applied compressive load per unit length, N_{xA}. It is assumed that N_{xA} is introduced at distance ζ from the middle surface. In addition, the external pressure p is acting on the lateral surface.

The work of the external forces then becomes:

$$W = -\int_0^{2\pi R}\Big[N_{xA}\,u_T\big|_{z=\zeta}\Big]_0^L dy + \int_0^L\int_0^{2\pi R} p\,w\,dx\,dy \tag{II-27}$$

Following (II-11), the first variation of W becomes:

$$\delta\int_{t_1}^{t_2} W\,dt = \int_{t_1}^{t_2}\Big\{-\int_0^{2\pi R}\Big[N_{xA}\,\delta(u-\zeta w_{,x})\Big]_0^L dy + \int_0^L\int_0^{2\pi R} p\,\delta w\,dx\,dy\Big\}\,dt$$

$$= \int_{t_1}^{t_2}\Big\{\int_0^L\int_0^{2\pi R} p\,\delta w\,dx\,dy - \int_0^{2\pi R}\Big[N_{xA}\,\delta u - N_{xA}\,\zeta\,\delta w_{,x}\Big]_0^L dy\Big\}\,dt \tag{II-28}$$

By combining (II-26), (II-28), and (II-22), we finally get:

$$\delta\int_{t_1}^{t_2}(T-U+W)dt=\int_{t_1}^{t_2}\Big\{\iint_{0\,0}^{L\;2\pi R}\Big[-D_{11}w_{,xxxx}-2D_{12}w_{,xxyy}-D_{22}w_{,yyyy}$$

$$-S_{11}f_{,xxxx}+2S_{12}f_{,xxyy}-S_{22}f_{,yyyy}+f_{,xx}w_{,yy}-2f_{,xy}w_{,xy}$$

$$+f_{,yy}w_{,xx}+\frac{f_{,xx}}{R}+p-\bar{m}w_{,tt}+I_{\bar{m}}(w_{,xxtt}+w_{,yytt})\Big]\delta w\,dx\,dy$$

$$+\int_0^L\Big[f_{,xy}\,\delta u-f_{,xx}\,\delta v+(f_{,xy}w_{,x}-f_{,xx}w_{,y}+S_{22}f_{,yyy}-S_{13}f_{,xxy}$$

$$+(D_{\nu}+F_{Rb}S_{11})w_{,xxy}+D_{22}w_{,yyy}-I_{\bar{m}}w_{,ytt})\,\delta w-(D_{nGS}+D_{nGR})w_{,xy}\,\delta w_{,x}$$

$$+(S_{13}f_{,xx}-S_{22}f_{,yy}-(D_{\nu}+F_{Rb}S_{11})w_{,xx}-D_{22}w_{,yy})\,\delta w_{,y}\Big]\Big|_0^{2\pi R}dx$$

$$+\int_0^{2\pi R}\Big[(-f_{,yy}-N_{xA})\,\delta u+f_{,xy}\,\delta v+(f_{,xy}w_{,y}-f_{,yy}w_{,x}+S_{11}f_{,xxx}$$

$$-S_{14}f_{,xyy}+(D_{\nu}+F_{Sb}S_{22})w_{,xyy}+D_{11}w_{,xxx}+(D_{nGS}+D_{nGR})w_{,xyy}$$

$$-I_{\bar{m}}w_{,xtt})\,\delta w+(-S_{11}f_{,xx}+S_{14}f_{,yy}-(D_{\nu}+F_{Sb}S_{22})w_{,yy}$$

$$-D_{11}w_{,xx}+N_{xA}f)\,\delta w_{,x}\Big]\Big|_0^{L}dy\Big\}\,dt=0 \qquad \text{(II-29)}$$

The above equation consists of three distinct parts: the first part contains a double integral with respect to x and y; the second part is characterized by an integral with respect to x; the third part features an integral with respect to y.

The integrand of the second part must be evaluated at the limits, y=0 and y=2πR. The geometric constraints (closure conditions) of the cylindrical shell require however that

u; v; w; $w_{,x}$; and $w_{,y}$ must assume identical values at y=0 and y=2πR. The same applies to their first variations. Consequently, the integrand reduces to zero if the closure conditions are satisfied.

The integrand of the third part has to be evaluated at x=0 and x=L (boundary conditions). Since the ends of the cylindrical shell can be mounted physically in various manners, the first variations of u; v; w; and $w_{,x}$, or their multiplying coefficients in parentheses, must assume specific values at x=0 and x=L. Selecting these values such that each term, when evaluated at x=0 and x=L, vanishes, leads to the following possible choices of boundary conditions:

$$
\left.
\begin{array}{llll}
f_{1yy} + N_{xA} = 0 & \text{or } u = 0 & \text{at} & x = 0; L \\
f_{1yy} = 0 & \text{or } v = 0 & \text{at} & x = 0; L \\
f_{1xy} w_{,y} - f_{1yy} w_{,x} + S_{11} f_{1xx} & & & \\
-S_{14} f_{1xyy} + (D_\nu + F_{Sb} S_{22}) w_{,xyy} & & & \\
+(D_{MGS} + D_{MGR}) w_{,xyy} - I_m w_{,xtt} = 0 & \text{or } w = 0 & \text{at} & x = 0; L \\
-S_{11} f_{1xx} + S_{14} f_{1yy} & & & \\
-(D_\nu + F_{Sb} S_{22}) w_{,yy} & & & \\
-D_{11} w_{,xx} + N_{xA} \zeta = 0 & \text{or } w_{,x} = 0 & \text{at} & x = 0; L
\end{array}
\right\}
\qquad \text{(II-30)}
$$

In terms of the stress resultants (II-2) and moments (I-27), (II-24), these boundary conditions can be stated equivalently as:

$$
\left.
\begin{array}{llll}
N_x + N_{xA} = 0 & \text{or} \quad \dot{u} = 0 & \text{at} & x = 0; L \\
N_{xy} = 0 & \text{or} \quad v = 0 & \text{at} & x = 0; L \\
M_{x,x} - m_y - (M_{xy,y} - M_{yx,y}) & & & \\
+ N_x w_{,x} + N_{xy} w_{,y} = 0 & \text{or} \quad w = 0 & \text{at} & x = 0; L \\
M_x + N_{xA} \zeta = 0 & \text{or} \quad w_{,x} = 0 & \text{at} & x = 0; L
\end{array}
\right\} \quad \text{(II-31)}
$$

Corresponding to the physical situation, an appropriate selection of boundary conditions from those listed above will reduce the integrand of the second part of (II-29) to zero. Satisfying the closure and boundary conditions, leaves therefore the first part of (II-29) equated to zero. Since δw is arbitrary, the integrand must vanish. The latter reproduces the dynamic equilibrium equation (II-10) obtained earlier.

The static counterparts of the boundary conditions (II-31) are identical with those of reference [35], where the the static equivalent of equations (II-1) was derived on the basis of the variation of the total potential without the use of a stress function.

4. The Field Equations.

Since equation (II-10) involves the stress function and the radial displacement, we need another equation to solve the problem. This additional relation is provided by the compatibility equation (I-18), which is repeated below:

$$\varepsilon_{x,yy} + \varepsilon_{y,xx} - \gamma_{xy,xy} = w_{,xy}^2 - w_{,xx}\, w_{,yy} - \frac{w_{,xx}}{R} \qquad \text{(I-18)}$$

Differentiating the strain equations (II-7) and introducing the result into (I-18), yields:

$$A_{11} f_{,xxxx} + 2\left(\frac{1}{2K_6} - A_{13}\right) f_{,xxyy} + A_{22} f_{,yyyy} - S_{11} w_{,xxxx}$$
$$+ (S_{13} + S_{14}) w_{,xxyy} - S_{22} w_{,yyyy} = w_{,xy}^2 - w_{,xx} w_{,yy} - \frac{w_{,xx}}{R} \qquad \text{(II-32)}$$

Defining,

$$A_{12} = \frac{1}{2K_6} - A_{13} \qquad \text{(II-33)}$$

and using the last expression of (II-9), the above equation becomes:

$$A_{11} f_{,xxxx} + 2A_{12} f_{,xxyy} + A_{22} f_{,yyyy} - S_{11} w_{,xxxx} + 2S_{12} w_{,xxyy}$$
$$- S_{22} w_{,yyyy} - w_{,xy}^2 + w_{,xx} w_{,yy} + \frac{w_{,xx}}{R} = 0 \qquad \text{(II-34)}$$

This equation will be referred to as the compatibility equation for the eccentrically reinforced cylindrical shell.

With equations (II-10) and (II-34), we have therefore succeeded to arrive at a complete system of equations. These are listed together below and will be called the field equations of the eccentrically reinforced cylindrical shell:

$$\left.\begin{aligned} &D_{11} w_{,xxxx} + 2 D_{12} w_{,xxyy} + D_{22} w_{,yyyy} + S_{11} f_{,xxxx} \\ &-2 S_{12} f_{,xxyy} + S_{22} f_{,yyyy} - f_{,xx} w_{,yy} + 2 f_{,xy} w_{,xy} \\ &- f_{,yy} w_{,xx} - \frac{f_{,xx}}{R} - p + \bar{m} w_{,tt} - I_{\bar{m}} (w_{,xxtt} + w_{,yytt}) = 0 \\ &A_{11} f_{,xxxx} + 2 A_{12} f_{,xxyy} + A_{22} f_{,yyyy} - S_{11} w_{,xxxx} \\ &+ 2 S_{12} w_{,xxyy} - S_{22} w_{,yyyy} - w_{,xy}^2 + w_{,xx} w_{,yy} + \frac{w_{,xx}}{R} = 0 \end{aligned}\right\} \quad \text{(II-35)}$$

5. Special Case Reductions.

If the stiffeners are arranged symmetrically about the monocoque shell middle surface, we can speak of a quasi-orthotropic shell. Its strain-stress function relations are readily available from (II-7) by setting the eccentricity parameters S to zero. Similarly, the field equations for the quasi-orthotropic shell are obtained from (II-35) by dropping the terms containing the eccentricity parameters. The coefficients of the field equations will be denoted with a superscript (0) in this case.

The reduction to the monocoque shell is also straight forward. Table (II-1) below lists the coefficients of the field equations as they reduce from the eccentrically reinforced shell to the quasi-orthotropic, to the monocoque shell.

Eccentrically Reinforced Shell	D_{11}	D_{12}	D_{22}	S_{11}	S_{12}	S_{22}
	Defined by equations (II-9) and (II-6)					
Quasi-Orthotropic Shell	$D_{11}^{(o)}$	$D_{12}^{(o)}$	$D_{22}^{(o)}$			
	$D+\frac{E_s I_{sc}}{d}$	$D+\frac{1}{2}\left(\frac{G_s J_s}{d}+\frac{G_R J_R}{\ell}\right)$	$D+\frac{E_R I_{Rc}}{\ell}$	0	0	0
Monocoque Shell	D	D	D	0	0	0

Eccentrically Reinforced Shell	A_{11}	A_{12}	A_{22}	$\bar{m}$	$I_{\bar{m}}$
	Defined by eqs. (II-6),(II-33),(I-23),(I-26)				
Quasi-Orthotropic Shell	$A_{11}^{(o)}=A_{11}$	$A_{12}^{(o)}=A_{12}$	$A_{22}^{(o)}=A_{22}$	$\bar{m}^{(o)}=\bar{m}$	$I_{\bar{m}}^{(o)}$
					$\frac{\rho h^3}{12}+\rho_s\frac{I_{sc}}{d}+\rho_R\frac{I_{Rc}}{\ell}$
Monocoque Shell	$\frac{1}{Eh}$	$\frac{1}{Eh}$	$\frac{1}{Eh}$	ρh	$\frac{\rho h^3}{12}$

Table (II-1) : Coefficients of the Field Equations for the Quasi-Orthotropic and Monocoque Shell.

On using the "orthotropic" coefficients, the system of field equations for the quasi-orthotropic cylindrical shell is written as:

$$\left.\begin{aligned}
&D_{11}^{(0)} w_{,xxxx} + 2D_{12}^{(0)} w_{,xxyy} + D_{22}^{(0)} w_{,yyyy} - f_{,xx} w_{,yy} + 2f_{,xy} w_{,xy} \\
&+ f_{,yy} w_{,xx} - \frac{f_{,xx}}{R} - p + \bar{m} w_{,tt} - I_{\bar{m}}^{(0)} (w_{,xxtt} + w_{,yytt}) = 0 \\
&A_{11}^{(0)} f_{,xxxx} + 2A_{12}^{(0)} f_{,xxyy} + A_{22}^{(0)} f_{,yyyy} - w_{,xy}^2 + w_{,xx} w_{,yy} + \frac{w_{,xx}}{R} = 0
\end{aligned}\right\} \quad \text{(II-36)}$$

The above equations correspond essentially to those derived by Thielemann [11] for the true orthotropic cylindrical shell. His equations contain an initial imperfection displacement and were derived only for the static case.
The field equations for the monocoque cylindrical shell represent the last reduction and become with the appropriate coefficients from Table (II-1):

$$\left.\begin{aligned}
&D \nabla^4 w - f_{,xx} w_{,yy} + 2f_{,xy} w_{,xy} - f_{,yy} w_{,xx} - \frac{f_{,xx}}{R} \\
&- p + \rho h w_{,tt} - \frac{\rho h^3}{12} (w_{,xxtt} + w_{,yytt}) = 0 \\
&\frac{1}{Eh} \nabla^4 f - w_{,xy}^2 + w_{,xx} w_{,yy} + \frac{w_{,xx}}{R} = 0
\end{aligned}\right\} \quad \text{(II-37)}$$

The static counterparts of equations (II-37) are widely known in the literature; they may be found in Volmir's book [49]. On reducing equations (II-37) to the static case and letting $R \to \infty$, the well-known von Kármán-Marguerre large deflection plate equations are obtained.

CHAPTER III : THE FIELD EQUATIONS FOR INITIAL IMPERFECTIONS.

1. Modifications of the Strain-Displacement Relations, Stress Resultants and Moments due to Initial Imperfections.

An initial imperfection displacement in the radial direction will be considered. Let us call the latter $w_{(0)}$, while we denote by $w_{(1)}$ the total radial displacement so that the net radial deflection w is given by $w = w_{(1)} - w_{(0)}$. Unfortunately, this somewhat cumbersome notation is necessary in connection with the comma-differentiation symbolism.

The strain-displacement relations for initial imperfections are taken from Volmir[49], given for the plate, and become for the cylindrical shell:

$$\left.\begin{aligned} \varepsilon_x &= u_{,x} + \frac{1}{2}\left(w_{(1),x}^2 - w_{(0),x}^2\right) \\ \varepsilon_y &= v_{,y} + \frac{1}{2}\left(w_{(1),y}^2 - w_{(0),y}^2\right) - \frac{1}{R}\left(w_{(1)} - w_{(0)}\right) \\ \gamma_{xy} &= u_{,y} + v_{,x} + w_{(1),x}\, w_{(1),y} - w_{(0),x}\, w_{(0),y} \end{aligned}\right\} \qquad \text{(III-1)}$$

These relations reduce to those of (I-17) when the initial imperfection displacement is set to zero.

In analogy to equations (I-19), the stress resultants and moments can be written as:

$$N_x = K_{MS}\left[u_{,x} + \tfrac{1}{2}\left(w_{(0),x}^2 - w_{(0),x}^2\right)\right] + K_\nu\left[v_{,y} + \tfrac{1}{2}\left(w_{(0),y}^2 - w_{(0),y}^2\right) - \tfrac{1}{R}\left(w_{(0)} - w_{(0)}\right)\right]$$
$$- F_{Sb}\left[w_{(0),xx} - w_{(0),xx}\right]$$

$$N_y = K_\nu\left[u_{,x} + \tfrac{1}{2}\left(w_{(0),x}^2 - w_{(0),x}^2\right)\right] + K_{MR}\left[v_{,y} + \tfrac{1}{2}\left(w_{(0),y}^2 - w_{(0),y}^2\right) - \tfrac{1}{R}\left(w_{(0)} - w_{(0)}\right)\right]$$
$$- F_{Rb}\left[w_{(0),yy} - w_{(0),yy}\right]$$

$$N_{xy} = N_{yx} = K_6\left[u_{,y} + v_{,x} + w_{(0),x}\, w_{(0),y} - w_{(0),x}\, w_{(0),y}\right]$$

$$M_x = F_{Sb}\left[u_{,x} + \tfrac{1}{2}\left(w_{(0),x}^2 - w_{(0),x}^2\right)\right] - D_{MS}\left[w_{(0),xx} - w_{(0),xx}\right] - D_\nu\left[w_{(0),yy} - w_{(0),yy}\right]$$

$$M_y = F_{Rb}\left[v_{,y} + \tfrac{1}{2}\left(w_{(0),y}^2 - w_{(0),y}^2\right) - \tfrac{1}{R}\left(w_{(0)} - w_{(0)}\right)\right] - D_\nu\left[w_{(0),xx} - w_{(0),xx}\right]$$
$$- D_{MR}\left[w_{(0),yy} - w_{(0),yy}\right]$$

$$M_{xy} = D_{MGS}\left[w_{(0),xy} - w_{(0),xy}\right]$$

$$M_{yx} = -D_{MGR}\left[w_{(0),xy} - w_{(0),xy}\right]$$

(III-2)

2. Modifications of the Field Equations due to Initial Imperfections.

Neglecting tangential inertia forces, the dynamic equilibrium equations can be expressed by:

$$\left.\begin{aligned} N_{x,x} + N_{yx,y} &= 0 \\ N_{y,y} + N_{xy,x} &= 0 \\ N_x\, w_{(0),xx} + 2N_{xy}\, w_{(0),xy} + N_y\, w_{(0),yy} + \frac{N_y}{R} + M_{x,xx} & \\ + M_{yx,xy} + M_{y,yy} - M_{xy,xy} + p = \bar{m}\, w_{(0),tt} - I_{\bar{m}}\left(w_{(0),xxtt} + w_{(0),yytt}\right) & \end{aligned}\right\} \text{(III-3)}$$

where the so-called reduced loads involve the total displacement, and where $w_{(i)}$ has been used in the inertia terms. This is permissible since $w_{(o)}$ is constant with respect to time. The first two equations of (III-3) can again be identically satisfied by a stress function $\Phi(x,y,t)$, defined such that,

$$\left.\begin{aligned} N_x &= \Phi_{,yy} \\ N_y &= \Phi_{,xx} \\ N_{xy} &= -\Phi_{,xy} \end{aligned}\right\} \qquad \text{(III-4)}$$

where Φ has been used as the stress function symbol for the case of initial imperfections in contrast to f of equations (II-2).

The remaining dynamic equilibrium equation from (III-3) can be stated as:

$$\begin{aligned} &-\left[D_{HS}\left(w_{(i),xxxx} - w_{(o),xxxx}\right) + 2D_2\left(w_{(i),xxyy} - w_{(o),xxyy}\right)\right. \\ &\left. + D_{HR}\left(w_{(i),yyyy} - w_{(o),yyyy}\right)\right] + \Phi_{,yy}\, w_{(i),xx} - 2\Phi_{,xy}\, w_{(i),xy} \\ &+ \Phi_{,xx}\, w_{(i),yy} + \frac{\Phi_{,xx}}{R} + F_{Sb}\left(u_{,xxx} + w_{(i),xx}^2 - w_{(o),xx}^2 + w_{(i),x}\, w_{(i),xxx}\right. \\ &\left. - w_{(o),x}\, w_{(o),xxx}\right) + F_{Rb}\left(v_{,yyy} + w_{(i),yy}^2 - w_{(o),yy}^2 + w_{(i),y}\, w_{(i),yyy}\right. \\ &\left. - w_{(o),y}\, w_{(o),yyy} - \frac{1}{R}\left(w_{(i),yy} - w_{(o),yy}\right) + p = \bar{m}\, w_{(i),tt} - I_{\bar{m}}\left(w_{(i),xxtt} + w_{(i),yytt}\right)\right. \end{aligned} \qquad \text{(III-5)}$$

We can again eliminate the tangential displacement terms. Solving the first two equations of (III-2) for $u_{,x}$ and $v_{,y}$, yields:

$$
\left.
\begin{aligned}
u_{1,x} &= -A_{13}\Phi_{1,xx} + A_{22}\Phi_{1,yy} + S_{14}\left(w_{(1),1,xx} - w_{(0),1,xx}\right) \\
&\quad - S_{22}\left(w_{(1),1,yy} - w_{(0),1,yy}\right) - \tfrac{1}{2}\left(w_{(1),1,x}^{2} - w_{(0),1,x}^{2}\right) \\
v_{1,y} &= A_{11}\Phi_{1,xx} - A_{13}\Phi_{1,yy} - S_{11}\left(w_{(1),1,xx} - w_{(0),1,xx}\right) \\
&\quad + S_{13}\left(w_{(1),1,yy} - w_{(0),1,yy}\right) - \tfrac{1}{2}\left(w_{(1),1,y}^{2} - w_{(0),1,y}^{2}\right) + \tfrac{1}{R}\left(w_{(1)} - w_{(0)}\right)
\end{aligned}
\right\} \quad \text{(III-6)}
$$

Differentiating these expressions appropriately and introducing the result into equation (III-5), yields the dynamic equilibrium equation:

$$
\left.
\begin{aligned}
&D_{11}\left[w_{(1),1,xxxx} - w_{(0),1,xxxx}\right] + 2D_{12}\left[w_{(1),1,xxyy} - w_{(0),1,xxyy}\right] \\
&+D_{22}\left[w_{(1),1,yyyy} - w_{(0),1,yyyy}\right] + S_{11}\Phi_{1,xxxx} - 2S_{12}\Phi_{1,xxyy} \\
&+S_{22}\Phi_{1,yyyy} - \Phi_{1,xx}w_{(1),1,yy} + 2\Phi_{1,xy}w_{(1),1,xy} - \Phi_{1,yy}w_{(1),1,xx} \\
&-\frac{\Phi_{1,xx}}{R} - p + \bar{m}w_{(1),1,tt} - I_{\bar{m}}\left[w_{(1),1,xxtt} + w_{(1),1,yytt}\right] = 0
\end{aligned}
\right\} \quad \text{(III-7)}
$$

The reduction to the case of zero initial imperfections transforms equation (III-7) readily back to the first of expressions (II-35).

The strain compatibility equation with initial imperfections is taken from Volmir [49], for the plate, and is modified for the cylindrical shell to become:

$$
\left.
\begin{aligned}
\varepsilon_{x,1,yy} + \varepsilon_{y,1,xx} - \gamma_{xy,1,xy} &= w_{(1),1,xy}^{2} - w_{(1),1,xx}w_{(1),1,yy} - w_{(0),1,xy}^{2} \\
&\quad + w_{(0),1,xx}w_{(0),1,yy} - \tfrac{1}{R}\left(w_{(1),1,xx} - w_{(0),1,xx}\right)
\end{aligned}
\right\} \quad \text{(III-8)}
$$

The strains can be expressed from equations (III-6) and (III-1) as follows:

$$\varepsilon_x = -A_{13}\Phi_{,xx} + A_{22}\Phi_{,yy} + S_{14}(w_{(1),xx} - w_{(0),xx}) - S_{22}(w_{(1),yy} - w_{(0),yy})$$

$$\varepsilon_y = A_{11}\Phi_{,xx} - A_{13}\Phi_{,yy} - S_{11}(w_{(1),xx} - w_{(0),xx}) + S_{13}(w_{(1),yy} - w_{(0),yy})$$

$$\gamma_{xy} = -\frac{1}{K_6}\Phi_{,xy}$$

(III-9)

Differentiating these strains appropriately and introducing the result into equation (III-8), leads to the displacement compatibility as the second of the field equations. The modified field equations for the case of initial imperfections thus follow as:

$$\left.\begin{aligned}
&D_{11}[w_{(1),xxxx} - w_{(0),xxxx}] + 2D_{12}[w_{(1),xxyy} - w_{(0),xxyy}] \\
&+ D_{22}[w_{(1),yyyy} - w_{(0),yyyy}] + S_{11}\Phi_{,xxxx} - 2S_{12}\Phi_{,xxyy} \\
&+ S_{22}\Phi_{,yyyy} - \Phi_{,xx}w_{(1),yy} + 2\Phi_{,xy}w_{(1),xy} - \Phi_{,yy}w_{(1),xx} \\
&- \frac{\Phi_{,xx}}{R} - p + \bar{m}w_{(1),tt} - I_{\bar{m}}[w_{(1),xxtt} + w_{(1),yytt}] = 0
\end{aligned}\right\}$$

$$\left.\begin{aligned}
&A_{11}\Phi_{,xxxx} + 2A_{12}\Phi_{,xxyy} + A_{22}\Phi_{,yyyy} \\
&- S_{11}[w_{(1),xxxx} - w_{(0),xxxx}] + 2S_{12}[w_{(1),xxyy} - w_{(0),xxyy}] \\
&- S_{22}[w_{(1),yyyy} - w_{(0),yyyy}] - w^2_{(1),xy} + w_{(1),xx}w_{(1),yy} \\
&+ w^2_{(0),xy} - w_{(0),xx}w_{(0),yy} + \frac{1}{R}[w_{(1),xx} - w_{(0),xx}] = 0
\end{aligned}\right\}$$

(III-10)

These field equations reduce readily to those of (II-35) when $w_{(0)}$ is set to zero. Using the coefficients of Table (II-1), the field equations for initial imperfections of the quasi-orthotropic and monocoque shell are deduced at once.

CHAPTER IV : DETERMINATION OF A STRESS FUNCTION FROM AN ASSUMED RADIAL DISPLACEMENT.

1. The Assumed Total and Initial Imperfection Displacements.

An exact closed-form solution to the system of fourth order nonlinear (second degree) partial differential equations (III-10) is not known. We shall therefore seek an approximate solution. One way of attempting a solution is to assume a total and an initial radial displacement. Both of these are then introduced into the compatibility equation of (III-10) which results in a fourth order partial differential equation for Φ . If we can find an integral to the latter, we have a suitable stress function which can be utilized in the process of satisfying the dynamic equilibrium equation of (III-10). This procedure will be given later.

In numerous static compression tests on monocoque cylindrical shells, the "diamond" buckling pattern was usually found in the postbuckling region. Occasionally, the "checker-board" pattern has also been observed. There seems to be a tendency of transition from the latter to the former. However, in most tests, there is no uniform distribution of a given pattern over the whole cylindrical surface, and only a number of "bands" conform to the pattern. A phenomenological theory of the dynamics of transition from local to postbuckling has been advanced by Evan-Iwanowski [54] .

For simplicity, let us assume a displacement pattern which is distributed over the entire shell surface. The initial and total radial displacements are assumed in the form,

$$\left.\begin{aligned} W_{(0)}(x,y) &= f_0 \sin\alpha x \sin\beta y + g_0 \sin^2\alpha x \sin^2\beta y \\ W_{(1)}(x,y,t) &= f_1(t)\sin\alpha x \sin\beta y + g_1(t)\sin^2\alpha x \sin^2\beta y \end{aligned}\right\} \qquad \text{(IV-1)}$$

where α and β are defined by,

$$\left.\begin{aligned} \alpha &= \frac{m\pi}{L} \\ \beta &= \frac{n}{R} \end{aligned}\right\} \qquad \text{(IV-2)}$$

The assumed form of (IV-1) implies that the imperfection displacement is in "spatial harmony" with the total displacement.

The radial displacement pattern (IV-1), and some of its variations, have been used extensively by Volmir [49]. The first term corresponds to the "checker board" pattern, while the second term describes the "diamond" shape. The time-dependent amplitudes $f_1(t)$ and $g_1(t)$ allow for a transition between the two patterns.

The shell literature is at times confusing when it comes to symmetry considerations. Let us therefore define the concepts that we shall use. We shall speak of two types of symmetries. The first refers to rotational symmetry about the cylinder axis, according to which a displacement is axisymmetric when it does not depend on y. The second refers

to symmetry with respect to the radial direction. Accordingly, the first term ("checker board" pattern) of (IV-1) is symmetric with respect to the radial direction, while the second term ("diamond" pattern) is asymmetric in this sense, since the deflection is only positive inward.

The radial displacement assumption (IV-1) has been utilized for simply-supported and clamped shells, although it satisfies neither boundary condition exactly. Volmir [49] claims that for shells, whose length is several times the mean radius, the influence of the end restraints becomes negligible.

Let us consider an eccentrically reinforced circular cylindrical shell which is terminated by stiff flanges on both ends. This case is often encountered in practical applications and corresponds to clamped boundary conditions. From the possible choice of boundary conditions for the radial displacement (II-31), modified for initial imperfections, we therefore select:

$$\begin{aligned} W_{(1)} - W_{(0)} &= 0 \quad \text{at} \quad x = 0; L \\ W_{(1),x} - W_{(0),x} &= 0 \quad \text{at} \quad x = 0; L \end{aligned} \qquad \text{(IV-3)}$$

The radial displacement assumption (IV-1) obviously satisfies the first boundary condition of (IV-3) at both ends exactly. For the second set of boundary conditions we calculate:

$$\left.\begin{aligned} W_{(1),x} - W_{(0),x} = \alpha \Big[& (f_1 - f_0)\cos\alpha x \sin\beta y + \tfrac{1}{2}(g_1 - g_0)\sin 2\alpha x \\ & - \tfrac{1}{2}(g_1 - g_0)\sin 2\alpha x \cos 2\beta y \Big] \end{aligned}\right\} \text{(IV-4)}$$

On account of the first term on the right hand side, the second part of the clamped boundary conditions is not satisfied. Taking however the average over the circumference at both ends, we obtain:

$$\frac{1}{2\pi R}\int_0^{2\pi R}\left[W_{(1),x}-W_{(0),x}\right]\Big|_{x=0;L}dy=\frac{1}{2\pi R}\alpha(f_1-f_0)\left[\cos\alpha x\right]\Big|_{x=0;L}\int_0^{2\pi R}\sin\beta y\,dy=0 \qquad \text{(IV-5)}$$

The second part of the clamped boundary conditions is therefore satisfied on the average.

2. <u>The Stress Function Differential Equation</u>.

The assumed radial displacement of the form (IV-1) is introduced into the compatibility equation of (III-10), which, after considerable algebra, results in:

$$\begin{aligned}
&A_{11}\Phi_{1,xxxx}+2A_{12}\Phi_{1,xxyy}+A_{22}\Phi_{1,yyyy}=\left\{(f_1-f_0)\left[\alpha^4S_{11}-2\alpha^2\beta^2S_{12}\right.\right.\\
&\left.\left.+\beta^4S_{22}+\frac{\alpha^2}{R}\right]-\alpha^2\beta^2(f_1g_1-f_0g_0)\right\}\sin\alpha x\sin\beta y\\
&+\tfrac{3}{2}\alpha^2\beta^2(f_1g_1-f_0g_0)\sin3\alpha x\sin\beta y+\tfrac{3}{2}\alpha^2\beta^2(f_1g_1-f_0g_0)\sin\alpha x\sin3\beta y\\
&+\left\{\tfrac{1}{2}\alpha^2\beta^2(f_1^2-f_0^2)+\tfrac{1}{2}\alpha^2\beta^2(g_1^2-g_0^2)-4\alpha^2\left(\alpha^2S_{11}+\tfrac{1}{4R}\right)(g_1-g_0)\right\}\cos2\alpha x\\
&+\left\{\tfrac{1}{2}\alpha^2\beta^2(f_1^2-f_0^2)+\tfrac{1}{2}\alpha^2\beta^2(g_1^2-g_0^2)-4\beta^4S_{22}(g_1-g_0)\right\}\cos2\beta y\\
&+\left\{4(g_1-g_0)\left[\alpha^4S_{11}-2\alpha^2\beta^2S_{12}+\beta^4S_{22}+\frac{\alpha^2}{4R}\right]-\alpha^2\beta^2(g_1^2-g_0^2)\right\}\cos2\alpha x\cos2\beta y\\
&-\tfrac{1}{2}\alpha^2\beta^2(g_1^2-g_0^2)\cos4\alpha x-\tfrac{1}{2}\alpha^2\beta^2(g_1^2-g_0^2)\cos4\beta y\\
&+\tfrac{1}{2}\alpha^2\beta^2(g_1^2-g_0^2)\cos4\alpha x\cos2\beta y+\tfrac{1}{2}\alpha^2\beta^2(g_1^2-g_0^2)\cos2\alpha x\cos4\beta y
\end{aligned} \qquad \text{(IV-6)}$$

Dividing the above equation by the leading coefficient, leads to the following expression,

$$\Phi_{,xxxx} + 2a_{12} + a_{22}\Phi_{,yyyy} = k_1 \sin\alpha x \sin\beta y + k_2 \sin 3\alpha x \sin\beta y + k_3 \sin\alpha x \sin 3\beta y + k_4 \cos 2\alpha x + k_5 \cos 2\beta y + k_6 \cos 2\alpha x \cos 2\beta y + k_7 \cos 4\alpha x + k_8 \cos 4\beta y + k_9 \cos 4\alpha x \cos 2\beta y + k_{10} \cos 2\alpha x \cos 4\beta y \tag{IV-7}$$

where the following abbreviations have been used.

$$a_{12} = \frac{A_{12}}{A_{11}}$$

$$a_{22} = \frac{A_{22}}{A_{11}}$$

$$k_1 = \frac{1}{A_{11}}\left\{(f_1 - f_0)\left[\alpha^4 S_{11} - 2\alpha^2\beta^2 S_{12} + \frac{\alpha^2}{R}\right] - \alpha^2\beta^2(f_1 g_1 - f_0 g_0)\right\}$$

$$k_2 = \frac{3\alpha^2\beta^2}{2A_{11}}(f_1 g_1 - f_0 g_0)$$

$$k_3 = \frac{3\alpha^2\beta^2}{2A_{11}}(f_1 g_1 - f_0 g_0) = k_2$$

$$k_4 = \frac{1}{A_{11}}\left\{\frac{1}{2}\alpha^2\beta^2(f_1^2 - f_0^2) + \frac{1}{2}\alpha^2\beta^2(g_1^2 - g_0^2) - 4\alpha^2\left(\alpha^2 S_{11} + \frac{1}{4R}\right)(g_1 - g_0)\right\}$$

$$k_5 = \frac{1}{A_{11}}\left\{\frac{1}{2}\alpha^2\beta^2(f_1^2 - f_0^2) + \frac{1}{2}\alpha^2\beta^2(g_1^2 - g_0^2) - 4\beta^4 S_{22}(g_1 - g_0)\right\}$$

$$k_6 = \frac{1}{A_{11}}\left\{4(g_1 - g_0)\left(\alpha^4 S_{11} - 2\alpha^2\beta^2 S_{12} + \beta^4 S_{22} + \frac{\alpha^2}{4R}\right) - \alpha^2\beta^2(g_1^2 - g_0^2)\right\}$$

$$k_7 = -\frac{\alpha^2\beta^2}{2A_{11}}(g_1^2 - g_0^2)$$

(IV-8)

$$k_8 = -\frac{\alpha^2\beta^2}{2A_{11}}\left(g_1^2 - g_0^2\right) = k_7$$

$$k_9 = \frac{\alpha^2\beta^2}{2A_{11}}\left(g_1^2 - g_0^2\right) = -k_7$$

$$k_{10} = \frac{\alpha^2\beta^2}{2A_{11}}\left(g_1^2 - g_0^2\right) = -k_7 \qquad \text{(IV-8)}$$

3. The Derivation of a Stress Function.

Due to the nature of the trigonometric terms on the right side of equation (IV-7), we can find an integral by assuming a stress function that is made-up of these same trigonometric terms. Φ is therefore written in the form,

$$\Phi(x,y,t) = \lambda_1 \sin\alpha x \sin\beta y + \lambda_2 \sin 3\alpha x \sin\beta y + \lambda_3 \sin\alpha x \sin 3\beta y$$
$$+ \lambda_4 \cos 2\alpha x + \lambda_5 \cos 2\beta y + \lambda_6 \cos 2\alpha x \cos 2\beta y + \lambda_7 \cos 4\alpha x$$
$$+ \lambda_8 \cos 4\beta y + \lambda_9 \cos 4\alpha x \cos 2\beta y + \lambda_{10} \cos 2\alpha x \cos 4\beta y$$
$$- \bar{N}_{0x}\frac{y^2}{2} - \bar{N}_{0y}\frac{x^2}{2} \qquad \text{(IV-9)}$$

where we have added the last two terms, following Volmir [49]. It is obvious that these two terms disappear in the differentiating process of (IV-7). Their physical meaning will be discussed shortly. The λ's above are determined by equating coefficients of equal trigonometric terms when (IV-9) is introduced into (IV-7). The somewhat tedious algebra is omitted here and only the result is given below:

$$\lambda_1 = \frac{(f_1-f_0)(\alpha^4 S_{11} - 2\alpha^2\beta^2 S_{12} + \beta^4 S_{22} + \frac{\alpha^2}{R}) - \alpha^2\beta^2(f_1 g_1 - f_0 g_0)}{\alpha^4 A_{11} + 2\alpha^2\beta^2 A_{12} + \beta^4 A_{22}}$$

$$\lambda_2 = \frac{\frac{3}{2}\alpha^2\beta^2 (f_1 g_1 - f_0 g_0)}{81\alpha^4 A_{11} + 18\alpha^2\beta^2 A_{12} + \beta^4 A_{22}}$$

$$\lambda_3 = \frac{\frac{3}{2}\alpha^2\beta^2 (f_1 g_1 - f_0 g_0)}{\alpha^4 A_{11} + 18\alpha^2\beta^2 A_{12} + 81\beta^4 A_{22}}$$

$$\lambda_4 = \frac{\alpha^2\beta^2(f_1^2 - f_0^2) + \alpha^2\beta^2(g_1^2 - g_0^2) - 8\alpha^2(\alpha^2 S_{11} + \frac{1}{4R})(g_1 - g_0)}{32\alpha^4 A_{11}}$$

$$\lambda_5 = \frac{\alpha^2\beta^2(f_1^2 - f_0^2) + \alpha^2\beta^2(g_1^2 - g_0^2) - 8\beta^4 S_{22}(g_1 - g_0)}{32\beta^4 A_{22}}$$

$$\lambda_6 = \frac{4(g_1 - g_0)(\alpha^4 S_{11} - 2\alpha^2\beta^2 + \beta^4 S_{22} + \frac{\alpha^2}{4R}) - \alpha^2\beta^2(g_1^2 - g_0^2)}{16(\alpha^4 A_{11} + 2\alpha^2\beta^2 A_{12} + \beta^4 A_{22})}$$

$$\lambda_7 = -\frac{\alpha^2\beta^2(g_1^2 - g_0^2)}{512\alpha^4 A_{11}}$$

$$\lambda_8 = -\frac{\alpha^2\beta^2(g_1^2 - g_0^2)}{512\beta^4 A_{22}}$$

$$\lambda_9 = \frac{\alpha^2\beta^2(g_1^2 - g_0^2)}{32(16\alpha^4 A_{11} + 8\alpha^2\beta^2 A_{12} + \beta^4 A_{22})}$$

$$\lambda_{10} = \frac{\alpha^2\beta^2(g_1^2 - g_0^2)}{32(\alpha^4 A_{11} + 8\alpha^2\beta^2 A_{12} + 16\beta^4 A_{22}}$$

(IV-10)

Let us investigate whether the so-found stress function satisfies the boundary conditions of our problem. From the possible boundary conditions listed in (II-30), we select the following pair,

$$\left.\begin{aligned} \Phi_{1yy} + N_{xA} &= 0 \qquad \text{at} \qquad x = 0;L \\ \Phi_{1xy} &= 0 \qquad \text{at} \qquad x = 0;L \end{aligned}\right\} \quad \text{(IV-11)}$$

where the stress function for initial imperfections, Φ , has replaced f in (II-30).

Evaluating Φ_{1yy} from (IV-9), yields:

$$\begin{aligned} \Phi_{1yy} = -\beta^2 \big[& \lambda_1 \sin\alpha x \sin\beta y + \lambda_2 \sin 3\alpha x \sin\beta y + 9\lambda_3 \sin\alpha x \sin 3\beta y \\ & + 4\lambda_5 \cos 2\beta y + 4\lambda_6 \cos 2\alpha x \cos 2\beta y + 16\lambda_8 \cos 4\beta y \\ & + 4\lambda_9 \cos 4\alpha x \cos 2\beta y + 16\lambda_{10} \cos 2\alpha x \cos 4\beta y + \frac{N_{0x}}{\beta^2} \big] \end{aligned} \quad \text{(IV-12)}$$

At both ends, this expression is written as:

$$\begin{aligned} \Phi_{1yy}\Big|_{x=0;L} = -\beta^2 \big[& 4\lambda_5 \cos 2\beta y + 4\lambda_6 \cos 2\alpha x \cos 2\beta y + 16\lambda_8 \cos 4\beta y \\ & + 4\lambda_9 \cos 4\alpha x \cos 2\beta y + 16\lambda_{10} \cos 2\alpha x \cos 4\beta y + \frac{\bar{N}_{0x}}{\beta^2} \big] \Big|_{x=0;L} \end{aligned} \quad \text{(IV-13)}$$

When the above expression is evaluated at x=0 and x=L, it still remains a function of y and cannot, therefore, be equal to a constant value, $-N_{xA}$, as the boundary condition requires. However, on taking the average value in the circumferential

direction, we obtain:

$$\frac{1}{2\pi R}\int_0^{2\pi R} \Phi_{,yy}\Big|_{x=0;L}\, dy = -\bar{N}_{ox} \qquad \text{(IV-14)}$$

Consequently, $\bar{N}_{ox}$ is the applied compressive load obtained from averaging $\Phi_{,yy}$ over the circumference. The first part of the boundary conditions (IV-11) is therefore satisfied on the average.

Calculating $\Phi_{,xy}$ from (IV-9), results in:

$$\Phi_{,xy} = \alpha\beta\left[\lambda_1 \cos\alpha x \cos\beta y + 3\lambda_2 \cos 3\alpha x \cos\beta y + 3\lambda_3 \cos\alpha x \cos 3\beta y + 4\lambda_6 \sin 2\alpha x \sin 2\beta y + 8\lambda_9 \sin 4\alpha x \sin 2\beta y + 8\lambda_{10} \sin 2\alpha x \sin 4\beta y\right] \qquad \text{(IV-15)}$$

At the ends, we have,

$$\Phi_{,xy}\Big|_{x=0;L} = \alpha\beta\left[\lambda_1 \cos\alpha x \cos\beta y + 3\lambda_2 \cos 3\alpha x \cos\beta y + 3\lambda_3 \cos\alpha x \cos 3\beta y\right]\Big|_{x=0;L} \qquad \text{(IV-16)}$$

which is obviously a function of y and nonvanishing.

By taking the circumferential average, however,

$$\frac{1}{2\pi R}\int_0^{2\pi R} \Phi_{,xy}\Big|_{x=0;L}\, dy = 0 \qquad \text{(IV-17)}$$

we can satisfy the second part of the boundary conditions (IV-11) on the average.

4. The Conditions of Closure.

Thus far, we have seen how the boundary conditions are satisfied by the assumed radial displacement (IV-1) and the derived stress function (IV-9).

In addition, the conditions of closure require that $w_{(1)} - w_{(0)}$; $w_{(1),x} - w_{(0),x}$; $w_{(1),y} - w_{(0),y}$; u; and v should assume the same values at y=0 and y=2πR.

Let us rewrite (IV-1) in a different form:

$$\left.\begin{aligned} w_{(0)}(x,y) &= f_0 \sin\alpha x \sin\beta y + \tfrac{1}{4} g_0 - \tfrac{1}{4} g_0 \cos 2\alpha x - \tfrac{1}{4} g_0 \cos 2\beta y \\ &\quad + \tfrac{1}{4} g_0 \cos 2\alpha x \cos 2\beta y \\ w_{(1)}(x,y,t) &= f_1 \sin\alpha x \sin\beta y + \tfrac{1}{4} g_1 - \tfrac{1}{4} g_1 \cos 2\alpha x - \tfrac{1}{4} g_1 \cos 2\beta y \\ &\quad + \tfrac{1}{4} g_1 \cos 2\alpha x \cos 2\beta y \end{aligned}\right\} \quad \text{(IV-18)}$$

The y-dependence of the above equation is trigonometric and was chosen such that the fundamental wavelength corresponds to the circumference. This characteristic is not changed in the differentiating process. Consequently, the conditions of closure for the radial displacement and its first partial derivatives with respect to x and y are therefore satisfied. We can write more formally:

$$\left.\begin{aligned} \int_0^{2\pi R} [w_{(1),y} - w_{(0),y}]\, dy &= 0 \\ \int_0^{2\pi R} [w_{(1),xy} - w_{(0),xy}]\, dy &= 0 \end{aligned}\right\} \quad \text{(IV-19)}$$

$$\int_0^{2\pi R} [W_{(1),yy} - W_{(0),yy}]\, dy = 0 \qquad \text{(IV-19)}$$

In order to check the closure conditions on u, we must determine $u_{,y}$ first. Integrating $u_{,x}$ from (III-6), we can write,

$$u = \mathcal{F}(y) + \int_0^x [-A_{13}\Phi_{,\xi\xi} + A_{22}\Phi_{,yy} + S_{14}(W_{(1),\xi\xi} - W_{(0),\xi\xi}) - S_{22}(W_{(1),yy} - W_{(0),yy}) - \tfrac{1}{2}(W_{(1),\xi}^2 - W_{(0),\xi}^2)]\, d\xi \qquad \text{(IV-20)}$$

where the dummy variable ξ replaces x of the first expression of (III-6) and $\mathcal{F}(y)$ is a yet undetermined function of y. Let us stipulate that $u|_{x=0}=0$, so that, as a consequence, $\mathcal{F}=0$. $u_{,y}$ then becomes:

$$u_{,y} = \int_0^x [-A_{13}\Phi_{,\xi\xi y} + A_{22}\Phi_{,yyy} + S_{14}(W_{(1),\xi\xi y} - W_{(0),\xi\xi y}) - S_{22}(W_{(1),yyy} - W_{(0),yyy}) - (W_{(1),\xi} W_{(1),\xi y} - W_{(0),\xi} W_{(0),\xi y})]\, d\xi \qquad \text{(IV-21)}$$

On substituting the derivatives of the stress function and the radial displacements, and after some algebra, we can write the condition of closure as:

$$\int_0^{2\pi R} u_{,y}\, dy = \int_0^x \int_0^{2\pi R} \{\alpha^2\beta^2 A_{13}[\lambda_1 \sin\alpha\xi \cos\beta y + 9\lambda_2 \sin 3\alpha\xi \cos\beta y + 3\lambda_3 \sin\alpha\xi \cos 3\beta y + 8\lambda_6 \cos 2\alpha\xi \sin 2\beta y + 32\lambda_9 \cos 4\alpha\xi \sin 2\beta y + 16\lambda_{10} \cos 2\alpha\xi \sin 4\beta y] + \beta^3 A_{22}[-\lambda_1 \sin\alpha\xi \cos\beta y - \lambda_2 \sin 3\alpha\xi \cos\beta y - 27\lambda_3 \sin\alpha\xi \cos 3\beta y + 8\lambda_5 \sin 2\beta y + 8\lambda_6 \cos 2\alpha\xi \sin 2\beta y$$

$$64\lambda_8 \sin 4\beta y + 8\lambda_9 \cos 4\alpha\{\sin 2\beta y + 64\lambda_{10}\cos 2\alpha\{\sin 4\beta y]$$
$$+ \alpha^2\beta S_{14}[-(f_1-f_0)\sin\alpha\{\cos\beta y + 2(g_1-g_0)\cos 2\alpha\{\sin 2\beta y]$$
$$+ \beta^3 S_{22}[(f_1-f_0)\sin\alpha\{\cos\beta y + 2(g_1-g_0)\sin 2\beta y$$
$$- 2(g_1-g_0)\cos 2\alpha\{\sin 2\beta y] - \alpha^2\beta[\tfrac{1}{2}(f_1^2-f_0^2)\sin\beta y\cos\beta y$$
$$+ \tfrac{1}{2}(f_1^2-f_0^2)\cos 2\alpha\{\sin\beta y\cos\beta y + \tfrac{1}{2}(f_1g_1-f_0g_0)\sin 2\alpha\{\cos\alpha\{\cos\beta y$$
$$- \tfrac{1}{2}(f_1g_1-f_0g_0)\sin 2\alpha\{\cos\alpha\{\cos 2\beta y + (f_1g_1-f_0g_0)\sin 2\alpha\{\cos\alpha\{\sin\beta y\sin 2\beta y$$
$$+ \tfrac{1}{4}(g_1^2-g_0^2)\sin 2\beta y - \tfrac{1}{4}(g_1^2-g_0^2)\cos 4\alpha\{\sin 2\beta y - \tfrac{1}{4}(g_1^2-g_0^2)\sin 2\beta y\cos\beta y$$
$$+ \tfrac{1}{4}(g_1^2-g_0^2)\cos 4\alpha\{\sin 2\beta y\cos 2\beta y]\}\,d\{\,dy$$

(IV-22)

When the integration is performed with respect to y, each term vanishes on account of the trigonometric terms in y. The condition of closure on u is therefore satisfied.

For v we can write:

$$\int_0^{2\pi R} v_{,y}\,dy = 0 \qquad \text{(IV-23)}$$

Introducing $v_{,y}$ from (III-6), yields:

$$\int_0^{2\pi R}[A_{11}\Phi_{,xx} - A_{13}\Phi_{,yy} - S_{11}(w_{(1),xx} - w_{(0),xx}) + S_{13}(w_{(1),yy} - w_{(0),yy})$$
$$- \tfrac{1}{2}(w_{(1),y}^2 - w_{(0),y}^2) + \frac{1}{R}(w_{(1)} - w_{(0)})]\,dy = 0$$

(IV-24)

On account of the third expression of (IV-19), the fourth term in the above equation can be deleted immediately.

The stress function and radial displacement terms are substituted from (IV-9) and (IV-18). After some algebra and cancellation of those trigonometric terms that integrate out to zero, one obtains:

$$\int_0^{2\pi R} \Big\{ -\alpha^2 A_{11} \Big[4\lambda_4 \cos 2\alpha x + 16\lambda_7 \cos 4\alpha x + \frac{\bar{N}_{oy}}{\alpha^2} \Big] + A_{13}\bar{N}_{ox} - \alpha^2 S_{11}(g_1 - g_o)\cos 2\alpha x - \frac{\beta^2}{8}\Big[f_1^2 - f_o^2\Big] + \frac{3}{4}(g_1^2 - g_o^2) - \Big((f_1^2 - f_o^2) + (g_1^2 - g_o^2)\Big)\cos 2\alpha x + \frac{1}{4}(g_1^2 - g_o^2)\cos 4\alpha x \Big] + \frac{1}{R}\Big[\frac{1}{4}(g_1 - g_o) - \frac{1}{4}(g_1 - g_o)\cos 2\alpha x\Big] \Big\} dy = 0 \qquad \text{(IV-25)}$$

Satisfaction of the condition of closure therefore requires that the above integrand is equal to zero, or:

$$A_{13}\bar{N}_{ox} - A_{11}\bar{N}_{oy} - \frac{\beta^2}{8}(f_1^2 - f_o^2) - \frac{3}{32}\beta^2(g_1^2 - g_o^2) + \frac{1}{4R}(g_1 - g_o) + \cos 2\alpha x \Big[\frac{\beta^2}{8}\Big((f_1^2 - f_o^2) + (g_1^2 - g_o^2)\Big) - 4\alpha^2 A_{11}\lambda_4 - \alpha^2 S_{11}(g_1 - g_o)\Big] + \cos 4\alpha x \Big[-16\alpha^2 A_{11}\lambda_7 - \frac{\beta^2}{32}(g_1^2 - g_o^2)\Big] = 0$$

When λ_4 and λ_7 are inserted from (IV-10), it can readily be shown that the coefficients of $\cos 2\alpha x$ and $\cos 4\alpha x$ reduce to zero. Omitting the algebraic details, we are left with:

$$A_{13}\bar{N}_{ox} - A_{11}\bar{N}_{oy} - \frac{\beta^2}{8}(f_1^2 - f_o^2) - \frac{3}{32}\beta^2(g_1^2 - g_o^2) + \frac{1}{4R}(g_1 - g_o) = 0 \qquad \text{(IV-26)}$$

The condition of closure therefore relates $\bar{N}_{ox}$ and $\bar{N}_{oy}$ of the stress function expression (IV-9).

Solving for $\bar{N}_{oy}$, yields:

$$\bar{N}_{oy} = \frac{A_{13}}{A_{11}} \bar{N}_{ox} - \frac{\beta^2}{8A_{11}} (f_1^2 - f_0^2) - \frac{3\beta^2}{32A_{11}} (g_1^2 - g_0^2) + \frac{1}{4A_{11}R} (g_1 - g_0) \qquad \text{(IV-27)}$$

CHAPTER V : THE DYNAMIC EQUILIBRIUM OF AN ECCENTRICALLY REINFORCED CYLINDRICAL SHELL SUBJECTED TO A CONTROLLED RATE OF ENDSHORTENING.

1. Controlled Rate of Endshortening.

The endshortening of the cylindrical shell is defined by:

$$e = -\int_0^L u_{,x}\, dx \qquad \text{(V-1)}$$

$u_{,x}$ is introduced from equation (III-6) so that one obtains:

$$e = -\int_0^L \{A_{22}\Phi_{,yy} - A_{13}\Phi_{,xx} + S_{14}(w_{(1),xx} - w_{(0),xx}) - S_{22}(w_{(1),yy} - w_{(0),yy}) - \tfrac{1}{2}(w_{(1),x}^2 - w_{(0),x}^2)\}\, dx \qquad \text{(V-2)}$$

Inserting the appropriate stress function and radial displacement terms from (IV-9) and (IV-18), leads to,

$$\begin{aligned} e = -\int_0^L \{ & -\beta^2 A_{22}[\lambda_1 \sin\alpha x \sin\beta y + \lambda_2 \sin 3\alpha x \sin\beta y + 9\lambda_3 \sin\alpha x \sin 3\beta y \\ & + 4\lambda_5 \cos 2\beta y + 16\lambda_8 \cos 4\beta y + \frac{\bar{N}_{ox}}{\beta^2}] \\ & + \alpha^2 A_{13}[\lambda_1 \sin\alpha x \sin\beta y + 9\lambda_2 \sin 3\alpha x \sin\beta y + \lambda_3 \sin\alpha x \sin 3\beta y \\ & + \frac{\bar{N}_{oy}}{\alpha^2}] - \alpha^2 S_{14}(f_1 - f_0)\sin\alpha x \sin\beta y + \beta^4 S_{22}[(f_1 - f_0)\sin\alpha x \sin\beta y \\ & - (g_1 - g_0)\cos 2\beta y] - \frac{\alpha^2}{8}[(f_1^2 - f_0^2) + \frac{3}{4}(g_1^2 - g_0^2) - ((f_1^2 - f_0^2) \\ & + (g_1^2 - g_0^2))\cos 2\beta y + 3(f_1 g_1 - f_0 g_0)\sin\alpha x \cos\beta y + 3(f_1 g_1 - f_0 g_0)\sin 3\alpha x \sin\beta y \\ & - (f_1 g_1 - f_0 g_0)\sin 3\alpha x \sin 3\beta y - (f_1 g_1 - f_0 g_0)\sin\alpha x \sin 3\beta y \\ & + \tfrac{1}{4}(g_1^2 - g_0^2)\cos 4\beta y]\}\, dx \end{aligned} \qquad \text{(V-3)}$$

where the terms containing cos $2\alpha x$ and cos $4\alpha x$ have been deleted since they vanish in the integration.

Regrouping the integrand in terms of its y-dependent components, there results:

$$
\begin{aligned}
e = -\int_0^L \{ & -A_{22}\bar{N}_{ox} + A_{13}\bar{N}_{oy} - \frac{\alpha^2}{8}(f_1^2 - f_0^2) - \frac{3}{32}\alpha^2(g_1^2 - g_0^2) \\
& + \sin\beta y\,[-\beta^2 A_{22}\lambda_1 \sin\alpha x - \beta^2 A_{22}\lambda_2 \sin 3\alpha x + \alpha^2 A_{13}\lambda_1 \sin\alpha x \\
& + 9\alpha^2 A_{13}\lambda_2 \sin 3\alpha x - \alpha^2 S_{14}(f_1 - f_0)\sin\alpha x \\
& + \beta^2 S_{22}(f_1 - f_0)\sin\alpha x - \tfrac{3}{8}\alpha^2(f_1 g_1 - f_0 g_0)\sin 3\alpha x\,] \\
& + \sin 3\beta y\,[-9\beta^2 A_{22}\lambda_3 \sin\alpha x + \alpha^2 A_{13}\lambda_3 \sin\alpha x \\
& + \tfrac{\alpha^2}{8}(f_1 g_1 - f_0 g_0)\sin 3\alpha x + \tfrac{\alpha^2}{8}(f_1 g_1 - f_0 g_0)\sin\alpha x\,] \\
& + \cos\beta y\,[-\tfrac{3}{8}\alpha^2(f_1 g_1 - f_0 g_0)\sin\alpha x\,] \\
& + \cos 2\beta y\,[-4\beta^2 A_{22}\lambda_5 - \beta^2 S_{22}(g_1 - g_0) + \tfrac{\alpha^2}{8}((f_1^2 - f_0^2) + (g_1^2 - g_0^2))] \\
& + \cos 4\beta y\,[-16\beta^2 A_{22}\lambda_8 - \tfrac{\alpha^2}{32}(g_1^2 - g_0^2)]\,\}\,dx
\end{aligned}
\qquad \text{(V-4)}
$$

The bracket terms associated with cos $2\beta y$ and cos $4\beta y$ vanish when λ_5 and λ_8 are substituted from (IV-10).

In the particular case of even integers for m in $\alpha = \frac{m\pi}{L}$, sin αx and sin $3\alpha x$ integrate out to zero so that e is not y-dependent for a buckling pattern which divides the shell length into an even number of axial half wavelengths.

Let us define a controlled rate of endshortening by,

$$\bar{e} = \int_0^t V(\tau)\, d\tau \qquad \text{(V-5)}$$

where V(t) is the prescribed uniform velocity, $- u_{,t}$, at x=L, taken positive in the negative x-direction and $\bar{e}$ is the average endshortening, given by:

$$\bar{e} = \frac{1}{2\pi R} \int_0^{2\pi R} e\, dy \qquad \text{(V-6)}$$

Inserting e from (V-4) and performing both integrations leads to:

$$\bar{e} = L \left\{ A_{22} \bar{N}_{0x} - A_{13} \bar{N}_{0y} + \frac{\alpha^2}{8}(f_1^2 - f_0^2) + \frac{3}{32}\alpha^2(g_1^2 - g_0^2) \right\} = \int_0^t V(\tau)\, d\tau \qquad \text{(V-7)}$$

Hoff [47] and his associates [48] investigated the dynamic buckling of columns in the form of (V-5) with a constant rate of endshortening. Similarly, Coppa and Nash [51] used this approach in the investigation of monocoque shells under impact, also utilizing a constant V.

In the present analysis the following rate of endshortening will be considered:

$$V(t) = V_0 e^{-\gamma t} \qquad \text{(V-8)}$$

Such an approach keeps the advantages of the previous analysis for $\gamma = 0$, e.g. for small values of V_0 a reduction to the static case is possible, while for large values of V_0 a fair representation of impact buckling is possible in the

sense of Coppa and Nash, neglecting wave propagation effects. The inclusion of a finite value for γ should improve the "impact model" in that the velocity at the end x=L usually decreases with time. This model might have some merits also in the consideration of axial impact on nonrigid surfaces.

Substituting $\bar{N}_{oy}$ from (IV-27) and V(t) from (V-8) into equation (V-7), and solving for $\bar{N}_{ox}$, results in:

$$\bar{N}_{ox} = \frac{V_o(1-e^{-\gamma t})}{\gamma L\left(A_{22}-\frac{A_{13}^2}{A_{11}}\right)} - \frac{1}{8}\,\frac{\alpha^2+\frac{A_{13}}{A_{11}}\beta^2}{A_{22}-\frac{A_{13}^2}{A_{11}}}\left[(f_1^2-f_0^2)+\frac{3}{4}(g_1^2-g_0^2)\right]+\frac{1}{4R}\,\frac{A_{13}}{A_{11}}\,\frac{(g_1-g_0)}{\left(A_{22}-\frac{A_{13}^2}{A_{11}}\right)} \qquad \text{(V-9)}$$

2. Application of the Bubnov-Galerkin Procedure.

In order to solve the problem of the eccentrically reinforced cylindrical shell subjected to a controlled rate of endshortening of the form (V-8), we must find a solution to the field equations (III-10). The second of these, the compatibility equation, is satisfied by the stress function (IV-9), which was derived from the assumed radial displacements (IV-1). Due to the controlled rate of endshortening(V-8), $\bar{N}_{ox}$ and $\bar{N}_{oy}$ of the stress function expression (IV-9) must be expressed by (V-9) and (IV-27).
The first of the field equations remains to be satisfied. Restricting ourselves to the problem of controlled rate of endshortening of an eccentrically reinforced cylindrical

shell which is terminated at both ends by rigid flanges, we can omit the pressure term in (III-10). The satisfaction of boundary and closure conditions has already been discussed. The dynamic equilibrium equation will be satisfied in the sense of Bubnov-Galerkin. For this purpose, let us rewrite the first equation of (III-10) with p=0 in the form:

$$
\begin{aligned}
H = {} & D_{11}\left[W_{(1),xxxx} - W_{(0),xxxx}\right] + 2D_{12}\left[W_{(1),xxyy} - W_{(0),xxyy}\right] \\
& + D_{22}\left[W_{(1),yyyy} - W_{(0),yyyy}\right] + S_{11}\Phi_{,xxxx} - 2S_{12}\Phi_{,xxyy} \\
& + S_{22}\Phi_{,yyyy} - \Phi_{,xx}W_{(1),yy} + 2\Phi_{,xy}W_{(1),xy} - \Phi_{,yy}W_{(1),xx} \\
& - \frac{\Phi_{,xx}}{R} + \bar{m}W_{(1),tt} - I_{\bar{m}}\left[W_{(1),xxtt} + W_{(1),yytt}\right] = 0
\end{aligned}
\tag{V-10}
$$

The Bubnov-Galerkin equations then become:

$$
\left.
\begin{aligned}
\int_0^{L}\int_0^{2\pi R} H \sin\alpha x \sin\beta y \, dx\,dy = 0 \\
\int_0^{L}\int_0^{2\pi R} H \sin^2\alpha x \sin^2\beta y \, dx\,dy = 0
\end{aligned}
\right\}
\tag{V-11}
$$

The evaluation of these two integrals is extremely tedious and lengthy. Some of the details are given in Appendix A. The result can be stated in a system of two second order simultaneous differential equations of the third degree in

in f_1 and g_1, the time-dependent amplitudes of the "checkerboard" and "diamond" buckling patterns. This system consists of the two equations (A-4) and (A-14) of Appendix A and is stated below:

$$\left.\begin{aligned}\frac{d^2 f_1}{dt^2} &= B_1 f_1 + B_2 g_1 + B_3 f_1 g_1 + B_4 f_1 g_1^2 + B_5 f_1^3 \\ &\quad + B_6 f_1 \frac{1-e^{-\gamma t}}{\gamma} + B_7 \\ \frac{d^2 g_1}{dt^2} &= C_1 g_1 + C_2 f_1 + C_3 g_1^2 + C_4 f_1^2 + C_5 f_1^2 g_1 \\ &\quad + C_6 g_1^3 + C_7 g_1 \frac{1-e^{-\gamma t}}{\gamma} + C_8 \frac{1-e^{-\gamma t}}{\gamma} + C_9\end{aligned}\right\} \quad \text{(V-12)}$$

The coefficients B and C are defined in Appendix A.

3. Reduction to the Case of Dynamic Buckling of a Column.

In the case of a column the "diamond" pattern amplitude $g_1(t)$ must be deleted so that only the first of the equations (V-12) is retained. The latter simplies further since the coupling terms drop out. On writing the B's with a superscript (C), indicating column, we are left with the following equation:

$$\frac{d^2 f_1}{dt^2} = B_1^{(C)} f_1 + B_5^{(C)} f_1^3 + B_6^{(C)} f_1 \frac{1-e^{-\gamma t}}{\gamma} + B_7^{(C)} \qquad \text{(V-13)}$$

The coefficients B are obtained by reduction of expressions (A-5) through (A-11) to the monocoque shell case; then letting $R \to \infty$, $\nu \to 0$, and on using the area moment of inertia I and the cross sectional area A of the column ($A \to h \cdot 1$; $D \to \frac{Eh^3}{12} \cdot 1 = EI$), these

coefficients become:

$$\left.\begin{aligned} B_1^{(c)} &= -\left(\frac{\pi}{L}\right)^4 \frac{EI}{\rho A} + \frac{3}{16}\left(\frac{\pi}{L}\right)^4 \frac{Ef_0^2}{\rho} \\ B_5^{(c)} &= -\frac{3}{16}\left(\frac{\pi}{L}\right)^4 \frac{E}{\rho} \\ B_6^{(c)} &= \left(\frac{\pi}{L}\right)^2 \frac{EV_0}{\rho L} \\ B_7^{(c)} &= \left(\frac{\pi}{L}\right)^4 \frac{EIf_0}{\rho} \end{aligned}\right\} \qquad \text{(V-14)}$$

The particular case of constant velocity of end approach is obtained from (V-13) by taking the limit as $\gamma \to 0$. There results:

$$\frac{d^2 f_1}{dt^2} = B_1^{(c)} f_1 + B_5^{(c)} f_1^3 + B_6^{(c)} f_1 t + B_7^{(c)} \qquad \text{(V-15)}$$

This equation coincides with that used by Hoff [47] for the column. A comparison of coefficients reveals a slight discrepancy in that Hoff has the factor 3/16 replaced by 1/4, which is not surprising when one recalls our method of derivation and satisfaction of boundary conditions (clamped). This difference is minor, however, and affects primarily $B_5^{(c)}$, at least for $f_0 \ll \frac{\sqrt{3}}{2} r_g$ where $r_g = \sqrt{\frac{I}{A}}$ is the radius of gyration of the column. Since $B_5^{(c)}$ multiplies with f_1^3, this slight difference becomes significant only in the postbuckling region.

4. The Linearized System of Differential Equations with Constant Coefficients.

Before plunging into numerical methods to integrate the system

of equations (V-12) for a particular shell, it seems worthwhile to consider certain simplifications of these equations. Let us therefore contemplate the linearized constant coefficient equivalent of (V-12) which is:

$$\left.\begin{aligned} \frac{d^2 f_1}{dt^2} &= B_1 f_1 + B_2 g_1 + B_7 \\ \frac{d^2 g_1}{dt^2} &= C_1 g_1 + C_2 f_1 + C_8 \frac{1-e^{-\gamma t}}{\gamma} + C_9 \end{aligned}\right\} \quad \text{(V-16)}$$

With the initial conditions,

$$\left.\begin{aligned} f_1(0) &= f_0 \\ g_1(0) &= g_0 \\ \frac{df_1}{dt}(0) &= \frac{dg_1}{dt}(0) = 0 \end{aligned}\right\} \quad \text{(V-17)}$$

and applying the Laplace transform method, the system becomes:

$$\left.\begin{aligned} (s^2 - B_1)\,\bar{f}_1(s) - B_2\,\bar{g}_1(s) &= s f_0 + \frac{B_7}{s} \\ -C_2\,\bar{f}_1(s) + (s^2 - C_1)\,\bar{g}_1(s) &= s g_0 + \frac{C_9}{s} + \frac{C_8}{s(s+\gamma)} \end{aligned}\right\} \quad \text{(V-18)}$$

The determinant of the homogeneous system becomes,

$$\Delta = s^4 - (B_1 + C_1)s^2 + B_1 C_1 - B_2 C_2$$

whose roots can be written as:

$$s_{1/2}^2 = \frac{1}{2}\left[(B_1 + C_1) \pm (B_1 - C_1)\sqrt{1 + \frac{4B_2 C_2}{(B_1 - C_1)^2}}\right]$$

On defining,

$$\theta = +\sqrt{1 + \frac{4B_2 C_2}{(B_1 - C_2)^2}} \quad \text{(V-19)}$$

and noting from the definitions of B_2 and C_2, equations (A-6) and (A-16), that B_2 and C_2 are related by,

$$C_2 = \frac{16}{9} B_2 \qquad \text{(V-20)}$$

we conclude that θ is always a real number. Let us introduce:

$$\left.\begin{aligned} \omega_1^2 &= -\tfrac{1}{2}\left[B_1(1+\theta) + C_1(1-\theta)\right] \\ \omega_2^2 &= -\tfrac{1}{2}\left[B_1(1-\theta) + C_1(1+\theta)\right] \end{aligned}\right\} \qquad \text{(V-21)}$$

so that the determinant Δ can be written as:

$$\Delta = (s^2+\omega_1^2)(s^2+\omega_2^2) \qquad \text{(V-22)}$$

Equations (V-19) and (V-21) provide some physical insight into the system (V-16). Noting from (A-6) and (A-16) that B_2 and C_2 vanish for zero imperfections, we conclude that θ is only slightly more than one, being one exactly for zero imperfections.
In the latter case, (V-21) becomes,

$$\left.\begin{aligned} \omega_1^{(0)2} &= -B_1^{(0)} \\ \omega_2^{(0)2} &= -C_1^{(0)} \end{aligned}\right\} \qquad \text{(V-23)}$$

where the superscript (0) has been added to indicate zero imperfections. $B_1^{(0)}$ and $C_1^{(0)}$ are obtained from (A-5) and (A-15) by deleting all terms with the factors f_o and g_o. They are:

$$B_1^{(0)} = -\frac{1}{\bar{m}_1}\left(\alpha^4 D_{11} + 2\alpha^2\beta^2 D_{12} + \beta^4 D_{22}\right) - \frac{\left(\alpha^4 S_{11} - 2\alpha^2\beta^2 S_{12} + \beta^4 S_{22} + \frac{\alpha^2}{R}\right)^2}{\bar{m}_1\left(\alpha^4 A_{11} + 2\alpha^2\beta^2 A_{12} + \beta^4 A_{22}\right)} \Bigg]$$

$$C_1^{(0)} = -\frac{16}{9\bar{m}_2}\left(3\alpha^4 D_{11} + 2\alpha^2\beta^2 D_{12} + 3\beta^4 D_{22} + \frac{1}{4A_{11}R^2}\right)$$
$$-\frac{16}{9\bar{m}_2}\frac{\left(\alpha^4 S_{11} - 2\alpha^2\beta^2 S_{12} + \beta^4 S_{22} + \frac{\alpha^2}{4R}\right)^2}{\left(\alpha^4 A_{11} + 2\alpha^2\beta^2 A_{12} + \beta^4 A_{22}\right)} - \frac{32}{9}\frac{\left(\alpha^2 S_{11} + \frac{1}{4R}\right)^2}{A_{11}\bar{m}_2}$$
$$-\frac{32\beta^4 S_{22}^2}{9A_{22}\bar{m}_2} - \frac{4}{9}\frac{A_{13}^2}{A_{11}^2 R^2 \bar{m}_2\left(A_{22} - \frac{A_{13}^2}{A_{11}}\right)} \qquad \text{(V-24)}$$

$\omega_1^{(0)}$ and $\omega_2^{(0)}$ are the circular natural frequencies in flexure of the "checkerboard", respectively, the "diamond" buckling amplitudes. The influence of the eccentric reinforcements on the natural frequencies is seen by the terms of (V-24) that contain the A's and S's . We also note that there is no coupling of the system (V-16), since $B_2 = C_2 = 0$ for zero imperfections. From the previous remarks, we can expect only slight coupling for nonvanishing imperfections. Both buckling pattern amplitudes are therefore almost independent of each other.

Looking back at the full nonlinear system (V-12), we conclude that interactions between the two buckling patterns occurs mainly due to the highly nonlinear coupling.

Solving the system (V-18) by Cramer's rule for the Laplace transformed variables $\bar{f}_1(s)$ and $\bar{g}_1(s)$, there results:

$$\bar{f}_1(s) = \frac{s^3 f_0}{(s^2+\omega_1^2)(s^2+\omega_2^2)} + \frac{s(B_7 + B_2 g_0 - C_1 f_0)}{(s^2+\omega_1^2)(s^2+\omega_2^2)}$$
$$+ \frac{B_2 C_9 - B_7 C_1}{s(s^2+\omega_1^2)(s^2+\omega_2^2)} + \frac{B_2 C_8}{s(s+\gamma)(s^2+\omega_1^2)(s^2+\omega_2^2)} \qquad \text{(V-25)}$$

$$\bar{g}_1(s) = \frac{s^3 g_0}{(s^2+\omega_1^2)(s^2+\omega_2^2)} + \frac{s(C_9 + C_2 f_0 - B_1 g_0)}{(s^2+\omega_1^2)(s^2+\omega_2^2)} + \frac{B_7 C_2 - B_1 C_9}{s(s^2+\omega_1^2)(s^2+\omega_2^2)} \approx$$

$$- \frac{B_1 C_8}{s(s+\gamma)(s^2+\omega_1^2)(s^2+\omega_2^2)} + \frac{C_8 s}{(s+\gamma)(s^2+\omega_1^2)(s^2+\omega_2^2)}$$

Most of the terms of (V-25) have known inversions and can be found in reference [55], for example; others are readily obtained by applying the convolution theorem. The inversion of (V-25) becomes:

$$f_1(t) = \frac{f_0}{\omega_1^2 - \omega_2^2}(\omega_1^2 \cos\omega_1 t - \omega_2^2 \cos\omega_2 t) - \frac{B_7 + B_2 g_0 - C_1 f_0}{\omega_1^2 - \omega_2^2}(\cos\omega_1 t - \cos\omega_2 t)$$

$$+ \frac{B_2 C_9 - B_7 C_1}{\omega_1^2 \omega_2^2}\left[1 + \frac{1}{\omega_1^2 - \omega_2^2}(\omega_2^2 \cos\omega_1 t - \omega_1^2 \cos\omega_2 t)\right]$$

$$+ \frac{B_2 C_8}{\omega_1^2 \omega_2^2}\left\{\frac{1 - e^{-\gamma t}}{\gamma} + \frac{1}{\omega_1^2 - \omega_2^2}\left[\frac{\omega_2^2(\gamma\cos\omega_1 t + \omega_1 \sin\omega_1 t - \gamma e^{-\gamma t})}{(\omega_1^2 + \gamma^2)}\right.\right.$$

$$\left.\left. - \frac{\omega_1^2(\gamma\cos\omega_2 t + \omega_2 \sin\omega_2 t - \gamma e^{-\gamma t})}{(\omega_2^2 + \gamma^2)}\right]\right\}$$

$$g_1(t) = \frac{g_0}{\omega_1^2 - \omega_0^2}(\omega_1^2 \cos\omega_1 t - \omega_2^2 \cos\omega_2 t) - \frac{(C_9 + C_2 f_0 - B_1 g_0)}{\omega_1^2 - \omega_2^2}(\cos\omega_1 t - \cos\omega_2 t)$$

$$+ \frac{B_7 C_2 - B_1 C_9}{\omega_1^2 \omega_2^2}\left[1 + \frac{1}{\omega_1^2 - \omega_2^2}(\omega_2^2 \cos\omega_1 t - \omega_1^2 \cos\omega_2 t)\right]$$

$$- \frac{B_1 C_8}{\omega_1^2 \omega_2^2}\left\{\frac{1 - e^{-\gamma t}}{\gamma} + \frac{1}{\omega_1^2 - \omega_2^2}\left[\frac{\omega_2^2(\gamma\cos\omega_1 t + \omega_1 \sin\omega_1 t - \gamma e^{-\gamma t}}{(\omega_1^2 + \gamma^2)}\right.\right.$$

$$\left.\left. - \frac{\omega_1^2(\gamma\cos\omega_2 t + \omega_2 \sin\omega_2 t - \gamma e^{-\gamma t})}{(\omega_2^2 + \gamma^2)}\right]\right\}$$

$$+ \frac{C_8 e^{-\gamma t}}{\omega_1^2 - \omega_2^2}\left\{\frac{-\gamma\cos\omega_1 t - \omega_1 \sin\omega_1 t + \gamma}{\omega_1^2 + \gamma^2} + \frac{\gamma\cos\omega_2 t + \omega_2 \sin\omega_2 t - \gamma}{\omega_2^2 + \gamma^2}\right\}$$

(V-26)

By collecting appropriate terms, these equations may be written as:

$$f_1(t) = U_1 \cos\omega_1 t + U_2 \cos\omega_2 t + U_3 \sin\omega_1 t + U_4 \sin\omega_2 t + U_5 e^{-\gamma t} + U_6$$

$$g_1(t) = (V_{11} + V_{12} e^{-\gamma t})\cos\omega_1 t + (V_{21} + V_{22} e^{-\gamma t})\cos\omega_2 t + (V_{31} + V_{32} e^{-\gamma t})\sin\omega_1 t + (V_{41} + V_{42} e^{-\gamma t})\sin\omega_2 t + V_5 e^{-\gamma t} + V_6$$

(V-27)

where the following abbreviations have been used:

$$U_1 = \frac{f_0\omega_1^2 - B_7 - B_2 g_0 + C_1 f_0 + \frac{1}{\omega_2^2}(B_2 C_9 - B_7 C_1)}{\omega_1^2 - \omega_2^2} + \frac{\gamma B_2 C_8}{\omega_1^2(\omega_1^2 - \omega_2^2)(\omega_1^2 + \gamma^2)}$$

$$U_2 = \frac{B_7 + B_2 g_0 - C_1 f_0 - f_0\omega_2^2 - \frac{1}{\omega_2^2}(B_2 C_9 - B_7 C_1)}{\omega_1^2 - \omega_2^2} - \frac{\gamma B_2 C_8}{\omega_2^2(\omega_1^2 - \omega_2^2)(\omega_2^2 + \gamma^2)}$$

$$U_3 = \frac{B_2 C_8}{\omega_1(\omega_1^2 - \omega_2^2)(\omega_1^2 + \gamma^2)}$$

$$U_4 = \frac{-B_2 C_8}{\omega_2(\omega_1^2 - \omega_2^2)(\omega_2^2 + \gamma^2)}$$

$$U_5 = -\frac{B_2 C_8}{\omega_1^2\omega_2^2}\left[\frac{1}{\gamma} + \frac{\gamma\omega_2^2}{(\omega_1^2 - \omega_2^2)(\omega_1^2 + \gamma^2)} - \frac{\gamma\omega_1^2}{(\omega_1^2 - \omega_2^2)(\omega_2^2 + \gamma^2)}\right]$$

$$V_{11} = \frac{g_0\omega_1^2 - C_9 - C_2 f_0 + B_1 g_0 + \frac{1}{\omega_2^2}(B_7 C_2 - B_1 C_9)}{\omega_1^2 - \omega_2^2} - \frac{\gamma B_1 C_8}{\omega_1^2(\omega_1^2 - \omega_2^2)(\omega_1^2 + \gamma^2)}$$

$$V_{12} = -\frac{\gamma C_8}{(\omega_1^2 - \omega_2^2)(\omega_1^2 + \gamma^2)}$$

$$V_{21} = \frac{C_9 + C_2 f_0 - B_1 g_0 - g_0 \omega_2^2 - \frac{1}{\omega_2^2}(B_7 C_2 - B_1 C_9)}{\omega_1^2 - \omega_2^2} + \frac{\gamma B_1 C_8}{\omega_2^2(\omega_1^2 - \omega_2^2)(\omega_2^2 + \gamma^2)}$$

$$V_{22} = \frac{\gamma C_8}{(\omega_1^2 - \omega_2^2)(\omega_2^2 + \gamma^2)}$$

$$V_{31} = -\frac{B_1 C_8}{\omega_1 (\omega_1^2 - \omega_2^2)(\omega_1^2 + \gamma^2)}$$

$$V_{32} = -\frac{\omega_1 C_8}{(\omega_1^2 - \omega_2^2)(\omega_1^2 + \gamma^2)}$$

$$V_{41} = \frac{B_1 C_8}{\omega_2 (\omega_1^2 - \omega_2^2)(\omega_2^2 + \gamma^2)}$$

$$V_{42} = \frac{\omega_2 C_8}{(\omega_1^2 - \omega_2^2)(\omega_2^2 + \gamma^2)}$$

$$V_5 = \frac{B_1 C_8}{\omega_1^2 \omega_2^2}\left[\frac{1}{\gamma} + \frac{\gamma \omega_2^2}{(\omega_1^2 - \omega_2^2)(\omega_1^2 + \gamma^2)} - \frac{\gamma \omega_1^2}{(\omega_1^2 - \omega_2^2)(\omega_2^2 + \gamma^2)}\right]$$

$$+ \frac{\gamma C_8}{\omega_1^2 - \omega_2^2}\left[\frac{1}{\omega_1^2 + \gamma^2} - \frac{1}{\omega_2^2 + \gamma^2}\right]$$

$$V_6 = \frac{B_7 C_2 - B_1 C_9 - \frac{B_1 C_8}{\gamma}}{\omega_1^2 \omega_2^2} \qquad \text{(V-27)}$$

The case of constant velocity of endshortening is of particular interest. Then the above equations simplify somewhat by taking the limit as $\gamma \to 0$. Since these equations were found useful in checking out one of the numerical methods that will be discussed later, they are also listed below:

$$f_1^{(0)}(t) = U_1^{(0)} \cos\omega_1 t + U_2^{(0)} \cos\omega_2 t + U_3^{(0)} \sin\omega_1 t + U_4^{(0)} \sin\omega_2 t + U_5^{(0)} t + U_6^{(0)}$$

$$g_1^{(0)}(t) = V_1^{(0)} \cos\omega_1 t + V_2^{(0)} \cos\omega_2 t + V_3^{(0)} \sin\omega_1 t + V_4^{(0)} \sin\omega_2 t + V_5^{(0)} t + V_6^{(0)}$$

(V-28)

The superscripts (0) refer to γ being zero. The coefficients are defined by:

$$U_1^{(0)} = \frac{f_0\omega_1^2 - B_7 - B_2 g_0 + C_1 f_0 + \frac{1}{\omega_1^2}(B_2 C_9 - B_7 C_1)}{\omega_1^2 - \omega_2^2}$$

$$U_2^{(0)} = \frac{B_7 + B_2 g_0 - C_1 f_0 - f_0\omega_2^2 - \frac{1}{\omega_2^2}(B_2 C_9 - B_7 C_1)}{\omega_1^2 - \omega_2^2}$$

$$U_3^{(0)} = \frac{B_2 C_8}{\omega_1^3(\omega_1^2 - \omega_2^2)}$$

$$U_4^{(0)} = -\frac{B_2 C_8}{\omega_2^3(\omega_1^2 - \omega_2^2)}$$

$$U_5^{(0)} = \frac{B_2 C_8}{\omega_1^2\omega_2^2}$$

$$U_6^{(0)} = \frac{B_2 C_9 - B_7 C_1}{\omega_1^2\omega_2^2}$$

$$V_1^{(0)} = \frac{g_0\omega_1^2 - C_9 - C_2 f_0 + B_1 g_0 + \frac{1}{\omega_1^2}(B_7 C_2 - B_1 C_9)}{\omega_1^2 - \omega_2^2}$$

$$V_2^{(0)} = \frac{C_9 + C_2 f_0 - B_1 g_0 - g_0\omega_1^2 - \frac{11}{\omega_2^2}(B_7 C_2 - B_1 C_9)}{\omega_1^2 - \omega_2^2}$$

$$V_3^{(0)} = -\frac{C_8(B_1 + \omega_1^2)}{\omega_1^3(\omega_1^2 - \omega_2^2)}$$

$$V_4^{(0)} = \frac{C_8(B_1 + \omega_2^2)}{\omega_2^3(\omega_1^2 - \omega_2^2)}$$

$$V_5^{(0)} = -\frac{B_1 C_8}{\omega_1^2\omega_2^2}$$

$$V_6^{(0)} = \frac{B_7 C_2 - B_1 C_9}{\omega_1^2\omega_2^2}$$

(V-29)

5. The Linearized Differential Equations for Very Small Imperfections and Constant Rate of Endshortening.

As pointed out in the previous section, the linearized system of equations (V-12) is almost decoupled. In this section, complete decoupling is assumed with γ being zero. This leads to two independent linear second order differential equations with variable coefficients of the form:

$$\left.\begin{aligned} \frac{d^2 f_1}{dt^2} &= B_1 f_1 + B_6 f_1 t + B_7 \\ \frac{d^2 g_1}{dt^2} &= C_1 g_1 + C_7 g_1 t + C_8 t + C_9 \end{aligned}\right\} \qquad \text{(V-30)}$$

In order to bring these equations into a more standardized form, the following transformations are made:

$$\left.\begin{aligned} B_6^{\frac{2}{3}} z &= -(B_1 + B_6 t) \\ f_1(t) &= u(z) \\ C_7^{\frac{2}{3}} \tau &= -(C_1 + C_7 t) \\ g_1(t) &= v(\tau) \end{aligned}\right\} \qquad \text{(V-31)}$$

The derivatives become:

$$\left.\begin{aligned} \frac{df_1}{dt} &= -B_6^{\frac{1}{3}} \frac{du}{dz} \\ \frac{d^2 f_1}{dt^2} &= B_6^{\frac{2}{3}} \frac{d^2 u}{dz^2} \\ \frac{dg_1}{dt} &= -C_7^{\frac{1}{3}} \frac{dv}{d\tau} \end{aligned}\right\} \qquad \text{(V-32)}$$

$$\frac{d^2 g_1}{dt^2} = C_7^{\frac{2}{3}} \frac{d^2 v}{d\tau^2} \qquad \int$$

Making use of these transformations and the derivatives, the equations (V-30) can be written in the form:

$$\left.\begin{aligned} \frac{d^2 u(z)}{dz^2} + z\,u(z) &= Q_1 \\ \frac{d^2 v(\tau)}{d\tau^2} + \tau\, v(\tau) &= Q_2 \tau + Q_3 \end{aligned}\right\} \qquad \text{(V-33)}$$

Use was made of the following abbreviations:

$$\left.\begin{aligned} Q_1 &= \frac{B_7}{B_6^{\frac{2}{3}}} \\ Q_2 &= -\frac{C_8}{C_7} \\ Q_3 &= \frac{C_9}{C_7^{\frac{2}{3}}} - \frac{C_1 C_8}{C_7^{\frac{5}{3}}} \end{aligned}\right\} \qquad \text{(V-34)}$$

The solutions to these differential equations can be shown to be:

$$u(z) = f_1(t) = Ai(-z)\left[\lambda_1 - \pi Q_1 \int_0^z Bi(-\theta)\,d\theta\right] + Bi(-z)\left[\lambda_2 + \pi Q_1 \int_0^z Ai(-\theta)\,d\theta\right]$$

$$\frac{df_1}{dt} = -B_6^{\frac{1}{3}}\left\{Ai'(-z)\left[\lambda_1 - \pi Q_1 \int_0^z Bi(-\theta)\,d\theta\right] + Bi'(-z)\left[\lambda_2 + \pi Q_1 \int_0^z Ai(-\theta)\,d\theta\right]\right.$$

$$v(\tau) = g_1(t) = Q_2 + Ai(-\tau)\left[\lambda_3 - \pi Q_3 \int_0^\tau Bi(-\theta)\,d\theta\right] + Bi(-\tau)\left[\lambda_4 + \pi Q_3 \int_0^\tau Ai(-\theta)\,d\theta\right]$$

$$\frac{dg_1}{dt} = -C_7^{\frac{1}{3}}\left\{Ai'(-\tau)\left[\lambda_3 - \pi Q_3 \int_0^\tau Bi(-\theta)\,d\theta\right] + Bi'(-\tau)\left[\lambda_4 + \pi Q_3 \int_0^\tau Ai(-\theta)\,d\theta\right]\right.$$

(V-35)

The Ai and Bi functions are so-called Airy functions. They are related to the one-third order Bessel functions when the argument is negative, as in (V-35). The reader is referred to the book [56] for further details. In arriving at (V-35), use was made of the property that the Wronskian of the Airy functions Ai and Bi equals $1/\pi$. The λ's are determined from the initial conditions such that,

$$\left.\begin{aligned}
\lambda_1 &= \pi\left[R_1\, Bi'(-z_0) - R_2 Bi(-z_0)\right] \\
\lambda_2 &= \pi\left[R_2\, Ai'(-z_0) - R_1 Ai'(-z_0)\right] \\
\lambda_3 &= \pi\left[R_3\, Bi'(-\tau_0) - R_4 Bi'(-\tau_0)\right] \\
\lambda_4 &= \pi\left[R_4\, Ai'(-\tau_0) - R_3 Ai'(-\tau_0)\right]
\end{aligned}\right\} \qquad \text{(V-36)}$$

where the R's are given by,

$$\left.\begin{aligned}
R_1 &= f_0 - \pi Q_1\left[Bi(-z_0)\int_0^{z_0} Ai(-\theta)\,d\theta - Ai(-z_0)\int_0^{z_0} Bi(-\theta)\,d\theta\right] \\
R_2 &= -\pi Q_1\left[Bi'(-z_0)\int_0^{z_0} Ai(-\theta)\,d\theta - Ai'(-z_0)\int_0^{z_0} Bi(-\theta)\,d\theta\right] \\
R_3 &= g_0 - Q_2 - \pi Q_3\left[Bi(-\tau_0)\int_0^{\tau_0} Ai(-\theta)\,d\theta - Ai(-\tau_0)\int_0^{\tau_0} Bi(-\theta)\,d\theta\right] \\
R_4 &= -\pi Q_3\left[Bi'(-\tau_0)\int_0^{\tau_0} Ai(-\theta)\,d\theta - Ai'(-\tau_0)\int_0^{\tau_0} Bi(-\theta)\,d\theta\right]
\end{aligned}\right\} \qquad \text{(V-37)}$$

and where,

$$\left.\begin{aligned}
z_0 &= -B_1 B_6^{-\frac{2}{3}} \\
\tau_0 &= -C_1 C_7^{-\frac{2}{3}}
\end{aligned}\right\} \qquad \text{(V-38)}$$

Equations (V-30) provide a closed-form solution to the differential equations (V-30), provided the Airy functions, their derivatives and integrals can be evaluated. A tabulation of such evaluations for an argument (negative) range from zero to ten is given in reference [56], p.477. In the (negative) argument range from ten to thirty, this reference lists certain asymptotic formulas for calculating the Airy functions and their derivatives by using certain values from the tables. In the same argument range, the integrals can be evaluated from asymptotic expansions given in the book [57], p.137. For (negative) arguments larger than thirty, the following Asmptotic expansions may be used [56] :

$$
\left.
\begin{aligned}
Ai(-\eta) &\sim 0.3989423\, \eta^{-\frac{1}{4}} (\cos\Lambda + \sin\Lambda) \\
Ai'(-\eta) &\sim -0.3989423\, \eta^{\frac{1}{4}} (\cos\Lambda - \sin\Lambda) \\
Bi(-\eta) &\sim 0.3989423\, \eta^{-\frac{1}{4}} (\cos\Lambda - \sin\Lambda) \\
Bi'(-\eta) &\sim 0.3989423\, \eta^{\frac{1}{4}} (\cos\Lambda + \sin\Lambda) \\
\int_0^{\eta} Ai(-\theta)\, d\theta &\sim \frac{2}{3} - \frac{1}{2}\sqrt{\frac{2}{\pi}}\, \eta^{-0.75} (\cos\Lambda - \sin\Lambda) \\
\int_0^{\eta} Bi(-\theta)\, d\theta &\sim \frac{1}{2}\sqrt{\frac{2}{\pi}}\, \eta^{-0.75} (\cos\Lambda + \sin\Lambda) \\
\Lambda &= \frac{2}{3}\eta^{\frac{3}{2}}
\end{aligned}
\right\} \qquad \text{(V-39)}
$$

In the above equations η is the generic variable and stands for z or τ of the other expressions.

In the (negative) argument range over thirty, the numerical calculation of the solutions (V-35) becomes relatively simple, using the above asymptotic expansions. From equations (V-31) and (V-38), we can put an upper time limit on the validity of these expansions and write:

$$\left.\begin{aligned} t_{f_1} &\leqq \frac{z_0 - 30}{B_6^{\frac{1}{3}}} = -\frac{B_1}{B_6} - \frac{30}{B_6^{\frac{1}{3}}} \\ t_{g_1} &\leqq \frac{z_0 - 30}{C_7^{\frac{1}{3}}} = -\frac{C_1}{C_7} - \frac{30}{C_7^{\frac{1}{3}}} \end{aligned}\right\} \qquad \text{(V-40)}$$

Recalling that B_6 and C_7 are proportional to the constant velocity of endshortening, V_o , these equations reflect the fact that the asymptotic expansions can be employed longer for smaller V_o .

These equations are useful in that they can give a comparison between linear and nonlinear theory for the case of very small imperfections and constant velocity of end approach.

For the particular case of the shell, considered in the next chapter, it turned out that the asymptotic expansions were valid during a portion of the time needed for dynamic buckling.

In order to solve for f_1 and g_1 for the rest of the time, a numerical evaluation becomes more complex. This effort was abandoned, since it involves about as much as to solve the full nonlinear system numerically.

A comparison of the first equation of (V-30) with (V-15) shows agreement with Hoff's linearized column equation. Hoff [47] solved this linearized equation numerically, using one-third

order Bessel functions without taking advantage of asymptotic expansions.

Reconsidering the full nonlinear system (V-12) and assuming very small imperfections and constant rate of endshortening, we could essentially divide the time history of dynamic buckling into three distinct periods:

a) The initial period: A comparison of the order of magnitude shows that all nonlinear terms, and also $B_6 f_1 t$ and $C_7 g_1 t$, are small in regard to the other terms. A reduction to a system of second order differential equations with constant coefficients is possible. On neglecting coupling, two separate equations may be solved by the method outlined in Section 5, setting $C_2=B_2=0$.

b) The intermediate period: As time proceeds, the terms $B_6 f_1 t$ and $C_7 g_1 t$ must be included, although the nonlinear terms may still be negligible. This period is covered by the development in this section. Until the end of the intermediate period the equations are practically uncoupled.

c) The final period: The beginning of this period is characterized by the onset of dynamic buckling with increasing f_1 and g_1 so that the nonlinear terms must be retained and strong nonlinear coupling occurs between "checkerboard" and "diamond" shape buckling amplitudes.

Having gained adequate physical insight into the governing equations (V-12), let us go on to the numerical solution of these equations for a particular shell.

CHAPTER VI : NUMERICAL SOLUTION OF THE DYNAMIC BUCKLING LOAD FOR CARD'S STRINGER SHELL.

1. Card's Stringer Shell.

In order to base any numerical calculation on a realistic basis, the stringer shells, labeled cylinder 1 and 2 in Card's report [34], will be used. Card measured the axial static buckling load and the pertinent data are shown in Table (VI-1) below:

CYLINDER	ALUMINUM ALLOY	TYPE STIFF.	STIFF. LOCAT.	h [in]	L [in]	R [in]	A [in^2]	P_{max} [Kips]	σ_{max} [ksi]	n .	d [in]	N_{ox} [lb/in]
1	2024-T351	Integral	Ext.	0.0283	38	9.55	3.69	112.6	30.5	6	1.0	800
2	2024-T351	Integral	Int.	0.0277	38	9.55	3.72	48.0	12.9	6	1.0	1875

Table (VI-1) : Card's Stringer Shell Data from Reference [34].

A refers to the total cross sectional area (stringer + monocoque shell), P_{max} is the total load obtained by multiplying σ_{max} by A; n is the number of circumferential diamond buckles, which corresponds to the definition used in this dissertation.

A sketch of the stringer cross sectional dimensions is given in Figure (VI-1) below:

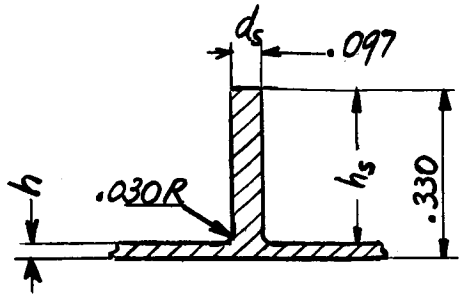

Figure (VI-1): Stringer Cross Section Dimensions

In the calculations of this report, the slight increase in area due to the fillet radius on the cross section is neglected. It is assumed, furthermore, that h=0.0283 in for both cylinders, 1 and 2. The necessary geometry and material input data are collected in Table (VI-2) below:

ν	$E=E_s$	E_R	G_s	G_R	ρ	ρ_s	ρ_R
	$[lb/in^2]$	$[lb/in^2]$	$[lb/in^2]$	$[lb/in^2]$	$[lb sec^2/in^4]$	$[lb sec^2/in^4]$	$[lb sec^2/in^4]$
0.3	10.5×10^6	0	4.038×10^6	0	2.59×10^{-4}	2.59×10^{-4}	0

h	A_s	A_R	d	ℓ	I_{sc}	I_{Rc}	J_s
[in]	$[in^2]$	$[in^2]$	[in]	[in]	$[in^4]$	$[in^4]$	$[in^4]$
0.0283	0.02926	0	1.0	1000*	2.216×10^{-4}	0	7.242×10^{-5}**

J_R	$\bar{z}_s$	$\bar{z}_R$	L	R
$[in^4]$	[in]	[in]	[in]	[in]
0	$\pm$ 0.165 ***	0	38.0	9.55

Table (VI-2) : Geometry and Material Input Parameters for Numerical Calculations of Card's Shell.

* This number is used in the computer program to prevent $K_R = \frac{E_R A_R}{\ell}$ from becoming zero over zero and does not actually enter into the calculations.

** Calculated on the basis of the theory of elasticity solution of twisting of a bar of rectangular cross section from reference [58], p.278, assuming free warping.

*** + for internal stiffeners, - for external stiffeners.

Since the data listed in Table (VI-2) are characteristic of the particular geometry and material composition of the eccentrically reinforced shell, they will be referred to as geometry and material input parameters.

It will be shown in the next chapter that the theory of the dynamic buckling of the eccentrically reinforced shell with its numerical method of solution can be applied successfully to the static case by assuming a small constant velocity V_o .

2. The Runge-Kutta Method of Integrating the Nonlinear Coupled Differential Equations.

The dynamic buckling of a monocoque cylindrical shell was investigated in reference [51]. A set of differential equations, similar to (V-12), was derived. The report indicated that a Runge-Kutta method was utilized in the numerical solution. No details are given, however, on the type of Runge-Kutta formula and the chosen step size.

It is convenient at this point to work with variables that are standard in numerical work. Let us therefore use:

$$\left.\begin{aligned} x &= t \\ y &= f_1 \\ z &= g_1 \end{aligned}\right\} \qquad \text{(VI-1)}$$

The nonlinear system of equations (V-12) can therefore be written as:

$$\left.\begin{aligned} y'' = F_1(x,y,z) &= B_1 y + B_2 z + B_3 yz + B_4 yz^2 + B_5 y^3 \\ &\quad + B_6 y \frac{1-e^{-\gamma x}}{\gamma} + B_7 \\ z'' = F_2(x,y,z) &= C_1 z + C_2 y + C_3 z^2 + C_4 y^2 + C_5 y^2 z \\ &\quad + C_6 z^3 + C_7 z \frac{1-e^{-\gamma x}}{\gamma} + C_8 \frac{1-e^{-\gamma x}}{\gamma} + C_9 \end{aligned}\right\} \qquad \text{(VI-2)}$$

The classical Runge-Kutta procedure is a fourth order method, e.g. a Taylor series expansion would agree with this method up to and including the fourth order term. It is self-starting in that no previous values of the function is required.

One of the serious drawbacks of the Runge-Kutta method is the lack of simple means for estimating the error. Even if the truncation error is small, a Runge-Kutta method may produce extremely inaccurate results under unfavorable conditions. Roundoff or truncation errors may become magnified as the solution is carried out for larger and larger x, which is pointed out in reference [59], p.329.

Despite these disadvantages, the method was tried out on the

strength that it worked apparently for the case of the monocoque shell of reference [51].

Since F_1 and F_2 of (VI-2) do not contain any first derivatives of y and z, we can make use of some specialized formula, given in reference [60], p.359, for $y'' = f(x,y)$. Extending this formula to a system of two simultaneous equations, we have:

$$
\left.
\begin{aligned}
k_1 &= h\,F_1(x_n; y_n; z_n) \\
k_2 &= h\,F_1\left(x_n + \tfrac{h}{2}; y_n + \tfrac{h}{2}y'_n + \tfrac{h}{8}k_1; z_n + \tfrac{h}{2}z'_n + \tfrac{h}{8}l_1\right) \\
k_3 &= h\,F_1\left(x_n + h; y_n + hy'_n + \tfrac{h}{2}k_2; z_n + hz'_n + \tfrac{h}{2}l_2\right) \\
\Delta y &= h\left[y'_n + \tfrac{1}{6}(k_1 + 2k_2)\right] \\
\Delta y' &= \tfrac{1}{6}(k_1 + 4k_2 + k_3) \\
l_1 &= h\,F_2(x_n; y_n; z_n) \\
l_2 &= h\,F_2\left(x_n + \tfrac{h}{2}; y_n + \tfrac{h}{2}y'_n + \tfrac{h}{2}k_1; z_n + \tfrac{h}{2}z'_n + \tfrac{h}{8}l_1\right) \\
l_3 &= h\,F_2\left(x_n + h; y_n + hy'_n + \tfrac{h}{2}k_2; z_n + hz'_n + \tfrac{h}{2}l_2\right) \\
\Delta z &= h\left[z'_n + \tfrac{1}{6}(l_1 + 2l_2)\right] \\
\Delta z' &= \tfrac{1}{6}(l_1 + 4l_2 + l_3)
\end{aligned}
\right\} \quad \text{(VI-3)}
$$

h refers here to the (constant) step size.

A computer program has been developed that calculates the B's and C's for the geometry and material input parameters of the particular shell under consideration for selected values of V_o, f_o, g_o, γ, m and n. The first program was based strictly on the above Runge-Kutta formulas and is not included in this dissertation.

3. The Application of the Runge-Kutta Method to Card's Stringer Shell and its Paradoxial Results.

This section discusses some results which were obtained by using the Runge-Kutta method. A critical review of these results, based strictly on physical insight, will reveal their paradoxial nature. The reasoning will be backed-up by an improved method, shown in a later section.

The geometry and material input parameters for Card's shell, Table(VI-2), are used. A constant rate of endshortening of 100 ips and initial imperfections of the order of half the monocoque shell thickness are assumed ($f_o=g_o=0.014$ in). Corresponding to each pair of mode numbers, m and n, there results a pair of amplitude functions, $f_1=f_1(t)$ and $g_1=g_1(t)$, after integrating the system (V-12). For each pair, m and n, an axial load $\bar{N}_{ox}=\bar{N}_{ox}(t)$ can be calculated from (V-9). Of the family of curves, $\bar{N}_{ox}=\bar{N}_{ox}(m;n;t)$, the lowest maximum will be defined as the critical dynamic buckling load.

Figures (VI-2) to (VI-4) depict results obtained by the Runge-Kutta method with a step size of 10 microseconds. The latter constitutes only a fraction of the natural period, corresponding to the lowest natural frequency of the linearized problem. In each Figure, the so-called aspect ratio of the buckle is kept constant. The aspect ratio is defined by:

$$\nu = \frac{b}{a} = \left(\frac{\pi R}{L}\right)\left(\frac{m}{n}\right) \qquad \text{(VI-4)}$$

Pairs of m and n, corresponding to aspect ratios of roughly 0.8, 1.2, and 1.6, were chosen.

In considering these Figures, it must be remarked that the arrows on the ends of the curves indicate a sharp drop of $\bar{N}_{ox}$ to a large negative value. This is physically not realizable, since it implies that the ends of the shell pull apart from each other, while they must approach each other by assumption.

It must be noted further that the maxima become lower and lower with increasing m and n. Intuitively, however, one would associate a "stiffer" configuration with higher modes.

The criterion for selecting the critical dynamic buckling load obviously fails, since it is expected that the maxima will get lower and lower with increasing mode numbers.

It is therefore apparent that the sharp drop-off of these curves is due to instability of the Runge-Kutta method. It is proposed to call this phenomenon somewhat facetiously "Runge-Kutta Buckling".

This conclusion is backed-up by Figure (VI-2*) which shows the curve $\bar{N}_{ox}=\bar{N}_{ox}(t)$ for m=n=12, calculated on the basis of an improved method. Comparing it with the corresponding curve of Figure (VI-2), the instability of the method becomes clear.

The Runge-Kutta method was also tried for small rates of end-shortening which approach static buckling. The method became unstable after a certain time, even though the same small step size of 10 microseconds was maintained.

A closed-form solution, based on the system of equations of

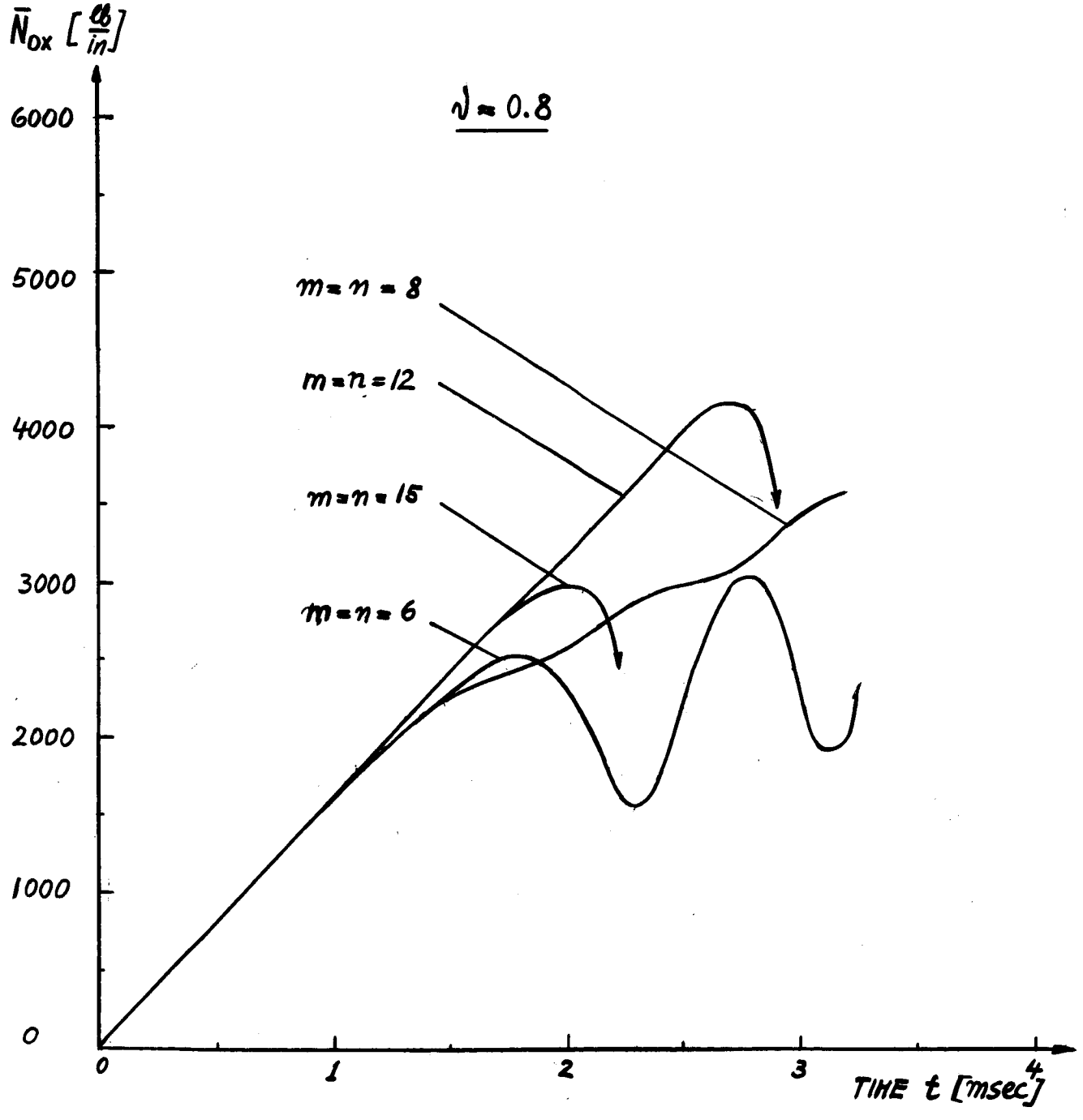

Figure (VI-2) : Dynamic Buckling Loads of Card's Shell by the Runge-Kutta Method, Int.Stiffened, Incl. Rot.Iner. Data: ν=0.8 ; V_o=100 ips ; γ=0 ; $f_o=g_o$=0.014 in

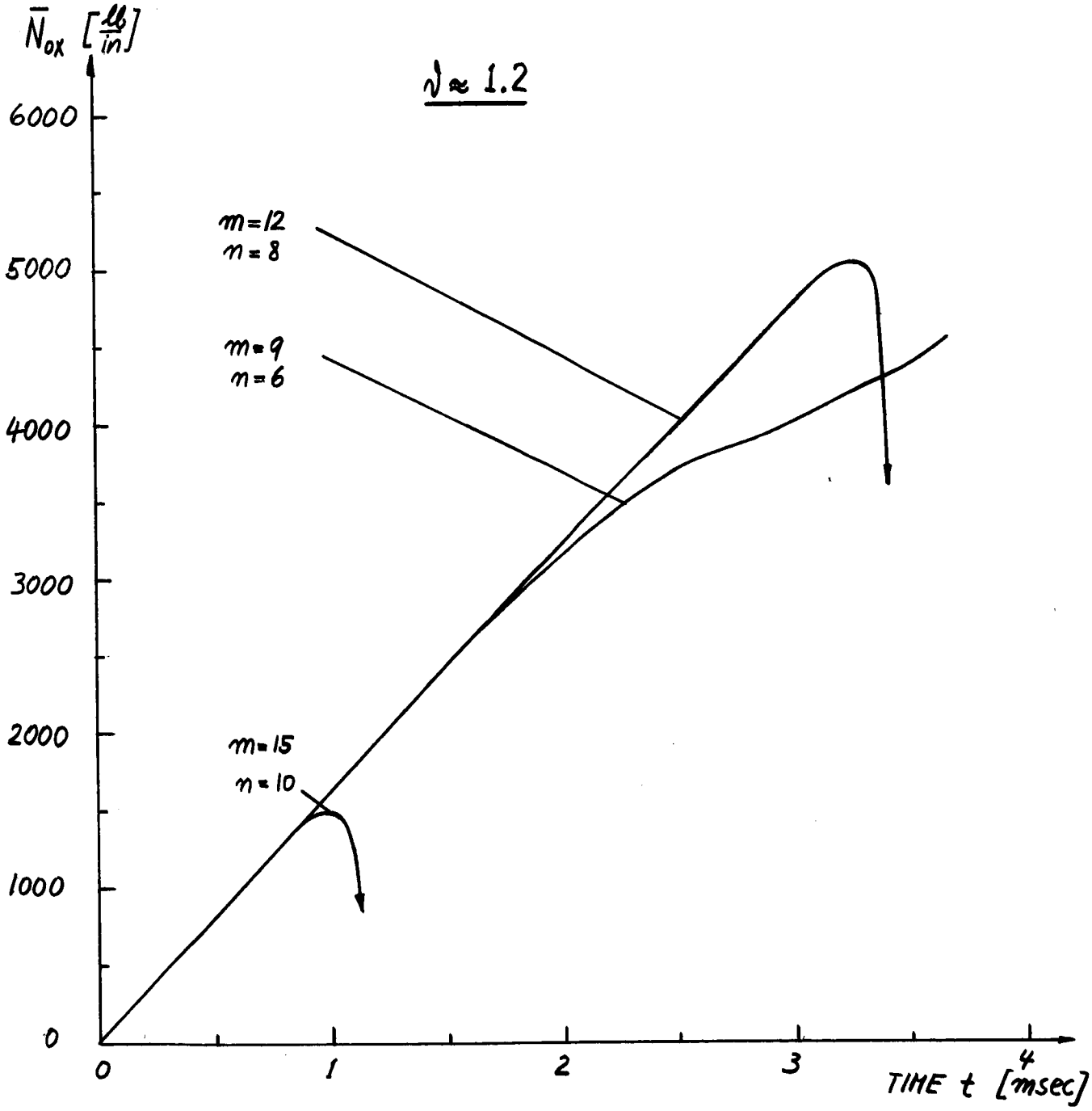

Figure (VI-3) : Dynamic Buckling Loads of Card's Shell by the Runge-Kutta Method, Int.Stiff.,Incl.Rot.Iner. Data: ν =1.2 ; V_o=100 ips ; γ=0 ; $f_o=g_o$=0.014 in.

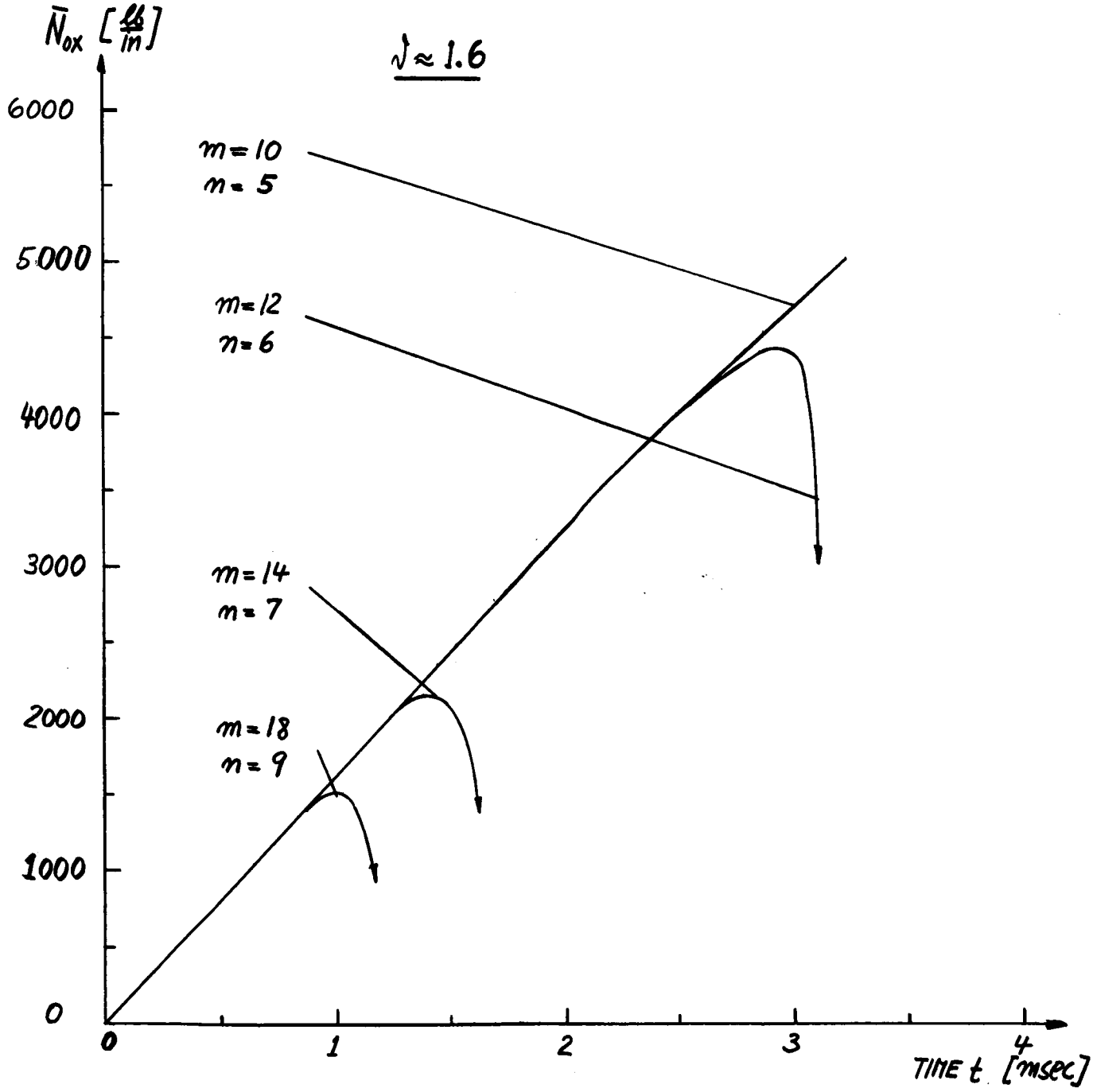

Figure (VI-4) : Dynamic Buckling Loads of Card's Shell by the Runge-Kutta Method, Int.Stiff.,Incl.Rot.Iner. Data: ν=1.6 ; V_o=100 ips ; γ=0 ; $f_o=g_o$=0.014 in.

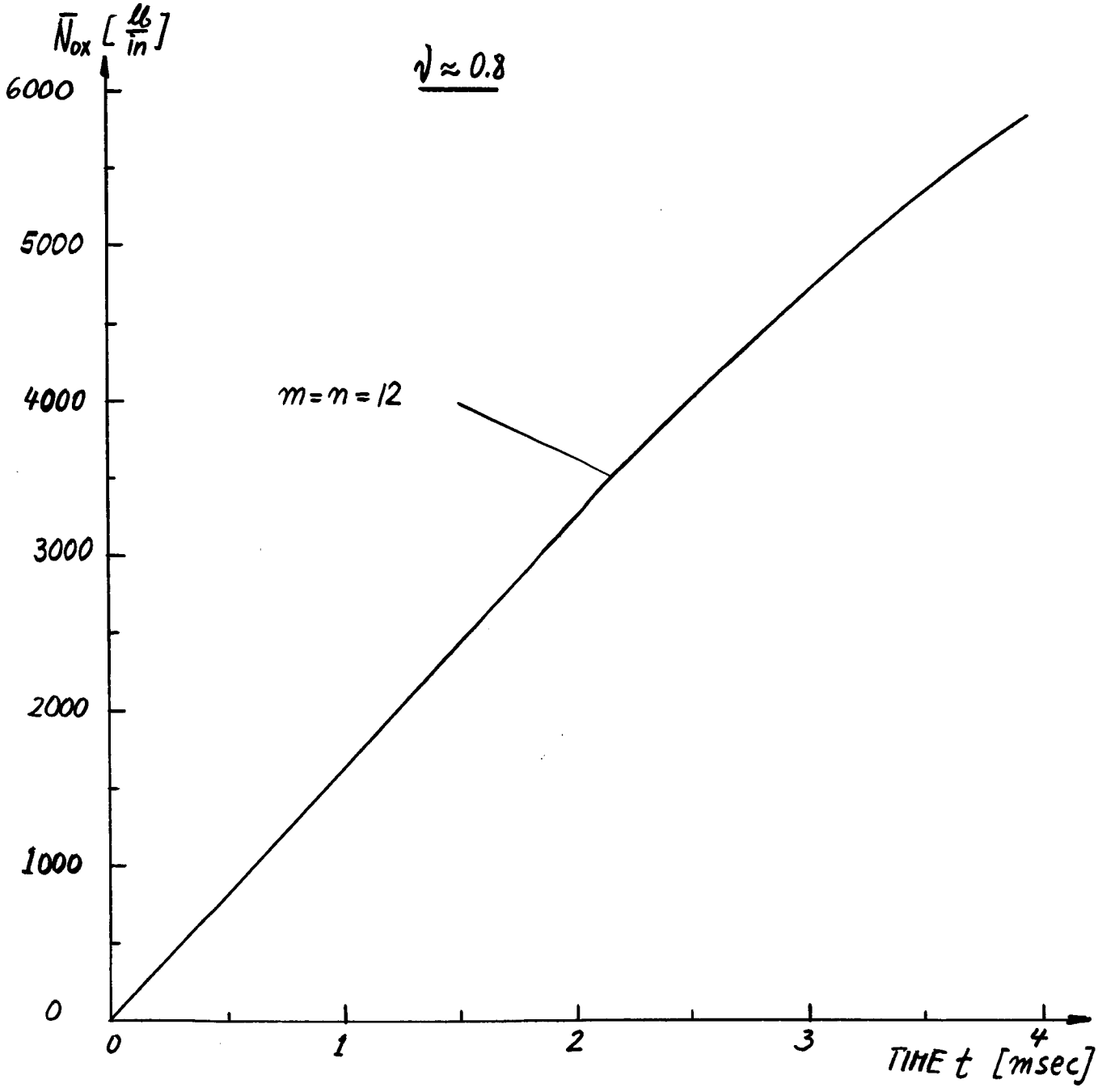

Figure (VI-2*) : Dynamic Buckling Load of Card's Shell by the Combined Method; Int.Stiff. Incl.Rot.Iner.
Data: ν =0.8 ; V_o=100 ips ; γ=0 ; $f_o=g_o$=0.014 in.

* See Section 4.

Section 5 (Linear Differential Equations with Constant Coefficients) was compared with a Runge-Kutta method solution of the same linearized problem. For V_o=0.01 ips, f_o=g_o=0.001 in, m=n=12 and γ=0, calculations were made every 10 microseconds, up to one millisecond. Both results compared quite favorably.

The results of reference [51] for the monocoque cylindrical shell, calculated on the basis of a Runge-Kutta method, are only given for equal m=n. They exhibit the same trend that the maxima of $\overline{N}_{ox}$ decrease with increasing m=n. A criterion for selecting the critical dynamic buckling load is based on the quantity $\zeta=(f_1+g_1)/h=\zeta(m;n;t)$. On plotting $\zeta(t)$ for various m=n values, it is argued that the ζ, corresponding to the critical dynamic buckling load, is the one that departs earliest from the time-axis and also assumes the maximum first. The plots of the $\zeta(t)$ curves for various m=n show, however, that the departure and the maximum value are attained earlier and earlier, as m=n increases. No definite conclusion can be reached. It is therefore strongly suspected that "Runge-Kutta Buckling" has not been recognized in the results of reference [51].

4. The Combined Runge-Kutta Predictor-Corrector Method.

A predictor-corrector method makes use of previously calculated values of the function, predicts the function at the next step ahead, uses this information to correct it with an improved value (iteration). This method is therefore not selfstarting, but is ideal to be combined with the Runge-Kutta method. This combination will henceforth be called simply the combined method.

We can again take advantage of the fact that F_1 and F_2 of (VI-2) do not contain the first derivatives of y and z. We select a set of fourth order formulas, which Hamming, see reference [61], p.214, calls very attractive. Further details can be obtained from this reference, since we only list these formulas:

$$\text{PREDICTORS} \left\{ \begin{aligned} y_{n+1} &= 2y_{n-1} - y_{n-3} + \frac{4h^2}{3}(y''_n + y''_{n-1} + y''_{n-2}) \\ z_{n+1} &= 2z_{n-1} - z_{n-3} + \frac{4h^2}{3}(z''_n + z''_{n-1} + z''_{n-2}) \end{aligned} \right\} \quad \text{(VI-5)}$$

$$\text{CORRECTORS} \left\{ \begin{aligned} y_{n+1} &= 2y_n - y_{n-1} + \frac{h^2}{12}(y''_{n+1} + 10y''_n + y''_{n-1}) \\ z_{n+1} &= 2z_n - z_{n-1} + \frac{h^2}{12}(z''_{n+1} + 10z''_n + z''_{n-1}) \end{aligned} \right\} \quad \text{(VI-6)}$$

Formulas (VI-5) use information of the current point n and reach back three steps to predict the value one step ahead. That value is then used in conjunction with F_1 and F_2 to calculate the second derivatives. As seen from (VI-6), these derivatives are utilized in the corrector, which also uses information of the current point, but reaches back only one step.

The predictor-corrector method can therefore be started, once the first four consecutive values are known. It is therefore only logical to calculate the first four points by the Runge-Kutta method and then carry on with the Predictor-Corrector procedure. This is done with the computer program given in Appendix B, where further comments are made.

5. Application of the Combined Method to Card's Shell.

The Figures of the following pages present the results of a calculation of the dynamic buckling loads of Card's shell, using the combined method. They are based on the data: V_o=100 ips γ =0; $f_o=g_o$=0.014 in. The mode numbers are varied according to the following scheme: for each fixed n (6;8;10), m is increased in steps of 2, starting with 2 and ending with 10. The lowest value of n was taken 6 since this corresponds to Card's static test. Figures (VI-5) through (VI-7) present the results for the internally reinforced shell. According to our criterion* for critical buckling, it is clear that the lowest maximum is obtained for m=4 and n=6, the corresponding critical dynamic buckling load being $\bar{N}_{oxc}$=2456 lb/in. This amounts to about three times the static buckling load measured by Card (See Table (VI-1)). Corresponding to the critical dynamic buckling load, the time histories of f_1 and g_1 are depicted in Figure (VI-8). Similar results are given for the externally reinforced shell in Figures (VI-9) through (VI-12). Notably, the critical dynamic buckling load occurs now for m=4 and n=8 and amounts to 3123 lb/in.

*the critical dynamic buckling load is the lowest maximum of $\bar{N}_{ox}(t)$

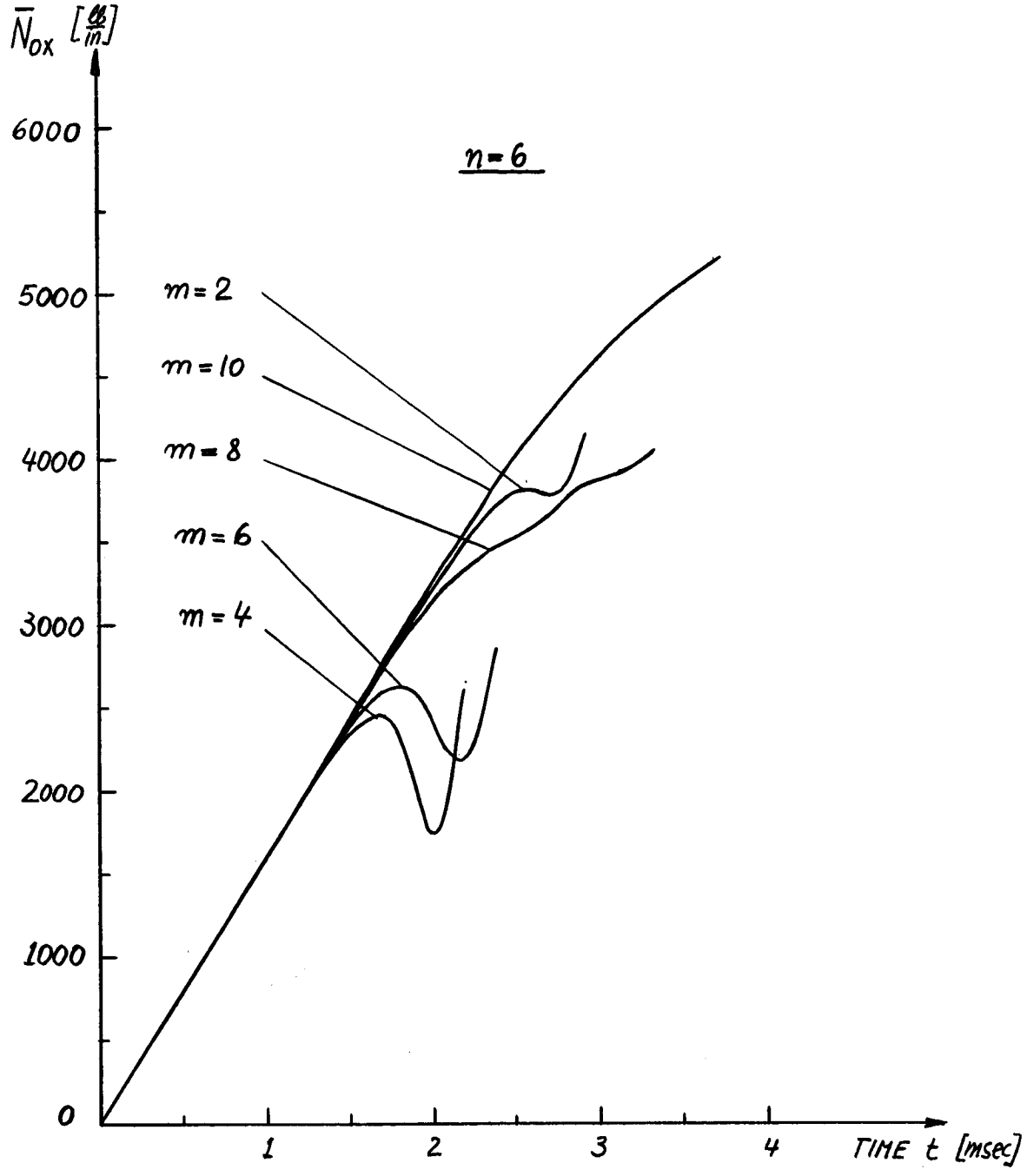

Figure (VI-5) : Dynamic Buckling Loads of Card's Shell by the Combined Method, Internally Stiffened, Including Rotatory Inertia.
Data: V_o=100 ips ; γ = 0 sec^{-1}; n=6 ;
$f_o=g_o$=0.014 in.

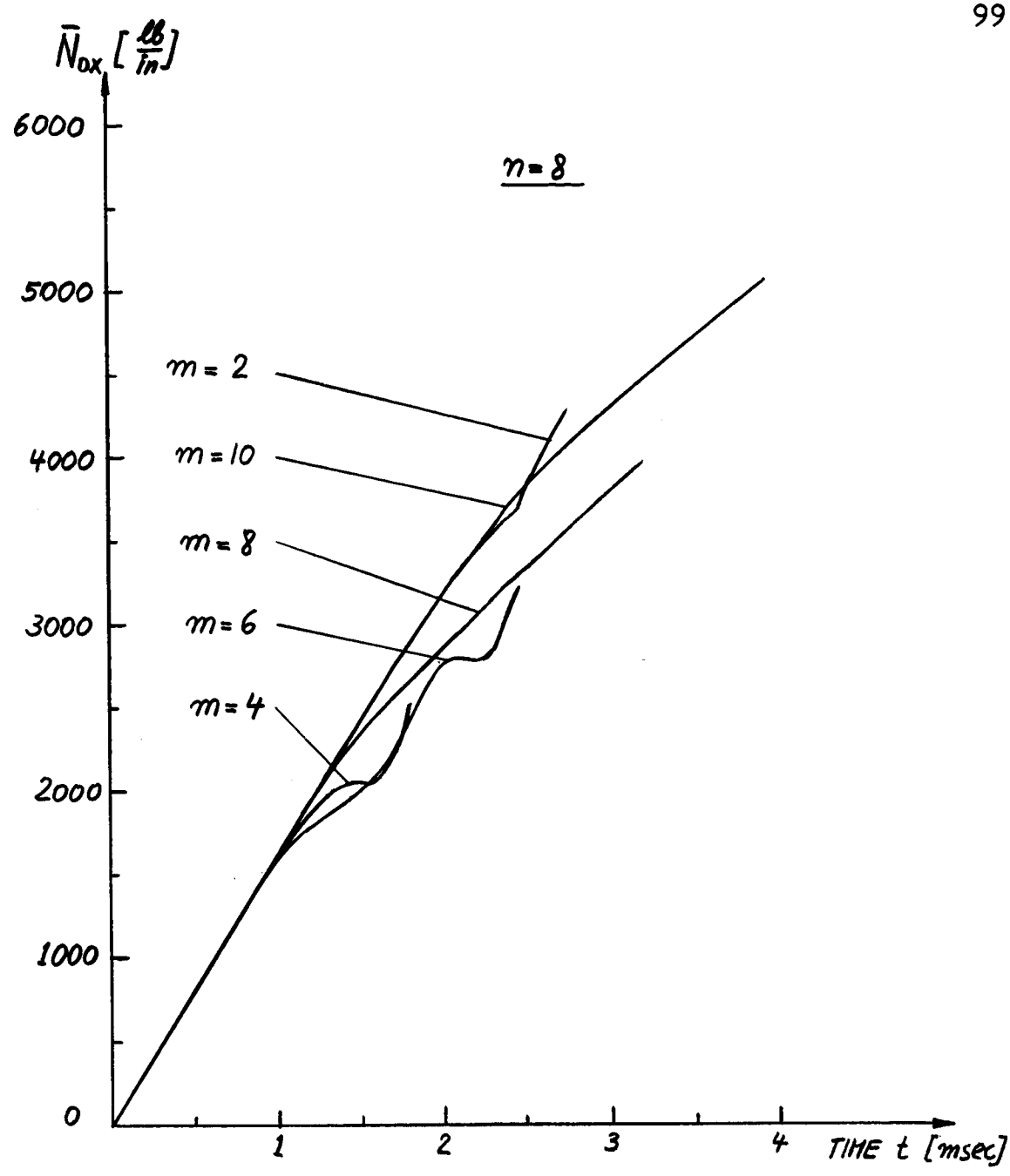

Figure (VI-6) : Dynamic Buckling Loads of Card's Shell by the Combined Method, Internally Stiffened, Including Rotatory Inertia.
Data: V_o=100 ips ; γ=0 sec^{-1} ; n=8 ;
$f_o=g_o$=0.014 in.

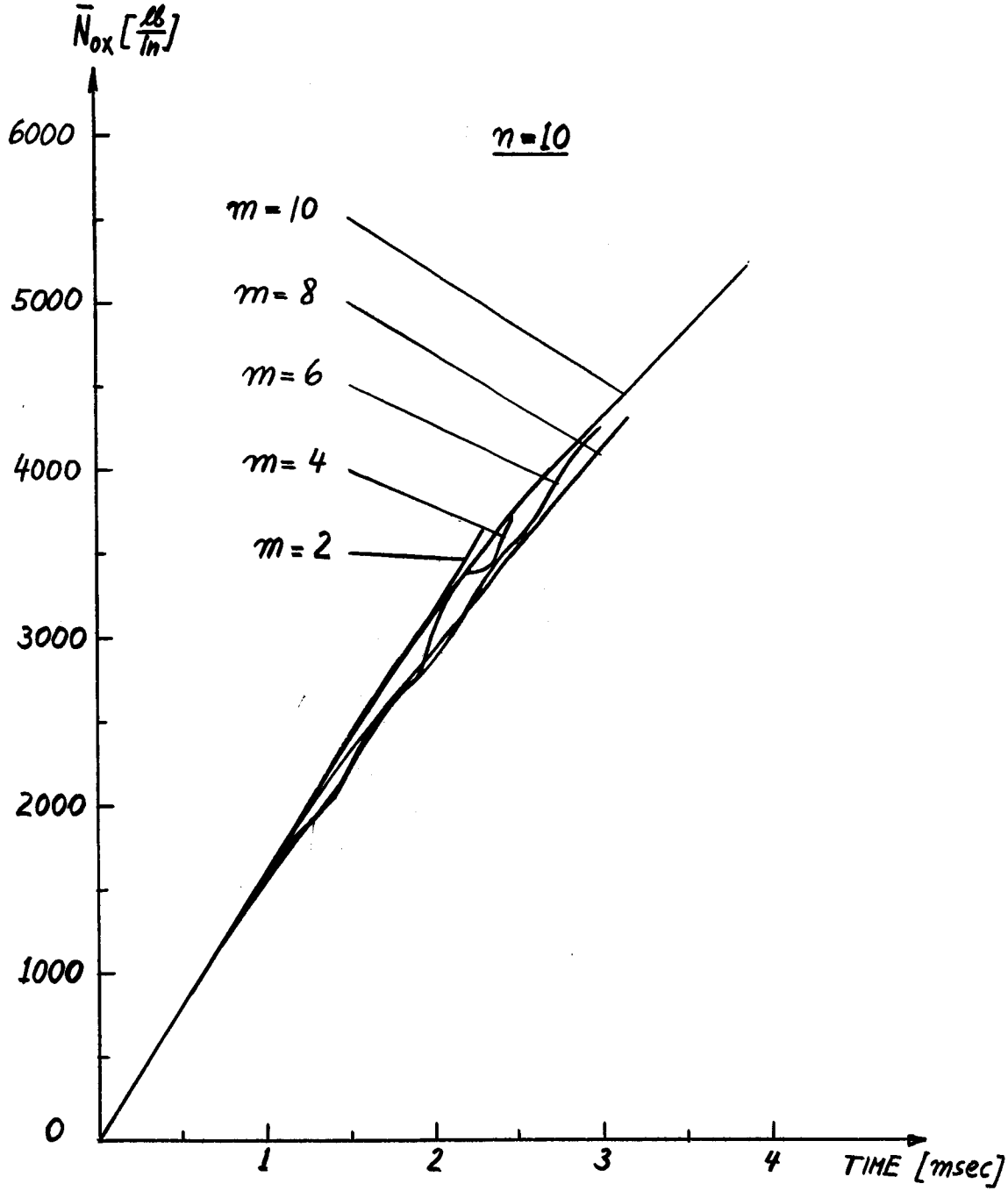

Figure (VI-7) : Dynamic Buckling Loads of Card's Shell by the Combined Method, Internally Stiffened, Including Rotatory Inertia.
Data: V_o=100 ips ; γ=0 sec^{-1} ; n=10 ;
$f_o=g_o$=0.014 in.

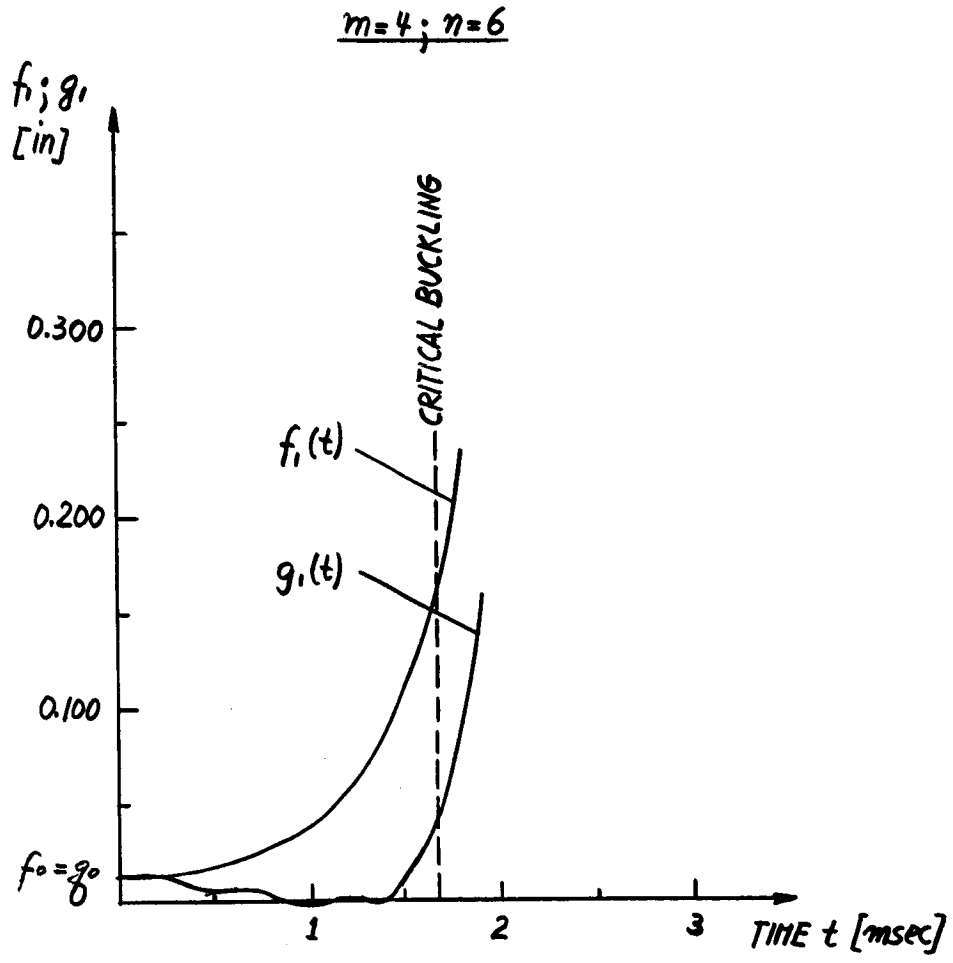

Figure (VI-8) : Critical Buckling Amplitudes of Card's Shell by the Combined Method, Internally Stiffened, Including Rotatory Inertia.
Data: V_o=100 ips ; γ=0 sec^{-1} ; m=4 ; n=6 ;
$f_o=g_o$=0.014 in.

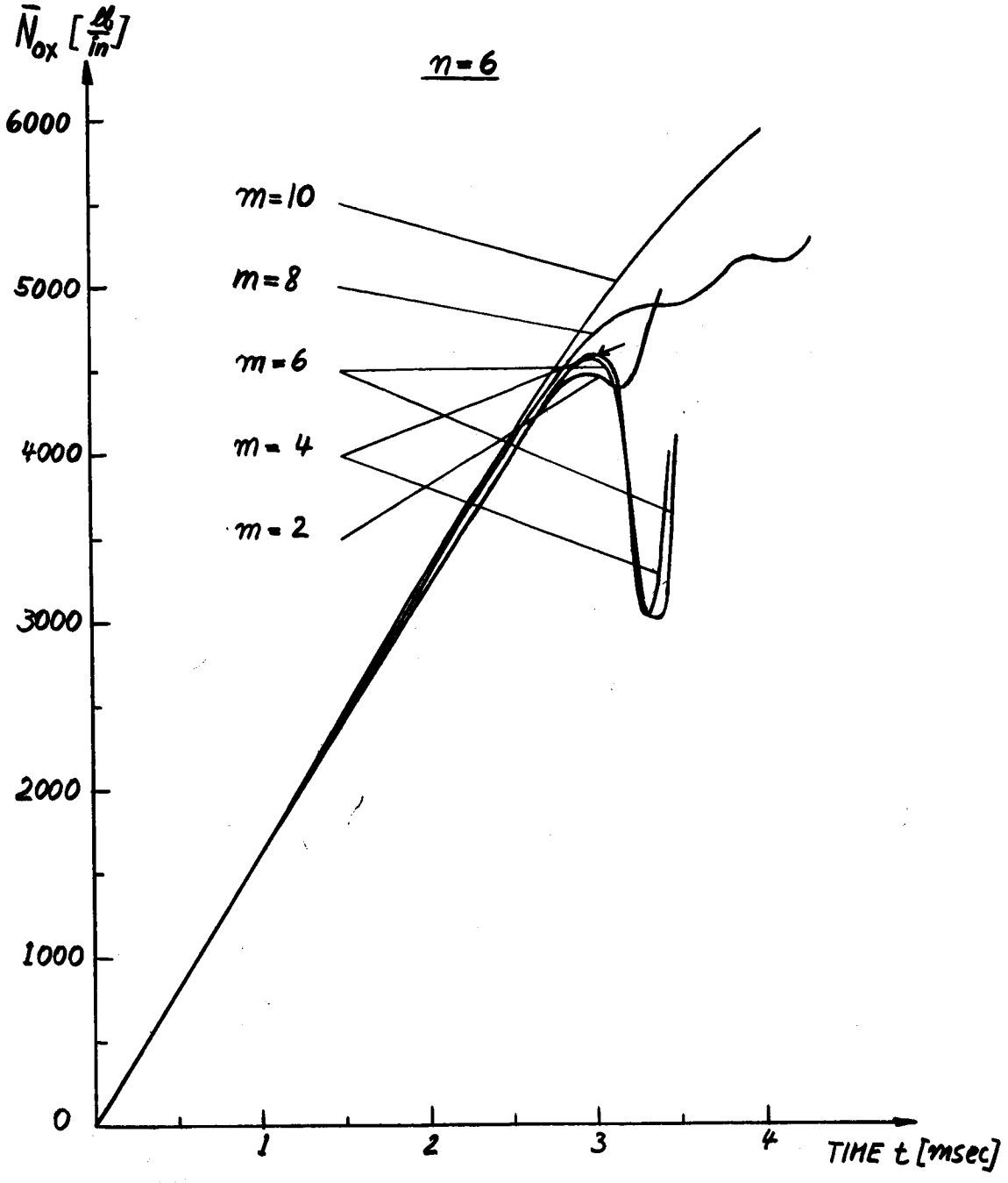

Figure (VI-9) : Dynamic Buckling Loads of Card's Shell by the Combined Method, Externally Stiffened, Including Rotatory Inertia.
Data: V_o=100 ips ; γ=0 sec^{-1} ; n=6 ;
$f_o=g_o$=0.014 in.

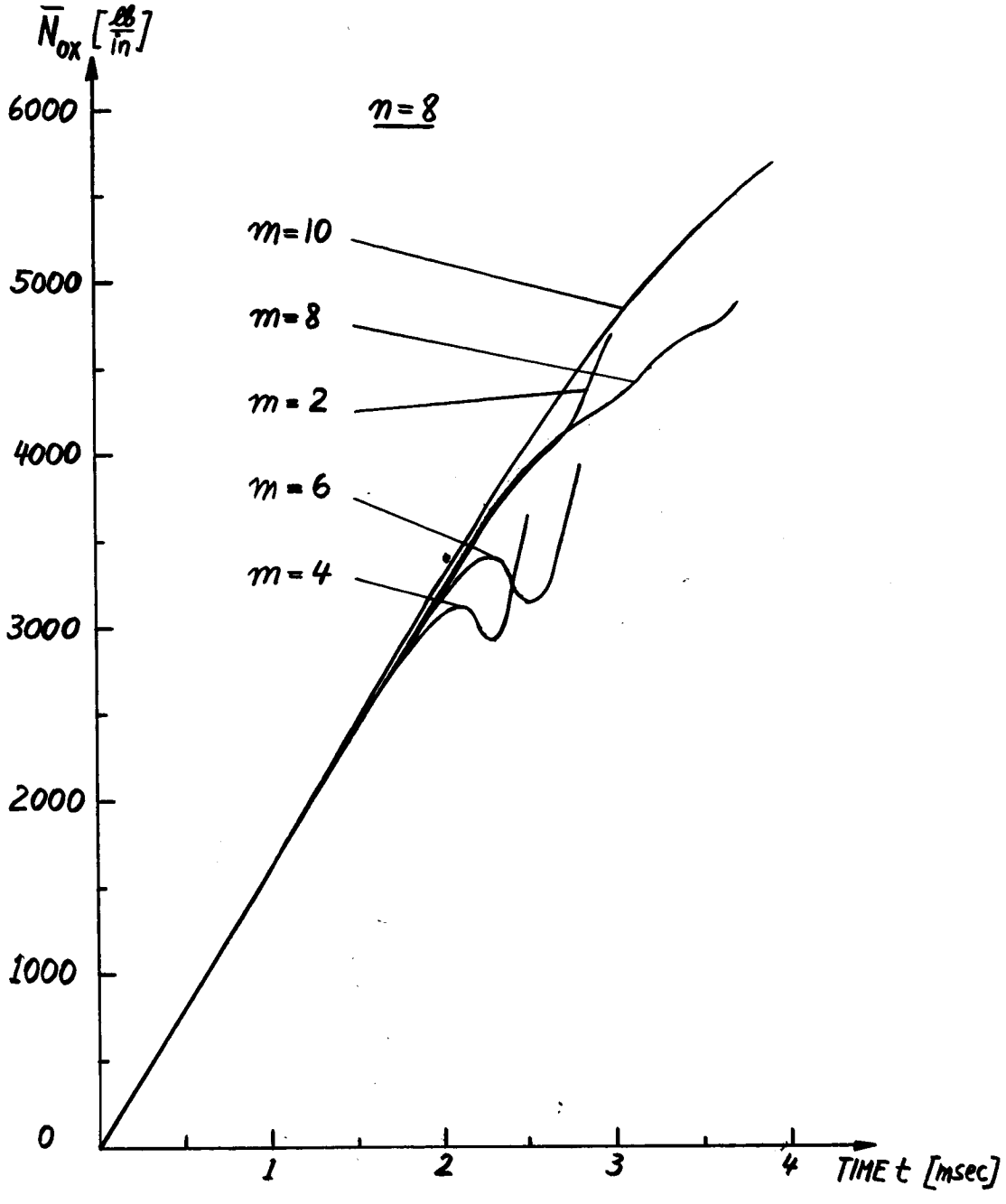

Figure (VI-10) : Dynamic Buckling Loads of Card's Shell by the Combined Method, Externally Stiffened, Including Rotatory Inertia.
Data: V_o=100 ips ; γ=0 sec^{-1} ; n=8 ;
$f_o=g_o$=0.014 in.

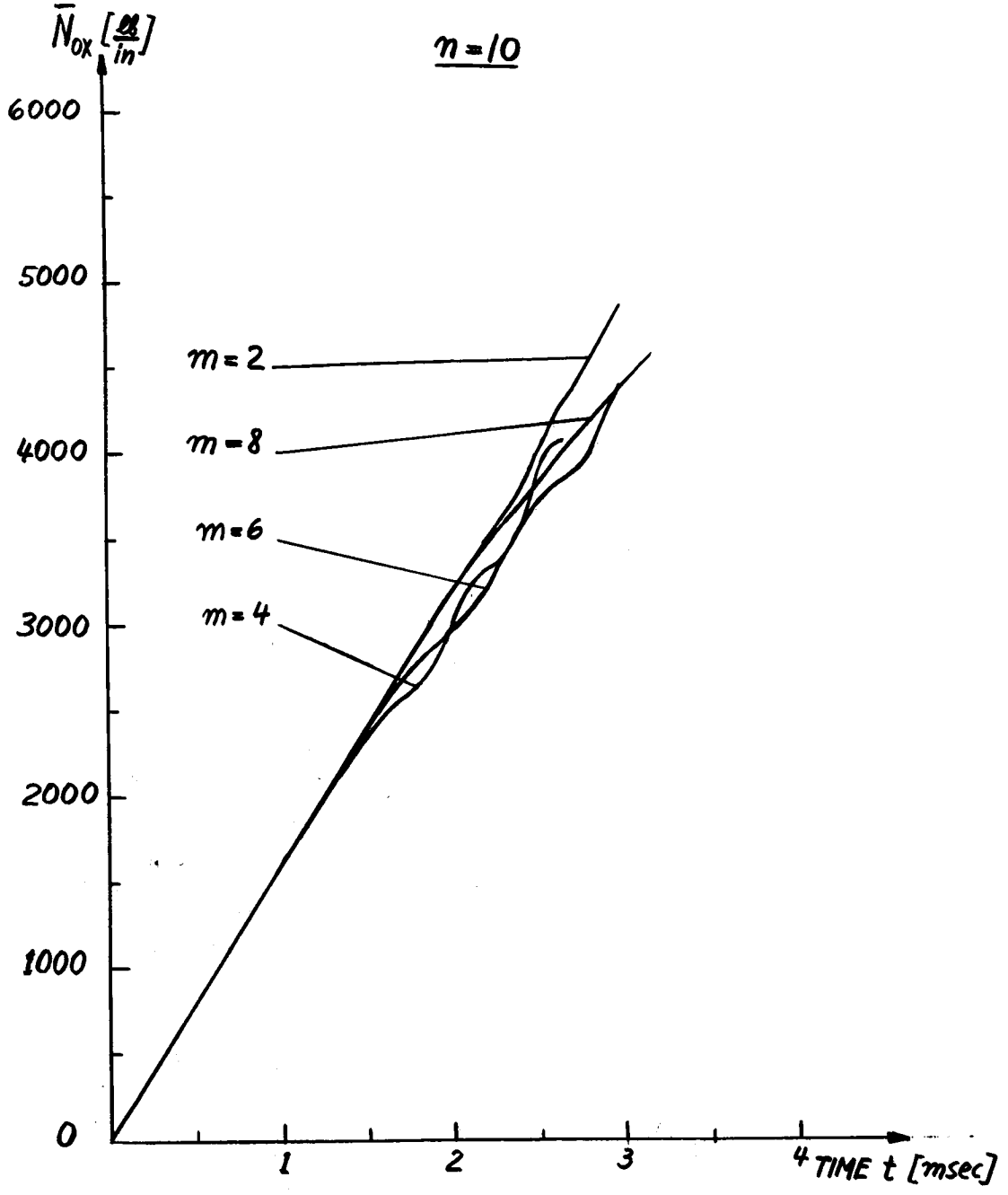

Figure (VI-11) : Dynamic Buckling Loads of Card's Shell by the Combined Method, Externally Stiffened, Including Rotatory Inertia.
Data: V_o=100 ips ; γ =0 sec^{-1} ; n=10 ;
$f_o=g_o$=0.014 in.

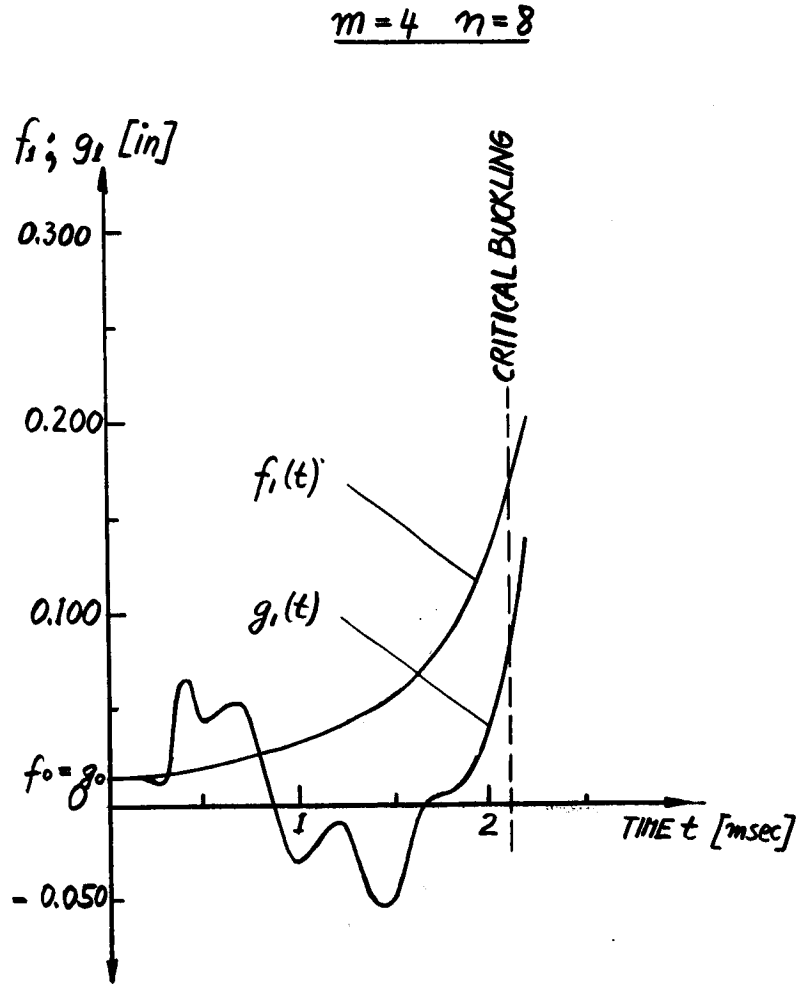

Figure (VI-12) : Critical Buckling Amplitudes of Card's Shell by the Combined Method, Externally Stiffened, Including Rotatory Inertia.
Data: V_o=100 ips ; γ = 0 sec^{-1} ; m=4 ; n=8 ;
$f_o=g_o$=0.014 in.

It can also be concluded that the dips of the $N_{ox}(t)$ curves after the first maximum are small. The smallness of the dip seems to be due to the reinforcements. This reasoning is based on a comparison with static data of the monocoque shell. In the latter, the buckling load is usually plotted versus unit endshortening. Since the rate of endshortening is constant for the curves of our Figures, the abscissa might as well be taken as unit endshortening. Nonlinear static monocoque curves rise only slowly after a considerable dip to the postbuckling value and reach soon into the super-large deflection region. Recalling analogous plate data, it must be concluded that the stringer-stiffened shell has more of a plate-like behavior, the transition being dependent on the stiffener-monocoque shell configuration.

Considering the time histories of f_1 and g_1 of Figures (VI-8) and (VI-12), it can be seen that theses amplitudes become quite large after the time, when N_{ox} has reached its critical value. All plots are therefore only carried out a small amount over the critical time, since much further, even the large deflection theory is no longer valid.

As a last remark, we observe that for large mode numbers, say $m > 6$ and $n > 8$, the curves $N_{ox}(t)$ no longer attain any maximum, in sharp contrast to the "Runge-Kutta Buckling" of Section 3. Our intuitive physical insight, that lead to clear up the previous paradoxial situation, is therefore confirmed by the calculations.

6. Factors Affecting the Critical Dynamic Buckling Load of Card's Stringer Shell.

It is quite clear that any extensive investigation of this type requires a large amount of computer time. Within the scope of this dissertation and the available computer time, it is therefore not possible to consider a wide variety of parameter changes and their effect on the results.
A modest effort was made, however, to show the influence of the following factors:

- Rotatory Inertia
- Magnitude of Constant Rate of Endshortening
- Size of the Initial Imperfections
- Direction of Initial Imperfections
- Time Constant of Exponentially Decaying Rate of Endshortening

a) The Effect of Rotatory Inertia

The rotatory inertia affects the coefficients B and C since $\bar{m}_1$ and $\bar{m}_2$ appear in the denominator of the definitions of these coefficients. $\bar{m}_1$ is defined by eqution (A-3), while $\bar{m}_2$ is given by (A-13). Both quatities are somewhat larger than the smeared-out mass $\bar{m}$, the increase being proportional to $I_{\bar{m}}$ and depending on the mode numbers m and n. $I_{\bar{m}}$ is defined by equation (I-26). In the particular case of Card's stringer

shell, the effect of rotatory inertia is expected to be somewhat smaller, since the contribution of the rings to $I_{\bar{m}}$ is absent. Since the increase over $\bar{m}$ is proportional to $(\alpha^2+\beta^2)\ I_{\bar{m}}$, large mode numbers are required to make this increase considerable, $I_{\bar{m}}$ being small for a stringer-only shell. It was shown in the last section that critical dynamic buckling occurs for relatively small mode numbers (m=4 ; n=6;8). Table (VI-3) below confirms these expectations.

m	n	INTERNALLY STIFF.		EXTERNALLY STIFF.	
		W. R. I.* $1^{st}\bar{N}_{ox\,max}$ [lb/in]	W.O.R.I** $1^{st}\bar{N}_{ox\,max}$ [lb/in]	W.R.I * $1^{st}\bar{N}_{ox\,max}$ [lb/in]	W.O.R.I** $1^{st}\bar{N}_{ox\,max}$ [lb/in]
2	6	3834	3834	4494	4494
4	6	<u>2456</u>	2449	4615	4612
6	6	2627	2623	4885	4583
4	8	-	-	<u>3123</u>	3115
6	8	2812	2801	3418	3412

* With Rotatory Inertia ** Without Rotatory Inertia

<u>Table (VI-3)</u> : Effect of Rotatory Inertia on the Dynamic Buckling of Card's Stringer Shell.
Data: V_o=1oo ips; γ=0 1/sec; $f_o=g_o$=0.014 in

The critical dynamic buckling loads, which were determined previously, are underligned in the above table.
In all cases, the effect of rotatory inertia is at most a fraction of one percent and can therefore be neglected in future considerations of Card's stringer shell.

b) The Effect of the Magnitude of Constant Rate of Endshortening

The magnitude of V_o affects primarily the coefficients B_6 and C_7 which are proportional to V_o. C_8 is also influenced through Poisson-type interaction. It is expected that smaller V_o will result in smaller critical dynamic buckling loads. With V_o approaching the static compression testing machine range, static buckling loads should be obtained. The latter will be demonstrated in the next chapter.

In Table (VI-4) below, calculated results are presented for V_o's of 100 ips and 50 ips.

m	n	INTERNALLY STIFF.		EXTERNALLY STIFF.	
		V_o=100 ips	V_o=50 ips	V_o=100 ips	V_o=50 ips
		1st $\bar{N}_{ox\,max}$	1st $\bar{N}_{ox\,max}$	1st $\bar{N}_{ox\,max}$	1st $\bar{N}_{ox\,max}$
		[lb/in]	[lb/in]	[lb/in]	[lb/in]
2	6	3834	2285	4494	2990
4	6	2449*	1815	4612	4029
6	6	2623	2347	4583	4287
4	8	-	2129	3115	2549
6	8	2801	-	3412	3130

*underligned values are critical dynamic buckling loads

Table (VI-4) : Effect of V_o on Dynamic Buckling Load of Card's Shell for Constant Rate of Endshortening. Data: γ=0 sec^{-1}; f_o=g_o=0.014 in; Rot.Iner. negl.

These results confirm our expectations.

c) The Effect of the Size of the Initial Imperfections.

It is expected that larger initial imperfections reduce the critical dynamic buckling load more drastically than smaller ones. In Table(VI-5) below, comparative data are presented for dynamic buckling loads calculated on the basis of $f_o=g_o=0.001$ in and $f_o=g_o=0.014$ in, for the same constant rate of endshortening $V_o=100$ ips.

m	n	INTERNALLY STIFF.		EXTERNALLY STIFF	
		$f_o=g_o$ [in]	$f_o=g_o$ [in]	$f_o=g_o$ [in]	$f_o=g_o$ [in]
		0.001	0.014	0.001	0.014
		1st $\bar{N}_{ox\,MAX}$	1st $\bar{N}_{ox\,MAX}$	1st $\bar{N}_{ox\,MAX}$	1st $\bar{N}_{ox\,MAX}$
		[lb/in]	[lb/in]	[lb/in]	[lb/in]
4	6	4042	<u>2449</u> *	7807	4612
4	8	3391	-	5621	<u>3115</u>

* underligned values are critical dynamic buckling loads

<u>Table (VI-5)</u> : Effect of the Initial Imperfection Size on the Dynamic Buckling Loads of Card's Shell. Data: $\gamma=0$ 1/sec; $V_o=100$ ips.

It is seen therefore that the effect of the imperfection size is extremely important.

It must be remarked in general that only the underligned values were minimized according to our definition of critical dynamic buckling load. The other values are just calculated by using the same mode numbers and determining the first maximum of $\bar{N}_{ox}$.

d) The Effect of the Direction of the Initial Imperfections.

Some interesting results may be obtained when the sign of f_o and g_o is reversed. The writer realizes that the discussion of this section is probably only of academic interest since existence of imperfection overshadows all other considerations. On an intuitive basis, a sign change in f_o alone should not change anything, at least for even m's. The reason is that the checkerboard pattern is made-up of sine waves which are always full waves in both axial (even m's) and circumferential directions. On an overall basis, there are as many inward as outward half waves and the order (sign of f_o) in which they are taken should not matter.

The sign of g_o does matter, however, since it is associated with a sine-square term.

Experience has shown that diamond buckling has a preference for inward bulging. If g_o is taken negative (outward), and the same tendency is assumed, it would appear that critical dynamic buckling is somewhat delayed, since the shell has to overcome the small artificial outward bulge first, before it can move inward. Since the first term of the $\bar{N}_{ox}(t)$ expression (V-9), is proportional to t for $\gamma=0$, it can build-up to a larger value before the other terms start to reduce it.

Numerical calculations confirm these speculations and are presented in Table (VI-6) below. It must be noted that these buckling values apply for $f_o=\pm 0.014$ in.

m	n	V_o = 50 ips				V_o = 100 ips			
		g_o = -0.014 in		g_o = +0.014 in		g_o = -0.014 in		g_o = +0.014 in	
		INT.*	EXT.	INT.	EXT.	INT.	EXT.	INT.	EXT.
		$1^{st}\bar{N}_{ox\,max}$ [lb/in]	$1^{st}\bar{N}_{ox\,max}$ [lb/in]	$1^{st}\bar{N}_{ox\,max}$ [lb/in]	$1^{st}\bar{N}_{ox\,max}$ [lb/in]	$1^{st}\bar{N}_{ox\,max}$ [lb/in]	$1^{st}\bar{N}_{ox\,max}$ [lb/in]	$1^{st}\bar{N}_{ox\,max}$ [lb/in]	$1^{st}\bar{N}_{ox\,max}$ [lb/in]
4	6	2127	4231	1815**	4029	2678	5184	2449	4612
4	8	-	3115	2129	2549	-	3663	-	3115

* INT. means internally stiffened shell.
EXT. means externally stiffened shell.
** underligned values are critical dynamic buckling loads.

Table(VI-6) : The Effect of the Direction of the Initial Imperfections on the Dynamic Buckling Loads of Card's Stringer Shell.
Data: γ=0 1/sec ; $f_o = \pm$ 0.014 in.

The effect of negative g_o is therefore to increase the dynamic buckling loads.
Figures (VI-13) and (VI-14) present the time histories of f_1 and g_1. In order to see the delay due to negative g_o, Figure (VI-13) must be compared with Figure (VI-8) for the same data but with positive g_o. The critical time, corresponding to critical buckling, is marked on these curves.
In Figure (VI-14), f_o=g_o=-0.014 in, and there is no difference in the g_1-curves of Figures (VI-13) and (VI-14); the f_1-curves take-off in opposite directions, however, even though the same critical dynamic buckling load results, since f_1 and f_o enter as squared quantities into the expression (V-9) for $\bar{N}_{ox}$.

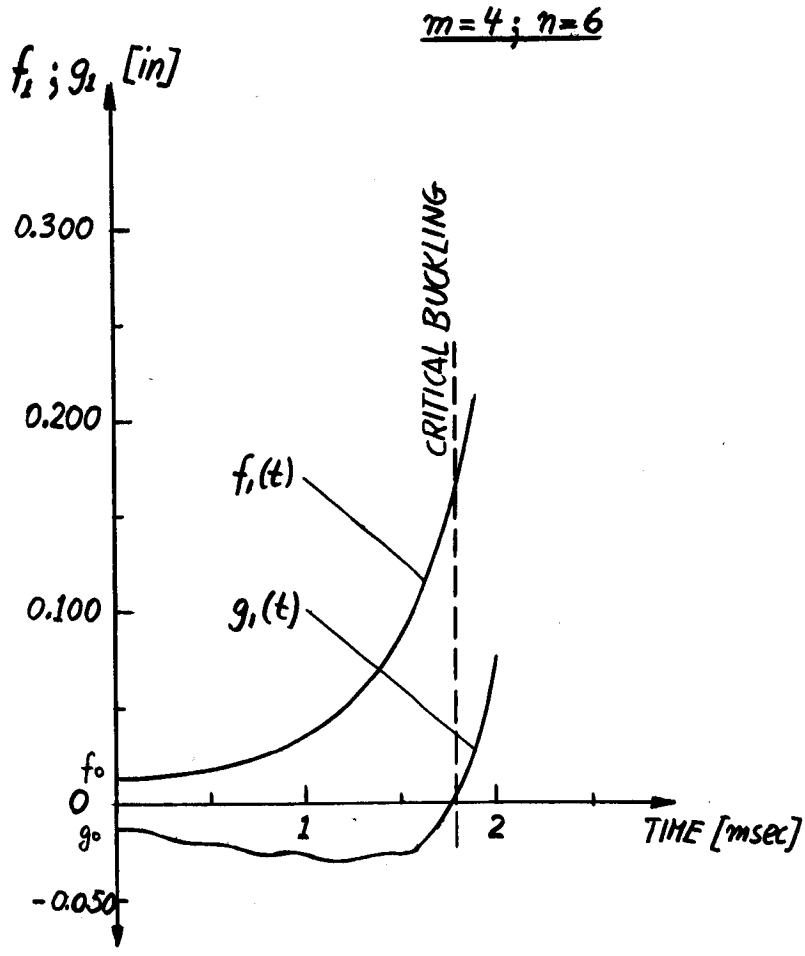

Figure (VI-13) : Critical Buckling Amplitudes of Card's Shell by the Combined Method, Internally Stiffened. Effect of Opposite Direction of Initial Imperfections. (Compare with Figure (VI-8))
Data: V_o=100 ips ; γ=0 sec^{-1} ; m=4 ; n=6 ;
f_o=+0.014 in ; g_o=-0.014 in.

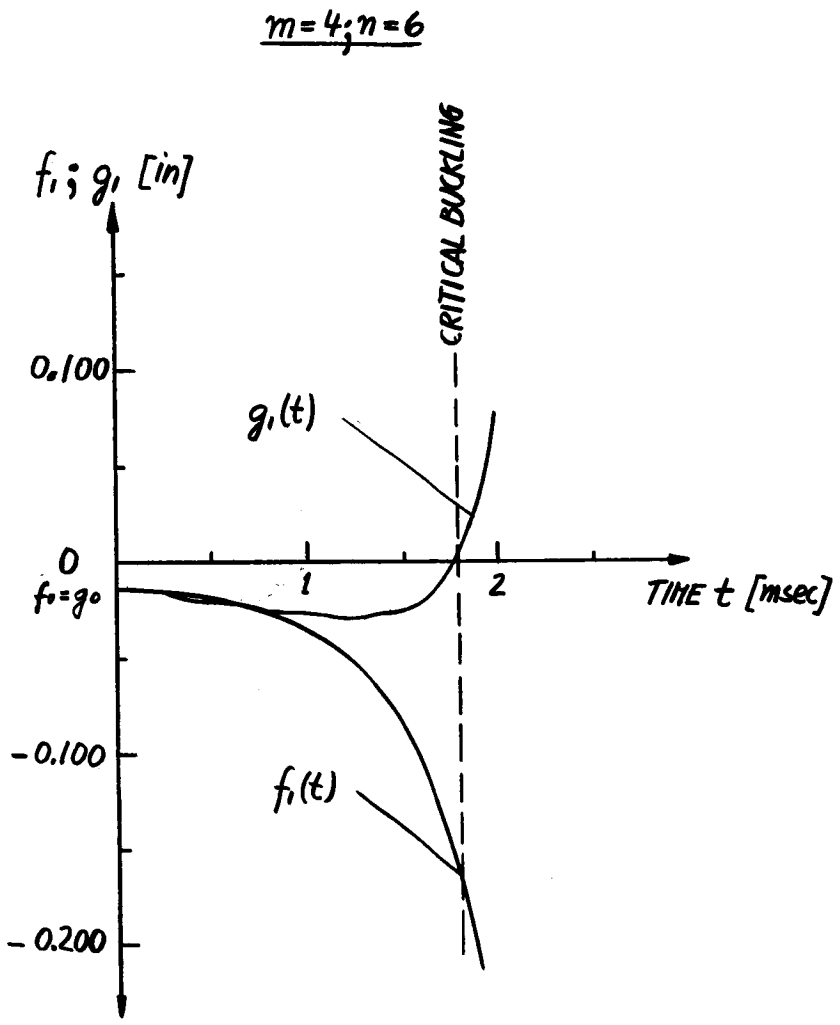

Figure (VI-14) : Critical Buckling Amplitudes of Card's Shell by the Combined Method, Internally Stiffened. Effect of Opposite Direction of Initial Imperfections. (Compare with Figure (VI-8))
Data: V_o=100 ips ; γ =0 sec^{-1} ; m=4 ; n=6 ;
$f_o=g_o$=-0.014 in.

e) The Effect of the Time Constant of the Exponentially Decaying Rate of Endshortening.

The time constant in this context is defined as the reciprocal of γ. In Table (VI-7) below, it is assumed that the time constant is 2 msec., e.g. V_o drops to 1/e of its value after that time. This particular value is chosen since critical buckling occurs approximately after such a duration, when V_o=100 ips and constant rate of endshortening are assumed. Calculations were made with V_o= 100 ips, γ =500 1/sec; the results are then compared with those obtained for constant rate of endshortening, with V_o=100 ips and V_o=50 ips.

m	n	INTERNALLY STIFFENED			EXTERNALLY STIFFENED		
		V_o=100 ips	V_o=50 ips	V_o=100 ips	V_o=100 ips	V_o=50 ips	V_o=100 ips
		γ=0 sec^{-1}	γ=0 sec^{-1}	γ=500 sec^{-1}	γ=0 sec^{-1}	γ=0 sec^{-1}	γ=500 sec^{-1}
		$1^{st}\bar{N}_{ox\,max}$	$1^{st}\bar{N}_{ox\,max}$	$1^{st}\bar{N}_{ox\,max}$	$1^{st}\bar{N}_{ox\,max}$	$1^{st}\bar{N}_{ox\,max}$	$1^{st}\bar{N}_{ox\,max}$
		[lb/in]	[lb/in]	[lb/in]	[lb/in]	[lb/in]	[lb/in]
4	6	2449*	1815	1793	4612	4029	3101
4	8	-	2129	2152	3115	2549	2324

* underligned values are critical dynamic buckling loads

Table (VI-7) : The Effect of the Time Constant of the Exponentially Decaying Rate of Endshortening on the Dynamic Buckling Loads of Card's Shell. Data: f_o=g_o= 0.014 in.

For the internally stiffened shell a reduction of the critical dynamic buckling load to roughly the values for V_o=50 ips, γ =0, is obtained, while it is somewhat less for the externally stiffened shell.

CHAPTER VII : SOME COMMENTS ON THE STATIC BUCKLING PROBLEM OF ECCENTRICALLY REINFORCED CYLINDRICAL SHELLS.

1. Prediction of the Static Buckling Load for Card's Stringer Shell from the "Dynamic" Theory.

It is recalled that the boundary conditions of the problem under consideration were not exactly satisfied. The clamped boundary conditions were satisfied on the average over the circumference.

In Card's tests, the stringer shell was ground flat at both ends so that the ends were bearing against the flat plates of head and base of the testing machine. It seems, therefore, that this arrangement approaches clamped boundary conditions, and a comparison of the calculated values from this theory and Card's test results can be made.

The combined method was applied to predict the static buckling load of Card's shell. Initial imperfections of $f_o=g_o=0.001$ in were assumed, accounting for careful machining of this shell. Photographs in Card's report [34] show mode numbers of m=2, and n=6. These mode numbers were selected and a constant rate of endshortening $V_o=0.1$ ips was chosen, maintaining the step size of integration of 10 microseconds. It goes without saying that this procedure is highly inefficient as far as computer time is concerned, but the purpose here was to demonstrate the reduction of the theory to the static case. For this reason only the internally reinforced shell was considered.

The result is presented in Figure (VII-1). Notice, that the general area around the dip has been expanded in scale. Buckling occurs at t=0.519 sec. with a buckling load N_{oxc}=833 lb/in. This compares quite favorably with Card's tested value of 800 lb/in.

2. The Static Buckling Equations.

Let us consider the field equations (II-35). On reducing these to the static case, we can write:

$$D_{11} w_{,xxxx} + 2 D_{12} w_{,xxyy} + D_{22} w_{,yyyy} + S_{11} f_{,xxxx} - 2S_{12} f_{,xxyy}$$
$$+S_{22} f_{,yyyy} - f_{,xx} w_{,yy} + 2 f_{,xy} w_{,xy} - f_{,yy} w_{,xx} - \frac{f_{,xx}}{R} - p = 0$$

$$A_{11} f_{,xxxx} + 2 A_{12} f_{,xxyy} + A_{22} f_{,yyyy} - S_{11} w_{,xxxx} + 2S_{12} w_{,xxyy}$$
$$- S_{22} w_{,yyyy} - w_{,xy}^2 + w_{,xx} w_{,yy} + \frac{w_{,xx}}{R} = 0 \qquad \text{(VII-1)}$$

Let us assume,

$$\left.\begin{aligned} f &= f_P + f_B \\ w &= w_P + w_B \end{aligned}\right\} \qquad \text{(VII-2)}$$

where the quantities with subscript P refer to prebuckling- those with B to buckling variables.

On introducing (VII-2) into (VII-1), we can subtract out the prebuckling terms, since they must satisfy the equilibrium and compatibility equations sparately. The prebuckling equations therefore become:

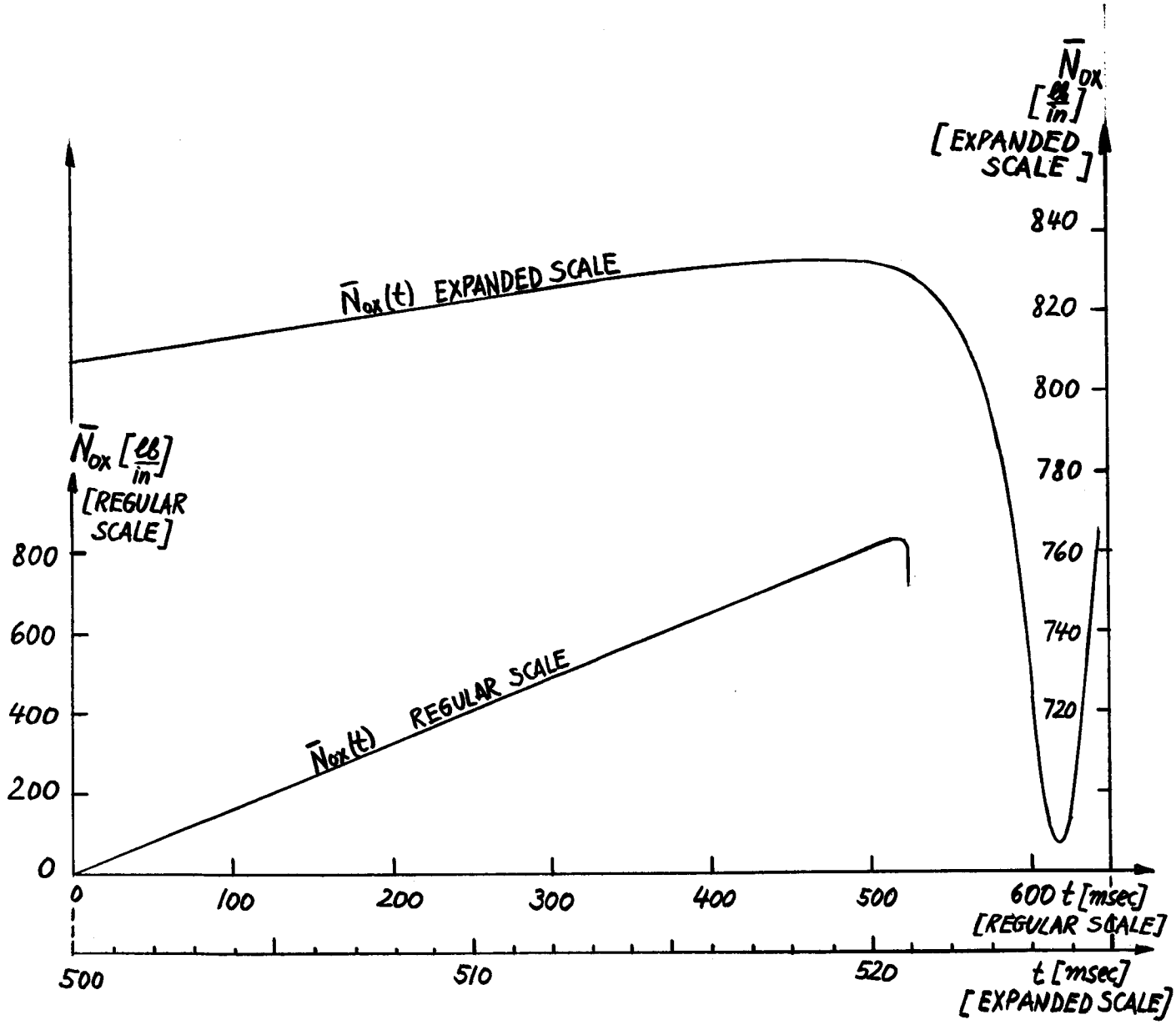

Figure (VII-1) : Prediction of the Static Buckling Load of Card's Shell from the "Dynamic" Theory, Internally Stiffened.

Data: V_o=0.1 ips ; γ = 0 sec^{-1} ; m=2 ; n=6 ;
$f_o=g_o$= 0.001 in.

$$D_{11} w_{P,xxxx} + 2 D_{12} w_{P,xxyy} + D_{22} w_{P,yyyy} + S_{11} f_{P,xxxx} - 2 S_{12} f_{P,xxyy}$$
$$+ S_{22} f_{P,yyyy} - f_{P,xx} w_{P,yy} + 2 f_{P,xy} w_{P,xy} - f_{P,yy} w_{P,xx} - \frac{f_{P,xx}}{R} - p = 0$$

$$A_{11} f_{P,xxxx} + 2 A_{12} f_{P,xxyy} + A_{22} f_{P,yyyy} - S_{11} w_{P,xxxx} + 2 S_{12} w_{P,xxyy}$$
$$- S_{22} w_{P,yyyy} - w^2_{P,xy} + w_{P,xx} w_{P,yy} + \frac{w_{P,xx}}{R} = 0$$

(VII-3)

The remainder yields the following equations:

$$D_{11} w_{B,xxxx} + 2 D_{12} w_{B,xxyy} + D_{22} w_{B,yyyy} + S_{11} f_{B,xxxx} - 2 S_{12} f_{B,xxyy} + S_{22} f_{B,yyyy}$$
$$- f_{B,yy} w_{B,xx} + 2 f_{P,xy} w_{B,xy} - f_{P,xx} w_{B,yy}$$
$$- f_{B,yy} w_{B,xx} + 2 f_{B,xy} w_{B,xy} - f_{B,xx} w_{B,yy}$$
$$- f_{B,yy} w_{P,xx} + 2 f_{B,xy} w_{P,xy} - f_{B,xx} w_{P,yy} - \frac{f_{B,xx}}{R} = 0$$

$$A_{11} f_{B,xxxx} + 2 A_{12} f_{B,xxyy} + A_{22} f_{B,yyyy} - S_{11} w_{B,xxxx} + 2 S_{12} w_{B,xxyy} - S_{22} w_{B,yyyy}$$
$$+ w_{P,xx} w_{B,yy} - 2 w_{P,xy} w_{B,xy} + w_{P,yy} w_{B,xx}$$
$$+ w_{B,xx} w_{B,yy} - w^2_{B,xy} + \frac{w_{B,xx}}{R} = 0$$

(VII-4)

Let us introduce:

$$\left.\begin{aligned} N_{xP} &= - f_{P,yy} \\ N_{yP} &= - f_{P,xx} \\ N_{xyP} &= - f_{P,xy} \end{aligned}\right\} \qquad \text{(VII-5)}$$

The stress resultants N_{xP} and N_{yP} correspond to compressive stresses.

We assume that the prebuckling deformations, slopes and curvatures are small so that products of such quantities can be neglected in (VII-4). In terms of the stress resultants (VII-5), these equations therefore become:

$$D_{11} w_{P,xxxx} + 2D_{12} w_{P,xxyy} + D_{22} w_{P,yyyy} + S_{11} f_{P,xxxx} - 2S_{12} f_{P,xxyy} + S_{22} f_{P,yyyy}$$
$$+ N_{yP} w_{P,yy} - 2N_{xyP} w_{P,xy} + N_{xP} w_{P,xx} + \frac{N_{yP}}{R} - p = 0$$

$$A_{11} f_{P,xxxx} + 2A_{12} f_{P,xxyy} + A_{22} f_{P,yyyy} - S_{11} w_{P,xxxx}$$
$$+ 2S_{12} w_{P,xxyy} - S_{22} w_{P,yyyy} + \frac{w_{P,xx}}{R} = 0 \qquad \text{(VII-6)}$$

Let us refer to (VII-6) as the linearized prebuckling equations. On using the stress resultants (VII-5) in (VII-4), there results:

$$D_{11} w_{B,xxxx} + 2D_{12} w_{B,xxyy} + D_{22} w_{B,yyyy} + S_{11} f_{B,xxxx} - 2S_{12} f_{B,xxyy}$$
$$+ S_{22} f_{B,yyyy} + N_{xP} w_{B,xx} - 2N_{xyP} w_{B,xy} + N_{yP} w_{B,yy} - \frac{f_{B,xx}}{R}$$
$$- f_{B,yy} w_{B,xx} + 2f_{B,xy} w_{B,xy} - f_{B,xx} w_{B,yy} - f_{B,yy} w_{P,xx}$$
$$+ 2f_{B,xy} w_{P,xy} - f_{B,xx} w_{P,yy} = 0$$

$$A_{11} f_{B,xxxx} + 2A_{12} f_{B,xxyy} + A_{22} f_{B,yyyy} - S_{11} w_{B,xxxx} + 2S_{12} w_{B,xxyy}$$
$$- S_{22} w_{B,yyyy} + w_{P,xx} w_{B,yy} - 2w_{P,xy} w_{B,xy} + w_{P,yy} w_{B,xx}$$
$$+ w_{B,xx} w_{B,yy} - w_{B,xy}^2 + \frac{w_{B,xx}}{R} = 0 \qquad \text{(VII-7)}$$

Let us call (VII-7) the buckling equations. The prebuckling- and buckling equations presented above cover the cases of

buckling due to axial compression, pressure and torsion, and they are therefore quite general.

With the assumption of axisymmetric prebuckling (in absence of torsion), the prebuckling equations can be simplified considerably and solutions may be possible that satisfy the given boundary conditions exactly. These prebuckling solutions are then introduced into the nonlinear buckling equations, whose solution must be attempted in some approximate manner. Such solutions were carried out for the monocoque cylindrical shell by Stein [22], Fischer [21], and Gorman [62]. Extensions of theses investigations to the eccentrically reinforced cylindrical shell should therefore also be possible. The equations derived in this section would provide the basis for such analyses.

3. The Linear Classical Buckling Equations for the Eccentrically Reinforced Cylindrical Shell in Axial Compression.

Neglecting the prebuckling deformation w_p, omitting the torsion term with N_{xyP}, and assuming that N_{xP} and N_{yP} do not depend on x and y, the fourth order derivatives of f_p in the prebuckling equations disappear on account of (VII-5).

The first equation of (VII-6) yields the simple result $N_{yP}=pR$ and the second equation is identically satisfied.

For the zero pressure case, we can therefore write a linearized version of the buckling equations (VII-7) in the form:

$$D_{11}\, w_{,xxxx} + 2D_{12}\, w_{,xxyy} + D_{22}\, w_{,yyyy} + S_{11}\, f_{,xxxx}$$
$$-2S_{12}\, f_{,xxyy} + S_{22}\, f_{,yyyy} + N_{ox}\, w_{,xx} - \frac{f_{,xx}}{R} = 0$$
$$S_{11}\, w_{,xxxx} - 2S_{12}\, w_{,xxyy} + S_{22}\, w_{,yyyy} - A_{11}\, f_{,xxxx}$$
$$-2A_{12}\, f_{,xxyy} - A_{22}\, f_{,yyyy} - \frac{w_{,xx}}{R} = 0 \qquad \text{(VII-8)}$$

The subscript B has been droped for easier writing. N_{ox} indicates no dependency on x and y. The second equation has been slightly rearranged to bring out term similarities between the above two equations.

Let us define the following linear operators:

$$\left.\begin{aligned}
\mathcal{L}_{11} &= D_{11}\frac{\partial^4}{\partial x^4} + 2D_{12}\frac{\partial^4}{\partial x^2\partial y^2} + D_{22}\frac{\partial^4}{\partial y^4} + N_{ox}\frac{\partial^2}{\partial x^2} \\
\mathcal{L}_{12} &= S_{11}\frac{\partial^4}{\partial x^4} - 2S_{12}\frac{\partial^4}{\partial x^2\partial y^2} + S_{22}\frac{\partial^4}{\partial y^4} - \frac{1}{R}\frac{\partial^2}{\partial x^2} \\
\mathcal{L}_{22} &= A_{11}\frac{\partial^4}{\partial x^4} + 2A_{12}\frac{\partial^4}{\partial x^2\partial y^2} + A_{22}\frac{\partial^4}{\partial y^4}
\end{aligned}\right\} \qquad \text{(VII-9)}$$

With the help of these operators, we can write (VII-8) much simpler as:

$$\left.\begin{aligned}
\mathcal{L}_{11}\, w + \mathcal{L}_{12}\, f &= 0 \\
\mathcal{L}_{12}\, w - \mathcal{L}_{22}\, f &= 0
\end{aligned}\right\} \qquad \text{(VII-10)}$$

On eliminating first f and then w, the following dual pair of equations results:

$$\left.\begin{aligned}
(\mathcal{L}_{11}\,\mathcal{L}_{22} + \mathcal{L}_{12}\,\mathcal{L}_{22})\, w = \mathcal{L}_8\, w = 0 \\
(\mathcal{L}_{11}\,\mathcal{L}_{22} + \mathcal{L}_{12}\,\mathcal{L}_{22})\, f = \mathcal{L}_8\, f = 0
\end{aligned}\right\} \qquad \text{(VII-11)}$$

The operator $\mathcal{L}_8$ is readily calculated from (VII-9) with the result:

$$\mathcal{L}_8 = (A_{11}D_{11} + S_{11}^2)\frac{\partial^8}{\partial x^8} + 2(A_{11}D_{12} + A_{12}D_{11} - 2S_{11}S_{12})\frac{\partial^8}{\partial x^6 \partial y^2}$$
$$+ [A_{11}D_{22} + 4A_{12}D_{12} + A_{22}D_{11} + 2(S_{11}S_{22} + 2S_{12}^2)]\frac{\partial^8}{\partial x^4 \partial y^4}$$
$$+ 2(A_{22}D_{12} + A_{12}D_{22} - 2S_{12}S_{22})\frac{\partial^8}{\partial x^2 \partial y^6} + (A_{22}D_{22} + S_{22}^2)\frac{\partial^8}{\partial y^8}$$
$$+ \frac{\partial^2}{\partial x^2}\left[(A_{11}N_{0x} - \frac{2S_{11}}{R})\frac{\partial^4}{\partial x^4} + 2(A_{12}N_{0x} + \frac{2S_{12}}{R})\frac{\partial^4}{\partial x^2 \partial y^2}\right.$$
$$\left. + (A_{22}N_{0x} - \frac{2S_{22}}{R})\frac{\partial^4}{\partial y^4}\right] + \frac{1}{R^2}\frac{\partial^4}{\partial x^4} \qquad \text{(VII-12)}$$

For completeness, if pressure and torsion are considered, this operator becomes:

$$\mathcal{L}_8 = (A_{11}D_{11} + S_{11}^2)\frac{\partial^8}{\partial x^8} + 2(A_{11}D_{12} + A_{12}D_{11} - 2S_{11}S_{12})\frac{\partial^8}{\partial x^6 \partial y^2}$$
$$+ [A_{11}D_{22} + 4A_{12}D_{12} + A_{22}D_{11} + 2(S_{11}S_{22} + 2S_{12}^2)]\frac{\partial^8}{\partial x^4 \partial y^4}$$
$$+ 2(A_{22}D_{12} + A_{12}D_{22} - 2S_{12}S_{22})\frac{\partial^8}{\partial x^2 \partial y^6} + (A_{22}D_{22} + S_{22}^2)\frac{\partial^8}{\partial y^8}$$
$$+ \frac{\partial^2}{\partial x^2}\left[(A_{11}N_{0x} - \frac{2S_{11}}{R})\frac{\partial^4}{\partial x^4} + 2(A_{12}N_{0x} + \frac{2S_{12}}{R} + A_{11}\frac{pR}{2})\frac{\partial^4}{\partial x^2 \partial y^2}\right.$$
$$\left. + (A_{22}N_{0x} - \frac{2S_{22}}{R} + 2A_{12}pR)\frac{\partial^4}{\partial y^4}\right] + \frac{1}{R^2}\frac{\partial^4}{\partial x^4}$$
$$- 2N_{0xy}\frac{\partial^2}{\partial x \partial y}\left[A_{11}\frac{\partial^4}{\partial x^4} + 2A_{12}\frac{\partial^4}{\partial x^2 \partial y^2} + A_{22}\frac{\partial^4}{\partial y^4}\right] + \frac{\partial^2}{\partial y^2}(A_{22}pR)\frac{\partial^4}{\partial y^4}$$

(VII-13)

On letting N_{oxy}=p=0, the latter operator reduces readily to the former of (VII-12).

Let us return to the case of axial compression only. The reduction of the operator (VII-12) to the monocoque shell case is readily achieved by letting $D_{11} \to D_{12} \to D_{22} \to D$; $S_{11} \to S_{12} \to S_{22} \to 0$; $A_{11} \to A_{12} \to A_{22} \to 1/Eh$. This operator then becomes:

$$\mathcal{L}_8^{(m)} = \frac{D}{Eh}\frac{\partial^8}{\partial x^8} + \frac{4D}{Eh}\frac{\partial^8}{\partial x^6 \partial y^2} + \frac{6D}{Eh}\frac{\partial^8}{\partial x^4 \partial y^4} + \frac{4D}{Eh}\frac{\partial^8}{\partial x^2 \partial y^6}$$
$$+ \frac{D}{Eh}\frac{\partial^8}{\partial y^8} + \frac{\partial^2}{\partial x^2}\left[\frac{N_{0x}}{Eh}\frac{\partial^4}{\partial x^4} + \frac{2N_{0x}}{Eh}\frac{\partial^4}{\partial x^2 \partial y^2} + \frac{N_{0x}}{Eh}\frac{\partial^4}{\partial y^4}\right] + \frac{1}{R^2}\frac{\partial^4}{\partial x^4} \qquad \text{(VII-14)}$$

With the usual operators for the monocoque case,

$$\nabla^4 = \frac{\partial^4}{\partial x^4} + 2\frac{\partial^4}{\partial x^2 \partial y^2} + \frac{\partial^4}{\partial y^4}$$
$$\nabla^8 = \nabla^4 \nabla^4 = \frac{\partial^8}{\partial x^8} + 4\frac{\partial^8}{\partial x^6 \partial y^2} + 6\frac{\partial^8}{\partial x^4 \partial y^4} + 4\frac{\partial^8}{\partial x^2 \partial y^6} + \frac{\partial^8}{\partial y^8} \qquad \text{(VII-15)}$$

the equation $\mathcal{L}_8^{(m)} W = 0$ can be written in the more familiar form

$$D\nabla^8 W + \frac{Eh}{R^2}\frac{\partial^4 W}{\partial x^4} + N_{0x}\nabla^4\frac{\partial^4 W}{\partial x^4} = 0 \qquad \text{(VII-16)}$$

which is known in this country as the linear Donnell equation for axial compression of the monocoque cylindrical shell. The same equation is given by Volmir [49], p.249, for example.

In order to find the classical static buckling load for the eccentrically reinforced cylindrical shell, we assume, as in the monocoque case, a radial displacement of the form:

$$W = \sum_{m=1}^{\infty} \sum_{n=1}^{\infty} \sin \frac{m\pi x}{L} \sin \frac{ny}{R} \qquad \text{(VII-17)}$$

If w is a solution then each term m;n satisfies $\mathcal{L}_8 W = 0$, where $\mathcal{L}_8$ is given by (VII-12). Performing the appropriate differentiations on w and introducing them into $\mathcal{L}_8 W = 0$ yields the following expression:

$$\begin{aligned}
&(A_{11}D_{11} + S_{11}^2)\left(\frac{m\pi}{L}\right)^8 + 2(A_{12}D_{11} + A_{11}D_{12} - 2S_{11}S_{12})\left(\frac{m\pi}{L}\right)^6\left(\frac{n}{R}\right)^2 \\
&+ [A_{22}D_{11} + 4A_{12}D_{12} + A_{11}D_{22} + 2(S_{11}S_{22} + 2S_{12}^2)]\left(\frac{m\pi}{L}\right)^4\left(\frac{n}{R}\right)^4 \\
&+ 2(A_{22}D_{12} + A_{12}D_{22} - 2S_{12}S_{22})\left(\frac{m\pi}{L}\right)^2\left(\frac{n}{R}\right)^6 + (A_{22}D_{22} + S_{22}^2)\left(\frac{n}{R}\right)^8 \\
&- \left(A_{11}N_{0x} - \frac{2S_{11}}{R}\right)\left(\frac{m\pi}{L}\right)^6 - 2\left(A_{12}N_{0x} + \frac{2S_{12}}{R}\right)\left(\frac{m\pi}{L}\right)^4\left(\frac{n}{R}\right)^2 \\
&- \left(A_{22}N_{0x} - \frac{2S_{22}}{R}\right)\left(\frac{m\pi}{L}\right)^2\left(\frac{n}{R}\right)^4 + \frac{1}{R^2}\left(\frac{m\pi}{L}\right)^4 = 0
\end{aligned} \qquad \text{(VII-18)}$$

Let us define the abbreviations:

$$\begin{aligned}
\theta &= \lambda^2 = \left(\frac{b}{a}\right)^2 = \left(\frac{\pi R}{L}\right)^2\left(\frac{m}{n}\right)^2 \\
\Omega &= \beta^2 = \left(\frac{n}{R}\right)^2 \\
\mu_1 &= A_{11}D_{11} + S_{11}^2 \\
\mu_2 &= 2(A_{11}D_{12} + A_{12}D_{11} - 2S_{11}S_{12}) \\
\mu_3 &= A_{22}D_{11} + 4A_{12}D_{12} + A_{11}D_{22} + 2(S_{11}S_{22} + 2S_{12}^2) \\
\mu_4 &= 2(A_{22}D_{12} + A_{12}D_{22} - 2S_{12}S_{22}) \\
\mu_5 &= A_{22}D_{22} + S_{22}^2
\end{aligned} \qquad \text{(VII-19)}$$

Solving (VII-18) for N_{ox} and using the above abbreviations leads to:

$$N_{ox} = \frac{\Omega}{\theta\,[\theta^2 A_{11} + 2\theta A_{12} + A_{22}]} \left\{ \theta^4 \mu_1 + \theta^3 \mu_2 + \theta^2 \mu_3 + \theta \mu_4 + \mu_5 + \frac{2}{R}\,\frac{\theta}{\Omega}\,(\theta^2 S_{11} - 2\theta S_{12} + S_{22}) + \frac{\theta^2}{\Omega^2 R^2} \right\} \tag{VII-20}$$

If the μ's are reduced to the case of the monocoque shell, there results:

$$\left.\begin{aligned} \mu_1^{(m)} &= \frac{D}{Eh} \\ \mu_2^{(m)} &= \frac{4D}{Eh} \\ \mu_3^{(m)} &= \frac{6D}{Eh} \\ \mu_4^{(m)} &= \frac{4D}{Eh} \\ \mu_5^{(m)} &= \frac{D}{Eh} \end{aligned}\right\} \tag{VII-21}$$

The superscript (m) refers to the monocoque shell.

N_{ox} then becomes for the monocoque shell:

$$N_{ox} = \frac{\Omega Eh}{\theta\,[\theta^2 + 2\theta + 1]} \left\{ \frac{D}{Eh} [\theta^4 + 4\theta^3 + 6\theta^2 + 4\theta + 1] + \frac{\theta^2}{\Omega^2 R^2} \right\}$$

$$= \frac{\Omega Eh}{\theta(\theta+1)^2} \left\{ \frac{D}{Eh} (\theta+1)^4 + \frac{\theta^2}{\Omega^2 R^2} \right\} = \frac{\Omega D (\theta+1)^2}{\theta} + \frac{\theta Eh}{\Omega R^2 (\theta+1)^2} \tag{VII-22}$$

Letting,

$$\xi = \frac{\Omega}{\theta}(\theta+1)^2 \tag{VII-23}$$

N_{ox} can be written as:

$$N_{ox} = D\xi + \frac{Eh}{R^2}\,\frac{1}{\xi} \tag{VII-24}$$

As it is recalled, the critical buckling load is then obtained by treating ξ as a continuous variable and seeking the minimum of N_{ox} as follows:

$$\frac{dN_{ox}}{d\xi} = D - \frac{Eh}{R^2}\frac{1}{\xi^2} = 0 \qquad \text{(VII-25)}$$

Solving for ξ and introducing the result into (VII-24), yields the critical static buckling load of the monocoque cylindrical shell:

$$N_{oxc} = \frac{2}{R}\sqrt{DEh} = \frac{Eh^2}{R\sqrt{3(1-\nu^2)}} \qquad \text{(VII-26)}$$

Thus a reduction to the monocoque cylindrical shell checks out. The last few steps follow the treatment of the monocoque cylindrical shell given by Volmir [49]and are only listed here as a means of comparing it with the eccentrically reinforced cylindrical shell. It is well to remember that the mode numbers m and n are undetermined and do not appear in the critical load expression.

Let us return to the eccentrically reinforced cylindrical shell and consider the expression for N_{ox} (VII-20).
A set of positive integer pairs m and n (θ and Ω) corresponds to a set of N_{ox} values. The smallest element in the N_{ox}-set is the critical static buckling load.
A minimization of the N_{ox} expression is not as easily achieved as in the case of the monocoque shell. Instead of trying to arrive at a closed-form solution for N_{oxC}, it seems more straight-

forward to write a relatively simple computer program which accepts all geometry and material input parameters, calculates N_{ox} according to (VII-20) for a whole range of pairs m and n, the lowest such value being the critical static buckling load. It must be kept in mind that the influence of boundary conditions has been neglected in this treatment.

4. Determination of the Classical Static Buckling Load for Card's Stringer Shell.

A separate computer program that executes the task prescribed above is not included in this dissertation, since it is relatively easy written from the program given in Appendix B, where all the parameters appearing in the μ expressions of (VII-19) are already available.

Table(VII-1) below presents the results of such calculations, obtained for Card's shell, internally and externally stiffened. Of the many calculated values of N_{ox} , only a few of the lowest values are given.

m	n	N_{ox} : INT. STIFF. [lb/in]	N_{ox} : EXT. STIFF. [lb/in]	η —	δ —
1	5	706	1176	1.67	0.1579
1	6	800	1138	1.42	0.1316
2	6	849	1928	2.27	0.2632
2	7	755	1610	2.14	0.2256

Table (VII-1) : Classical Static Buckling Loads for Card's Shell.

The quantity η in the table will be discussed in more detail in the next section. η is defined as the ratio of the buckling load of the externally reinforced shell to that of the internally stiffened cylinder:

$$\eta = \frac{N_{ox\ EXT.}}{N_{ox\ INT.}} \qquad \text{(VII-27)}$$

η might be appropriately called the stiffener location effectiveness, since it gives a measure of the effectiveness of putting the stiffeners externally.

Comparing the data of the table with Card's measured results, one finds good agreement for the mode numbers m=2 and n=6. Following the established criterion, however, we have to pick the lowest values, which occur for m=1 and n=5. These values are on the low side, particularly low for the externally stiffened shell, where it doesn't matter much whether one picks the "true low" for m=1 and n=6, or selects m=1 and n=5. It is apparently the mode number m that affects the buckling load for the externally stiffened Card shell in a drastic way.
We might therefore conclude, that the classical static analysis provides good results in connection with some experimental knowledge about the mode numbers, particularly m.
In the case of the monocoque cylindrical shell it has been shown [21] that clamping of the ends somewhat increases the buckling load, the increase being more pronounced for shorter shells. The radial displacement assumption (VII-7), on which

the classical theory is based, corresponds to the simply-supported boundary conditions. The classical theory would therefore inherently predict somewhat lower buckling loads than might be expected with a corresponding theory that takes clamped boundary conditions into account.

The calculated data therefore suggest that clamping seems to play an even more important role in the case of the eccentrically reinforced cylindrical shell. This is intuitively not surprising, since the stringers might be looked upon as an array of clamped columns.

5. The Effect of the Mode Numbers on the Stiffener Location Effectiveness.

The effect of the stiffener eccentricities on N_{ox} is seen clearly from equation (VII-20). The term in parentheses, containing the S's, is the important one. The expression for $N_{ox\ EXT.}$ is the same as (VII-20), except for a sign change in the S quantities. Assuming the same mode numbers for the internally and the externally stiffened cylindrical shell, the stiffener location effectiveness can be written in the form:

$$\eta = \frac{\theta^4\mu_1 + \theta^3\mu_2 + \theta^2\mu_3 + \theta\mu_4 + \mu_5 + \frac{\theta^2}{\Omega^2R^2} - \frac{2}{R}\frac{\theta}{\Omega}(\theta^2 S_{11} - 2\theta S_{12} + S_{22})}{\theta^4\mu_1 + \theta^3\mu_2 + \theta^2\mu_3 + \theta\mu_4 + \mu_5 + \frac{\theta^2}{\Omega^2R^2} + \frac{2}{R}\frac{\theta}{\Omega}(\theta^2 S_{11} - 2\theta S_{12} + S_{22})} \qquad \text{(VII28)}$$

It must be noted that the eccentricity parameters S must be taken positive for the development in this section, since

the minus sign for external stiffening is already incorporated into the above expression.

Let us introduce the abbreviation,

$$\rho_1 = -\frac{\frac{2}{R}\frac{\theta}{\Omega}\left(\theta^2 S_{11} - 2\theta S_{12} + S_{22}\right)}{\theta^4\mu_1 + \theta^3\mu_2 + \theta^2\mu_3 + \theta\mu_4 + \mu_5 + \frac{\theta^2}{\Omega^2 R^2}} \qquad \text{(VII-29)}$$

so that the stiffener location effectiveness can be written as:

$$\eta = \frac{1 + \rho_1}{1 - \rho_1} \qquad \text{(VII-30)}$$

For the case of a "stringer-only" cylindrical shell, ρ_1 can be simplified somewhat. Writing it as ρ_{1S} for this particular case and expressing it in terms of n and ϑ, it can be shown to be:

$$\rho_{1S} = \frac{2R\vartheta^4 S_{11}\left(\frac{1}{\nu} - \vartheta^2\right)}{n^2\left[\vartheta^8\mu_1 + \vartheta^6\mu_2 + \vartheta^4\left(\mu_3 + \frac{R^2}{n^4}\right) + \vartheta^2\mu_4 + \mu_5\right]} \qquad \text{(VII-31)}$$

The Poisson ratio appears since $2\,S_{12}/S_{11} \to \nu$ in the case of a stringer-only shell.

It is interesting to observe that ρ_{1S} becomes negative for aspect ratios $\vartheta > \frac{1}{\sqrt{\nu}}$ (> 1.83 for $\nu = 0.3$), so that the stiffener location effectiveness becomes less than one by (VII-30).

It is therefore theoretically possible that internally reinforced stringer shells may yield higher buckling loads than their externally stiffened counterparts, if the buckling aspect ratio exceeds a certain limit.

Recalling the physical meaning of $\nu = b/a$, this would imply that the buckles would have to stretch out considerably in the circumferential direction, as compared with the axial direction. On the other hand, a particular shell is expected to show an optimum stiffener location effectiveness for a certain pair of mode numbers. Figure (VII-2) presents a graphical optimization chart for Card's shell. η is plotted versus ν, with n as a parameter. The graph is arranged such that points on the $\eta = \eta(\nu)$ curves can be located which correspond to integer values of m and n. This was done simply by plotting $m = n\left(\frac{L}{\pi R}\right)\nu$, or $m = m(\nu)$, in the same diagram with common ν-axis, and labelling the straight lines with its corresponding n-values.

As an illustration, let us see whether we can get into the peak region with some reasonable pair m; n. Selecting for example m=3 on the ordinate axis (See Figure), we move horizontally over until we intersect the ray n=7, where the latter is chosen since its curve $\eta = \eta(\nu)$ exhibits the highest peak; we then move vertically to intersect the η-curve for n=7. The resulting stiffener location effectiveness is therefore around 2.5, which is about as much, as can be obtained. Figure (VII-2) also exhibits the sensitivity of $N_{ox\ EXT}$ to changes in mode numbers. In the peak region, $N_{ox\ EXT}$ will increase for increasing n up to n=7, and then decrease again. This peak region is in the range of $0.2 < \nu < 0.5$.

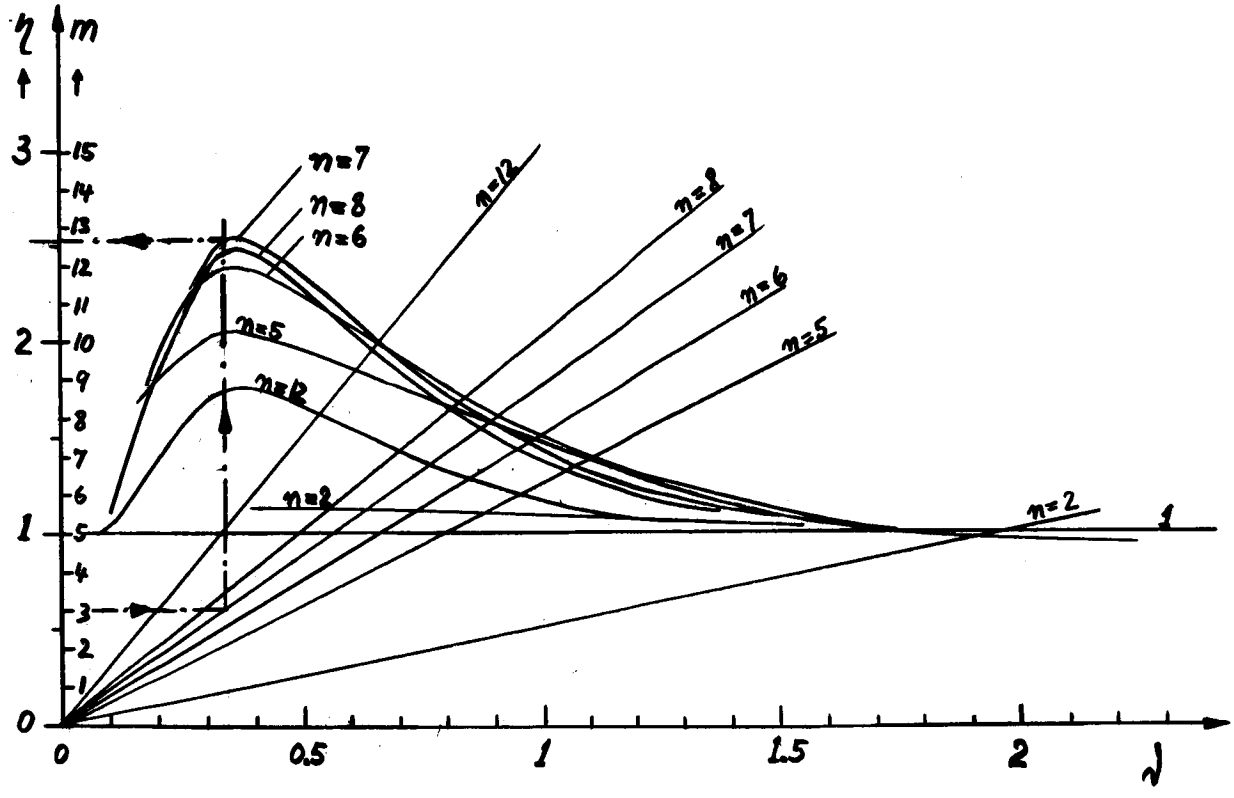

Figure (VII-2) : Stiffener Location Effectiveness Optimization Chart for Card's Shell.

CHAPTER VIII : SUMMARY, CONCLUSIONS AND FUTURE WORK.

1. Summary.

Chapters I and II provide the theoretical basis for the dynamic treatment of an eccentrically reinforced shallow cylindrical shell with closely spaced stiffeners and rings. This basis is provided by a new set of field equations which are shown to reduce to known equations in the literature.

Chapter III extends the field equations to include initial imperfections.

In Chapter IV, a radial displacement assumption is made on the basis of expected buckling pattern and initial imperfections are assumed in "spatial harmony" with the total displacements. A stress function is derived which satisfies the compatibility equation for the assumed radial displacements.

In Chapter V, the problem of a clamped eccentrically reinforced cylindrical shell is taken up, where the dynamic axial load results from some prescribed rate of endshortening. The dynamic equilibrium equations are being satisfied in the sense of Bubnov-Galerkin which results in a system of two non-linear second-order differential equations in the buckling pattern amplitudes. These important equations are then discussed in great detail. The reduction to the case of dynamic buckling of a column is shown. The chapter ends with a description of three distinct periods in the range of these equations, during which some physical insight may be obtained from certain simplifications.

In Chapter VI, the specific case of Card's stringer shell is treated on a numerical basis. Results based on the Runge-Kutta method are shown to be contrary to physical interpretations and "apparent" dynamic buckling occurs due to instability of the Runge-Kutta method. A combined Runge-Kutta Predictor-Corector method leads to dynamic buckling loads which are in agreement with intuitive physical expectations. The remaining portion of this chapter is devoted to a discussion of the influence of various factors on the critical dynamic buckling load, namely rotatory inertia, the magnitude of the constant rate of endshortening, the size of the initial imperfections, the direction of the initial imperfections and the time constant of the exponentially decaying rate of endshortening.

Chapter VII is concerned with static buckling in contradistinction to the other chapters and has been added mainly to give a more complete treatment of the eccentrically reinforced circular cylindrical shell. It is shown that Card's static test buckling load for the internally reinforced shell is theoretically predicted quite closely by a "static" rate of endshortening with initial imperfections of the order of manufacturing tolerances. Static buckling equations are derived from the field equations and a separation into prebuckling and buckling is made. A linear classic Donnell-type equation is derived, and classical buckling loads for Card's shell are compared with test results. The effect of the mode numbers is discussed and the concept of stiffener location effectiveness is explored in detail.

2. Conclusions.

Since no closed-form solution appears to be possible for the dynamic stability of an eccentrically reinforced cylindrical shell, conclusions must be based on relatively few numerical results for some specific shell.

- On the basis of available data for Card's stringer shell, we may conclude that rotatory inertia can be neglected in determining the critical dynamic buckling load. For other, cases it seems advisable to include it in the first numerical calculations.
- As expected, the magnitude of V_o for constant rate of end-shortening plays an important role. Magnifications of the static buckling loads of the order of two and three were obtained for the internally reinforced shell for V_o=50 ips and for V_o=100 ips, as compared with Card's static test results. These magnifications are considerably less for the externally stiffened shell, the reason being, that the critical dynamic buckling load is associated with different mode numbers for that shell as compared with the internally reinforced one. Card's static tests gave the same mode numbers for both shells. If the same mode numbers are taken for a basis of comparison from Table (VI-4), the range of these magnifications is similar to the one for the internally reinforced shell.
- The size of the imperfection amplitudes affects the critical dynamic buckling load drastically, as evidenced from Table (VI-4).

Starting with values of reasonable manufacturing tolerance (0.001 in), it is seen that an increase to approximately half the monocoque shell thickness (0.014 in) reduces the buckling loads by a factor of 1.6-1.8 for the same V_o=100 ips. It is sometimes argued that imperfections are not as important in reinforced cylindrical shells, since there is more "smeared-out" thickness available so that manufacturing tolerances become a smaller percentage than for thin monocoque shells. If the middle-surface amplitudes of the initial imperfections are of the sizes indicated, then such drastic reductions are possible. Whether these magnitudes of the imperfections are realistic,or not, depends on the method of manufacturing and assembly.

- The effect of the direction of the initial imperfections seems to be more of academic interest since imperfections should be eliminated as well as possible. If they do occur, one has ordinarily no control over their directions anyway. The effect of increasing the critical dynamic buckling load by a negative g_o is connected with the somewhat artificial assumption that the initial imperfections are in "spatial harmony" with the total displacements.
- The effect of an exponentially decaying rate of endshortening is to reduce the critical dynamic buckling load, as expected. The amount of reduction depends on the time constant $1/\gamma$. In the case of Card's shell, a time constant was selected of the order of the time it takes to reach buckling with a constant rate of endshortening V_o=100 ips. For the inter-

nally stiffened shell a reduction occurs to roughly the values obtained from assuming constant rate of endshortening V_o=50 ips, while it is somewhat more drastic for the externally stiffened shell.

- The theory of dynamic buckling yields a static buckling load for Card's internally stiffened shell which is in close agreement with the experimental value when "static" values for V_o and initial imperfections of the order of manufacturing tolerances are used.
- Within the scope of the classical static theory and the "stiffener" assumption of equal mode numbers, it is shown that maximum stiffener location effectiveness for Card's shell lies within the aspect ratio range of $0.3 < \eta < 0.5$; the best possible value ($\eta = 2.52$) occurs for the mode numbers m=3 and n=7.

3. Future Work.

A complex problem like the dynamic stability of eccentrically reinforced cylindrical shells offers a challenge to many approaches and for each solution, there will be an improved version. Extensions and improvements of the present work may be classified into:

- Improvements of the present solution of the same problem
- Extension of the problem to include other loading conditions.
- Extension of the problem to include other reinforcement configurations.
- Experimental work.

The present solution could possibly be improved in various aspects. A more realistic representation of the impact problem would have to include effects due to wave propagation and the elastic response should be extended into the plastic range. Within the scope of the present solution, the initial imperfection displacement assumption should be made more realistic. It would be desirable to have radial displacement assumptions which not only describe a physical buckling pattern, but also satisfy the given boundary conditions exactly. In addition to the present free parameters f_1 and g_1, there is a need for additional parameters. α and β should be made to be free parameters also. Then the mode numbers would become time-dependent in the analysis. It is of course obvious that any of these suggestions add considerable complexity to an already lengthy development. Before plunging into such improvements of the present approach, it is suggested to check for "passage" of the main bottle necks: Is it possible to find an integral for the stress function from the compatibility equation ? Does the assumed radial displacement offer advantages in evaluating the Galerkin integrals, such as orthogonality relations? What kind of nonlinear coupled differential equation system is to be expected in the selected free parameters, and can it be tackled within the state of the art of numerical methods ?

The scope of the present work is restricted to axial loads resulting from a prescribed rate of endshortening. There are, of course, many other loading possibilities, including simultaneous interaction of various spatial load distributions.

Generally speaking, we might look at the shell contour surfaces (lateral surfaces and faces) as a closed system which is acted upon by external disturbances. The boundary of this system is subjected to certain categories of disturbances which we choose to classify in the manner shown in Figure (VIII-1). The reaction of the internal shell system is then the response (deflection, strain, stress). Extensions of the present work to other loading situations is therefore possible in many ways.

The present analysis is limited to closely spaced stiffeners of an orthogonal array parallel to the generators and circles of the cylinder. The present analysis might be extended to include other reinforcement configurations in the same "equivalent shell" treatment. For the development of a theory to investigate "discreet" stiffening elements, the basic developments of the earlier chapters would have to be changed.

As already indicated, it is entirely feasible to consider the influence of boundary conditions on the prebuckling deformations in the static analysis.

Except for the verification of the static reduction of the present theory with Card's experimental results, a comparison of the "dynamic" theory with practical experiments is lacking. A short discussion of such possibilities is given below.

The Applied Mechanics Laboratory of Syracuse University has

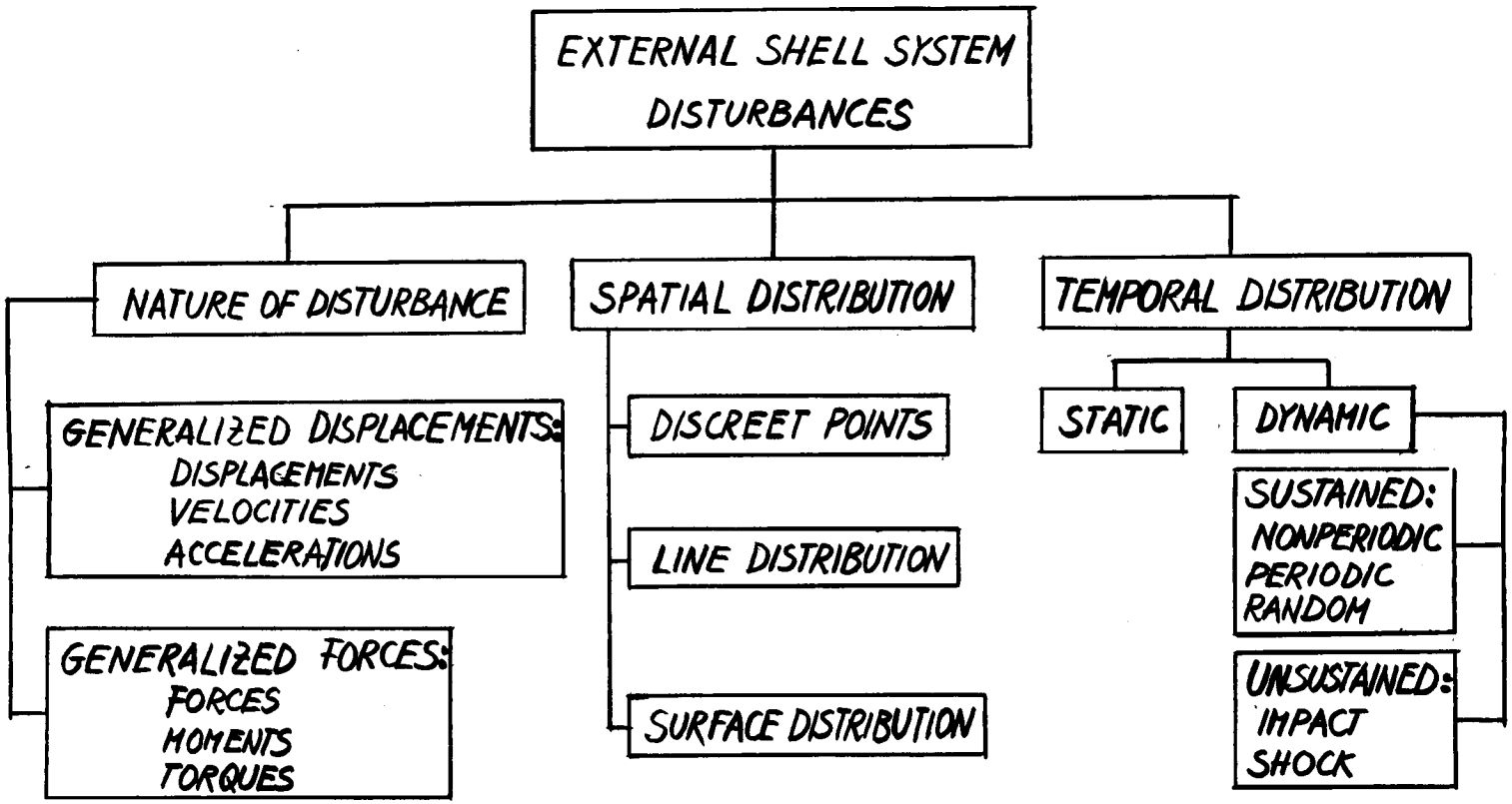

FIGURE (VIII-1): CLASSIFICATION OF POSSIBLE LOAD CONFIGURATIONS ON A SHELL.

successfully developed a process to make photoelastic monocoque cylindrical shells of extreme accuracy within certain dimensional ranges. No such process is presently available to produce stiffened cylindrical shells. The writer spent a considerable amount of time to put together a six-stringer externally stiffened cylindrical shell. Unfortunately, it collapsed under the slightest touch of a static load. The stringers were carefully cut from an available photoelastic cylinder as segments of the lateral side, thus providing the appropriate curvature to match the monocoque cylinder to which these segments were glued. This method is inadequate, however, toproduce closely-spaced stringer- and ring-stiffened circular cylindrical shells in large quantities, and it provides for no variation of the dimensions and geometries of the stiffener-shell structure. In dynamic testing, it is to be expected that the sample will be destroyed in each test run, in contrast to the slowly-run static test, which can be readily confined to the elastic regime, thus allowing for repetition. In addition, the presently used photoelastic material seems to lack toughness for impact-type loading. Embrittlement seems to increase as storage time increases. A research program is envisioned in order to study the manufacturing of closely-spaced stiffened cylinders made out of photoelastic material. Such shells could be loaded dynamically on the MB-testing machine which allows for proramming the endshortening. Possibly, the AVCO-Shocktester could be utilized. The history of the buckling process could be recorded with a high-speed movie camera (Photoeleastic patterns).

APPENDIX A : SOME DETAILS OF THE BUBNOV-GALERKIN PROCEDURE.

The algebraic evaluation of the Bubnov-Galerkin equations (V-11) is extremely lengthy. While it is not intended to present all detailed calculations, some intermediate results are given in this appendix.

H is calculated in (V-10) by substituting the radial displacement terms from (IV-18) and the stress function terms from (IV-19). In the latter, $\bar{N}_{oy}$ is replaced by (IV-27). Thus, one obtains:

$$
\begin{aligned}
H = {} & \alpha^4 D_{11}\left[(f_1-f_0)\sin\alpha x\sin\beta y - 4(g_1-g_0)\cos 2\alpha x + 4(g_1-g_0)\cos 2\alpha x\cos 2\beta y\right] \\
& + 2\alpha^2\beta^2 D_{12}\left[(f_1-f_0)\sin\alpha x\sin\beta y + 4(g_1-g_0)\cos 2\alpha x\cos 2\beta y\right] \\
& + \beta^4 D_{22}\left[(f_1-f_0)\sin\alpha x\sin\beta y - 4(g_1-g_0)\cos 2\beta y + 4(g_1-g_0)\cos 2\alpha x\cos 2\beta y\right] \\
& + \alpha^4 S_{11}\left[\lambda_1\sin\alpha x\sin\beta y + 81\lambda_2\sin 3\alpha x\sin\beta y + \lambda_3\sin\alpha x\sin 3\beta y\right. \\
& + 16\lambda_4\cos 2\alpha x + 16\lambda_6\cos 2\alpha x\cos 2\beta y + 256\lambda_7\cos 4\alpha x \\
& \left. + 256\lambda_9\cos 4\alpha x\cos 2\beta y + 16\lambda_{10}\cos 2\alpha x\cos 4\beta y\right] \\
& - 2\alpha^2\beta^2 S_{12}\left[\lambda_1\sin\alpha x\sin\beta y + 9\lambda_2\sin 3\alpha x\sin\beta y + 9\lambda_3\sin\alpha x\sin 3\beta y\right. \\
& \left. + 16\lambda_6\cos 2\alpha x\cos 2\beta y + 64\lambda_9\cos 4\alpha x\cos 2\beta y + 64\lambda_{10}\cos 2\alpha x\cos 4\beta y\right] \\
& + \beta^4 S_{22}\left[\lambda_1\sin\alpha x\sin\beta y + \lambda_2\sin 3\alpha x\sin\beta y + 81\lambda_3\sin\alpha x\sin 3\beta y\right. \\
& + 16\lambda_5\cos 2\beta y + 16\lambda_6\cos 2\alpha x\cos 2\beta y + 256\lambda_8\cos 4\beta y \\
& \left. + 16\lambda_9\cos 4\alpha x\cos 2\beta y + 256\lambda_{10}\cos 2\alpha x\cos 4\beta y\right] \\
& + \alpha^2\beta^2\left[-\lambda_1 f_1\sin^2\alpha x\sin^2\beta y - 9\lambda_2 f_1\sin\alpha x\sin 3\alpha x\sin^2\beta y\right.
\end{aligned}
$$

(continued next page)

$$
\begin{aligned}
&- \lambda_3 f_1 \sin^2\alpha x \sin\beta y \sin 3\beta y - 4\lambda_4 f_1 \sin\alpha x \cos 2\alpha x \sin\beta y \\
&- 4\lambda_6 f_1 \sin\alpha x \cos 2\alpha x \sin\beta y \cos 2\beta y - 16\lambda_7 f_1 \sin\alpha x \cos 4\alpha x \sin\beta y \\
&- 16\lambda_9 f_1 \sin\alpha x \cos 4\alpha x \sin\beta y \cos 2\beta y - 4\lambda_{10} f_1 \sin\alpha x \cos 2\alpha x \sin\beta y \cos 4\beta y \\
&- \frac{A_{13}}{A_{11}} \frac{\bar{N}_{0x}}{\alpha^2} f_1 \sin\alpha x \sin\beta y + \frac{\beta^2}{\alpha^2} \frac{1}{8A_{11}} (f_1^3 - f_1 f_0^2) \sin\alpha x \sin\beta y \\
&+ \frac{\beta^2}{\alpha^2} \frac{3}{32A_{11}} (f_1 g_1^2 - f_1 g_0^2) \sin\alpha x \sin\beta y - \frac{1}{\alpha^2} \frac{1}{4A_{11}R} (f_1 g_1 - f_1 g_0) \sin\alpha x \sin\beta y \\
&+ \lambda_1 g_1 \sin\alpha x \sin\beta y \cos 2\beta y + 9\lambda_2 g_1 \sin 3\alpha x \sin\beta y \cos 2\beta y \\
&+ \lambda_3 g_1 \sin\alpha x \sin 3\beta y \cos 2\beta y + 4\lambda_4 g_1 \cos 2\alpha x \cos 2\beta y + 4\lambda_6 g_1 \cos 2\alpha x \cos^2 2\beta y \\
&+ 16\lambda_7 g_1 \cos 4\alpha x \cos 2\beta y + 16\lambda_9 g_1 \cos 4\alpha x \cos^2 2\beta y \\
&+ 4\lambda_{10} g_1 \cos 2\alpha x \cos 2\beta y \cos 4\beta y + \frac{A_{13}}{A_{11}} \frac{\bar{N}_{0x}}{\alpha^2} g_1 \cos 2\beta y \\
&- \frac{\beta^2}{\alpha^2} \frac{1}{8A_{11}} (f_1^2 g_1 - f_0^2 g_1) \cos 2\beta y - \frac{\beta^2}{\alpha^2} \frac{3}{32A_{11}} (g_1^3 - g_0^2 g_1) \cos 2\beta y \\
&+ \frac{1}{\alpha^2} \frac{1}{4A_{11}R} (g_1^2 - g_0 g_1) \cos 2\beta y - \lambda_1 g_1 \sin\alpha x \cos 2\alpha x \sin\beta y \cos 2\beta y \\
&- 9\lambda_2 g_1 \sin 3\alpha x \cos 2\alpha x \sin\beta y \cos 2\beta y - \lambda_3 g_1 \sin\alpha x \cos 2\alpha x \sin 3\beta y \cos 2\beta y \\
&- 4\lambda_4 g_1 \cos^2 2\alpha x \cos 2\beta y - 4\lambda_6 g_1 \cos^2 2\alpha x \cos^2 2\beta y - 16\lambda_7 g_1 \cos 2\alpha x \cos 4\alpha x \cos 2\beta y \\
&- 16\lambda_9 g_1 \cos 2\alpha x \cos 4\alpha x \cos^2 2\beta y - 4\lambda_{10} g_1 \cos^2 2\alpha x \cos 2\beta y \cos 4\beta y \\
&- \frac{A_{13}}{A_{11}} \frac{N_{0x}}{\alpha^2} g_1 \cos 2\alpha x \cos 2\beta y + \frac{\beta^2}{\alpha^2} \frac{1}{8A_{11}} (f_1^2 g_1 - f_0^2 g_1) \cos 2\alpha x \cos 2\beta y \\
&+ \frac{\beta^2}{\alpha^2} \frac{3}{32A_{11}} (g_1^3 - g_1 g_0^2) \cos 2\alpha x \cos 2\beta y - \frac{1}{\alpha^2} \frac{1}{4A_{11}R} (g_1^2 - g_0 g_1) \cos 2\alpha x \cos 2\beta y \Big] \\
&+ 2\alpha^2\beta^2 \Big[\lambda_1 f_1 \cos^2\alpha x \cos^2\beta y + 3\lambda_2 f_1 \cos\alpha x \cos 3\alpha x \cos^2 2\beta y \\
&+ 3\lambda_3 f_1 \cos^2\alpha x \cos\beta y \cos 3\beta y + 4\lambda_6 f_1 \sin 2\alpha x \cos\alpha x \sin 2\beta y \cos\beta y \\
&+ 8\lambda_9 f_1 \sin 4\alpha x \cos\alpha x \sin 2\beta y \cos\beta y + 8\lambda_{10} f_1 \sin 2\alpha x \cos\alpha x \sin 4\beta y \cos\beta y
\end{aligned}
$$

(continued next page)

$$+\lambda_1 g_1 \sin 2\alpha x \cos\alpha x \sin 2\beta y \cos\beta y + 3\lambda_2 g_1 \sin 2\alpha x \cos 3\alpha x \sin 2\beta y \cos\beta y$$
$$+ 3\lambda_3 g_1 \sin 2\alpha x \cos\alpha x \sin 2\beta y \cos 3\beta y + 4\lambda_6 g_1 \sin^2 2\alpha x \sin^2 2\beta y$$
$$+ 8\lambda_9 g_1 \sin 2\alpha x \sin 4\alpha x \sin^2 2\beta y + 8\lambda_{10} g_1 \sin^2 2\alpha x \sin 2\beta y \sin 4\beta y]$$
$$+\alpha^2\beta^2[-\lambda_1 f_1 \sin^2\alpha x \sin^2\beta y - \lambda_2 f_1 \sin\alpha x \sin 3\alpha x \sin^2\beta y$$
$$- 9\lambda_3 f_1 \sin^2\alpha x \sin\beta y \sin 3\beta y - 4\lambda_5 f_1 \sin\alpha x \sin\beta y \cos 2\beta y$$
$$- 4\lambda_6 f_1 \sin\alpha x \cos 2\alpha x \sin\beta y \cos 2\beta y - 16\lambda_8 f_1 \sin\alpha x \sin\beta y \cos 4\beta y$$
$$- 4\lambda_9 f_1 \sin\alpha x \cos 4\alpha x \sin\beta y \cos 2\beta y - 16\lambda_{10} f_1 \sin\alpha x \cos 2\alpha x \sin\beta y \cos 4\beta y$$
$$- \frac{\bar{N}_{0x}}{\beta^2} f_1 \sin\alpha x \sin\beta y + \lambda_1 g_1 \sin\alpha x \cos 2\alpha x \sin\beta y$$
$$+\lambda_2 g_1 \sin 3\alpha x \cos 2\alpha x \sin\beta y + 9\lambda_3 g_1 \sin\alpha x \cos 2\alpha x \sin 3\beta y$$
$$+ 4\lambda_5 g_1 \cos 2\alpha x \cos 2\beta y + 4\lambda_6 g_1 \cos^2 2\alpha x \cos 2\beta y + 16\lambda_8 g_1 \cos 2\alpha x \cos 4\beta y$$
$$+ 4\lambda_9 g_1 \cos 2\alpha x \cos 4\alpha x \cos 2\beta y + 16\lambda_{10} g_1 \cos^2 2\alpha x \cos 4\beta y$$
$$+ \frac{\bar{N}_{0x}}{\beta^2} g_1 \cos 2\alpha x - \lambda_1 g_1 \sin\alpha x \cos 2\alpha x \sin\beta y \cos 2\beta y$$
$$- \lambda_2 g_1 \sin 3\alpha x \cos 2\alpha x \sin\beta y \cos 2\beta y - 9\lambda_3 g_1 \sin\alpha x \cos 2\alpha x \sin 3\beta y \cos 2\beta y$$
$$- 4\lambda_5 g_1 \cos 2\alpha x \cos^2 2\beta y - 4\lambda_6 g_1 \cos^2 2\alpha x \cos^2 2\beta y$$
$$- 16\lambda_8 g_1 \cos 2\alpha x \cos 2\beta y \cos 4\beta y - 4\lambda_9 g_1 \cos 2\alpha x \cos 4\alpha x \cos^2 2\beta y$$
$$- 16\lambda_{10} g_1 \cos^2 2\alpha x \cos 2\beta y \cos 4\beta y - \frac{\bar{N}_{0x}}{\beta^2} g_1 \cos 2\alpha x \cos 2\beta y]$$
$$+\frac{\alpha^2}{R}[\lambda_1 \sin\alpha x \sin\beta y + 9\lambda_2 \sin 3\alpha x \sin\beta y + \lambda_3 \sin\alpha x \sin 3\beta y$$
$$+ 4\lambda_4 \cos 2\alpha x + 4\lambda_6 \cos 2\alpha x \cos 2\beta y + 16\lambda_7 \cos 4\alpha x$$
$$+ 16\lambda_9 \cos 4\alpha x \cos 2\beta y + 4\lambda_{10} \cos 2\alpha x \cos 4\beta y + \frac{A_{13}}{A_{11}} \frac{\bar{N}_{0x}}{\alpha^2}$$

(continued next page)

$$- \frac{\beta^2}{\alpha^2}\frac{1}{8A_{11}}(f_1^2 - f_0^2) - \frac{\beta^2}{\alpha^2}\frac{3}{32A_{11}}(g_1^2 - g_0^2) + \frac{1}{\alpha^2}\frac{1}{4A_{11}R}(g_1 - g_0)\Big]$$

$$+ \bar{m}\Big[\frac{d^2f_1}{dt^2}\sin\alpha x \sin\beta y + \frac{1}{4}\frac{d^2g_1}{dt^2} - \frac{1}{4}\frac{d^2g_1}{dt^2}\cos 2\alpha x$$

$$- \frac{1}{4}\frac{d^2g_1}{dt^2}\cos 2\beta y + \frac{1}{4}\frac{d^2g_1}{dt^2}\cos 2\alpha x \cos 2\beta y\Big]$$

$$+ (\alpha^2+\beta^2) I_{\bar{m}}\Big[\frac{d^2f_1}{dt^2}\sin\alpha x \sin\beta y + \frac{d^2g_1}{dt^2}\cos 2\alpha x \cos 2\beta y\Big]$$

$$- I_{\bar{m}}\frac{d^2g_1}{dt^2}(\alpha^2\cos 2\alpha x + \beta^2 \cos 2\beta y) \qquad \text{(A-1)}$$

The first Bubnov-Galerkin equation, e.g.

$$\int_0^L \int_0^{2\pi R} H \sin\alpha x \sin\beta y \, dx\, dy = 0$$

is evaluated with H from (A-1). On integrating the above expression, a great many terms vanish. After a considerable amount of algebra, the following equation results:

$$(f_1 - f_0)\left[\alpha^4 D_{11} + 2\alpha^2\beta^2 D_{12} + \beta^4 D_{22}\right] + \lambda_1\left[\alpha^4 S_{11} - 2\alpha^2\beta^2 S_{12}\right.$$

$$\left. + \beta^4 S_{22} + \frac{\alpha^2}{R}\right] + \alpha^2\beta^2 f_1\left[2(\lambda_4+\lambda_5) - \frac{\bar{N}_{0x}}{\alpha^2\beta^2}\left(\alpha^2 + \frac{A_{13}}{A_{11}}\beta^2\right)\right]$$

$$+ \alpha^2\beta^2\left[-\lambda_1 + \frac{3}{2}\lambda_2 + \frac{3}{2}\lambda_3\right] + \frac{\beta^4}{8A_{11}}(f_1^3 - f_1 f_0^2)$$

$$+ \frac{3\beta^4}{32A_{11}}(f_1 g_1^2 - f_1 g_0^2) - \frac{\beta^2}{4A_{11}R}(f_1 g_1 - f_1 g_0) + \bar{m}_1 \frac{d^2f_1}{dt^2} = 0 \qquad \text{(A-2)}$$

where the abbreviation,

$$\bar{m}_1 = \bar{m} + (\alpha^2+\beta^2) I_{\bar{m}} \qquad \text{(A-3)}$$

has been introduced.

Inserting the λ's from (IV-10) and $\bar{N}_{ox}$ from (V-9) into equation (A-2), solving for $\frac{d^2 f_1}{dt^2}$, leads to,

$$\frac{d^2 f_1}{dt^2} = B_1 f_1 + B_2 g_1 + B_3 f_1 g_1 + B_4 f_1 g_1^2 + B_5 f_1^3 + B_6 f_1 \frac{1-e^{-\gamma t}}{\gamma} + B_7 \qquad \text{(A-4)}$$

where a considerable amount of algebra has been omitted, and where the coefficients B are defined by:

$$B_1 = -\frac{1}{\bar{m}_1}(\alpha^4 D_{11} + 2\alpha^2\beta^2 D_{12} + \beta^4 D_{22}) - \frac{(\alpha^4 S_{11} - 2\alpha^2\beta^2 S_{12} + \beta^4 S_{22} + \frac{\alpha^2}{R})^2}{\bar{m}_1(\alpha^4 A_{11} + 2\alpha^2\beta^2 A_{12} + \beta^4 A_{22})}$$

$$+ \frac{\alpha^4(f_0^2 + g_0^2)}{16 A_{22}\bar{m}_1} + \frac{\beta^4(3f_0^2 + \frac{5}{2}g_0^2)}{16 A_{11}\bar{m}_1} - \frac{\alpha^2\beta^2 g_0 S_{22}}{2A_{22}\bar{m}_1}$$

$$+ \frac{(\alpha^2 + \frac{A_{13}}{A_{11}}\beta^2)^2(f_0^2 + \frac{3}{4}g_0^2)}{8\bar{m}_1(A_{22} - \frac{A_{13}^2}{A_{11}})} - \frac{\beta^2 g_0}{4A_{11}R\bar{m}_1} - \frac{\beta^2(\alpha^2 S_{11} + \frac{1}{4R})g_0}{2A_{11}\bar{m}_1} \qquad \text{(A-5)}$$

$$B_2 = -\frac{\alpha^2\beta^2 f_0(\alpha^4 S_{11} - 2\alpha^2\beta^2 S_{12} + \beta^4 S_{22} + \frac{\alpha^2}{R})}{\bar{m}_1(\alpha^4 A_{11} + 2\alpha^2\beta^2 A_{12} + \beta^4 A_{22})}$$

$$+ \frac{\alpha^4\beta^4 f_0 g_0}{\bar{m}_1(\alpha^4 A_{11} + 2\alpha^2\beta^2 A_{12} + \beta^4 A_{22})} + \frac{9\alpha^4\beta^4 f_0 g_0}{4\bar{m}_1(81\alpha^4 A_{11} + 18\alpha^2\beta^2 A_{12} + \beta^4 A_{22}}$$

$$+ \frac{9\alpha^4\beta^4 f_0 g_0}{4\bar{m}_1(\alpha^4 A_{11} + 18\alpha^2\beta^2 A_{12} + 81\beta^4 A_{22})} \qquad \text{(A-6)}$$

$$B_3 = \frac{2\alpha^2\beta^2(\alpha^4 S_{11} - 2\alpha^2\beta^2 S_{12} + \beta^4 S_{22} + \frac{\alpha^2}{R})}{\bar{m}_1(\alpha^4 A_{11} + 2\alpha^2\beta^2 A_{12} + \beta^4 A_{22})} + \frac{\beta^2(\alpha^2 S_{11} + \frac{1}{4R})}{2A_{11}\bar{m}_1}$$

$$+ \frac{\alpha^2\beta^2 S_{22}}{2A_{22}\bar{m}_1} + \frac{\beta^2}{4A_{11}R\bar{m}_1} + \frac{A_{13}(\alpha^2 + \frac{A_{13}}{A_{11}}\beta^2)}{4A_{11}R\bar{m}_1(A_{22} - \frac{A_{13}^2}{A_{11}})}$$

(A-7)

$$B_4 = -\frac{\alpha^4\beta^4}{\bar{m}_1(\alpha^4 A_{11} + 2\alpha^2\beta^2 A_{12} + \beta^4 A_{22})} - \frac{9\alpha^4\beta^4}{4\bar{m}_1(81\alpha^4 A_{11} + 18\alpha^2\beta^2 A_{12} + \beta^4 A_{22})}$$

$$- \frac{9\alpha^4\beta^4}{4\bar{m}_1(\alpha^4 A_{11} + 18\alpha^2\beta^2 A_{12} + 81\beta^4 A_{22})} - \frac{5\beta^4}{32A_{11}\bar{m}_1}$$

$$- \frac{\alpha^4}{16A_{22}\bar{m}_1} - \frac{3(\alpha^2 + \frac{A_{13}}{A_{11}}\beta^2)^2}{32\bar{m}_1(A_{22} - \frac{A_{13}^2}{A_{11}})}$$

(A-8)

$$B_5 = -\frac{\alpha^4}{16A_{22}\bar{m}_1} - \frac{3\beta^4}{16A_{11}\bar{m}_1} - \frac{(\alpha^2 + \frac{A_{13}}{A_{11}}\beta^2)^2}{8\bar{m}_1(A_{22} - \frac{A_{13}^2}{A_{11}})}$$

(A-9)

$$B_6 = \frac{(\alpha^2 + \frac{A_{13}}{A_{11}}\beta^2)V_0}{\bar{m}_1 L(A_{22} - \frac{A_{13}^2}{A_{11}})}$$

(A-10)

$$B_7 = \frac{f_0}{\bar{m}_1}(\alpha^4 D_{11} + 2\alpha^2\beta^2 D_{12} + \beta^4 D_{22}) + \frac{f_0(\alpha^4 S_{11} - 2\alpha^2\beta^2 S_{12} + \beta^4 S_{22} + \frac{\alpha^2}{R})^2}{\bar{m}_1(\alpha^4 A_{11} + 2\alpha^2\beta^2 A_{12} + \beta^4 A_{22})}$$

$$- \frac{\alpha^2\beta^2 f_0 g_0(\alpha^4 S_{11} - 2\alpha^2\beta^2 S_{12} + \beta^4 S_{22} + \frac{\alpha^2}{R})}{\bar{m}_1(\alpha^4 A_{11} + 2\alpha^2\beta^2 A_{12} + \beta^4 A_{22})}$$

(A-11)

Turning now to the second Bubnov-Galerkin equation, e.g.

$$\int_0^L \int_0^{2\pi R} H \sin^2 \alpha x \sin^2 \beta y \, dx \, dy = 0$$

and proceeding as before, leads to:

$$(g_1 - g_0)\left[3\alpha^4 D_{11} + 2\alpha^2\beta^2 D_{12} + 3\beta^4 D_{22} + \frac{1}{4A_{11}R^2}\right]$$
$$- 8\alpha^2\lambda_4\left[\alpha^2 S_{11} + \frac{1}{4R}\right] + 4\lambda_6\left[\alpha^4 S_{11} - 2\alpha^2\beta^2 S_{12} + \beta^4 S_{22} + \frac{\alpha^2}{4R}\right]$$
$$- 8\beta^4\lambda_5 S_{22} + \alpha^2\beta^2 f_1\left[-\lambda_1 + \frac{3}{2}(\lambda_2 + \lambda_3) + \alpha^2\beta^2 g_1\left[2(\lambda_4 + \lambda_5$$
$$- \lambda_6 - \lambda_7 - \lambda_8) + \lambda_9 + \lambda_{10} - \frac{3}{4}\frac{\bar{N}_{0x}}{\alpha^2\beta^2}\left(\alpha^2 + \frac{A_{13}}{A_{11}}\beta^2\right)\right]$$
$$+ \frac{\beta^4}{16A_{11}}(f_1^2 g_1 - f_0^2 g_1) + \frac{3\beta^4}{64A_{11}}(g_1^3 - g_0^2 g_1) + \frac{\beta^4}{32A_{11}}(f_1^2 g_1 - f_0^2 g_1)$$
$$+ \frac{3\beta^4}{128A_{11}}(g_1^3 - g_1 g_0^2) - \frac{\beta^2}{8A_{11}R}(f_1^2 - f_0^2) - \frac{3\beta^2}{32A_{11}R}(g_1^2 - g_0^2)$$
$$- \frac{3\beta^2}{16A_{11}R}(g_1^2 - g_0 g_1) + \frac{A_{13}}{A_{11}}\frac{\bar{N}_{0x}}{R} + \frac{9}{16}\bar{m}_2\frac{d^2 g_1}{dt^2} = 0 \qquad \text{(A-12)}$$

where the abbreviation,

$$\bar{m}_2 = \bar{m} + \frac{4}{3}(\alpha^2 + \beta^2) I_{\bar{m}} \qquad \text{(A-13)}$$

has been introduced.

The λ's from (IV-10) and $\bar{N}_{0x}$ from (V-9) are introduced into (A-12). After considerable algebra, the resulting expression is solved for $\frac{d^2 g_1}{dt^2}$, which becomes:

$$\frac{d^2 g_1}{dt^2} = C_1 g_1 + C_2 f_1 + C_3 g_1^2 + C_4 f_1^2 + C_5 f_1^2 g_1 + C_6 g_1^3 + C_7 g_1 \frac{1-e^{-\gamma t}}{\gamma} + C_8 \frac{1-e^{-\gamma t}}{\gamma} + C_9$$

(A-14)

The coefficients C are defined by:

$$C_1 = -\frac{16}{9\bar{m}_2}\left(3\alpha^4 D_{11} + 2\alpha^2\beta^2 D_{12} + 3\beta^4 D_{22} + \frac{1}{4A_{11}R^2}\right)$$

$$- \frac{32\left(\alpha^2 S_{11} + \frac{1}{4R}\right)^2}{9 A_{11}\bar{m}_2} - \frac{16\left(\alpha^4 S_{11} - 2\alpha^2\beta^2 S_{12} + \beta^4 S_{22} + \frac{\alpha^2}{4R}\right)^2}{9\bar{m}_2\left(\alpha^4 A_{11} + 2\alpha^2\beta^2 A_{12} + \beta^4 A_{22}\right)}$$

$$- \frac{32\beta^4 S_{22}^2}{9 A_{22}\bar{m}_2} - \frac{8\beta^2 g_0\left(\alpha^2 S_{11} + \frac{1}{4R}\right)}{9 A_{11}\bar{m}_2} + \frac{\beta^4\left(f_0^2 + g_0^2\right)}{9 A_{11}\bar{m}_2}$$

$$- \frac{8\alpha^2\beta^2 S_{22} g_0}{9 A_{22}\bar{m}_2} + \frac{\alpha^4\left(f_0^2 + g_0^2\right)}{9 A_{22}\bar{m}_2} - \frac{8\alpha^2\beta^2 g_0\left(\alpha^4 S_{11} - 2\alpha^2\beta^2 S_{12} + \beta^4 S_{22} + \frac{\alpha^2}{4R}\right)}{9\bar{m}_2\left(\alpha^4 A_{11} + 2\alpha^2\beta^2 A_{12} + \beta^4 A_{22}\right)}$$

$$+ \frac{2\alpha^4\beta^4 g_0^2}{9\bar{m}_2\left(\alpha^4 A_{11} + 2\alpha^2\beta^2 A_{12} + \beta^4 A_{22}\right)} + \frac{\alpha^4 g_0^2}{144 A_{22}\bar{m}_2} + \frac{\beta^4 g_0^2}{144 A_{11}\bar{m}_2}$$

$$+ \frac{\alpha^4\beta^4 g_0^2}{18\bar{m}_2\left(16\alpha^4 A_{11} + 8\alpha^2\beta^2 A_{12} + \beta^4 A_{22}\right)} + \frac{\alpha^4\beta^4 g_0^2}{18\bar{m}_2\left(\alpha^4 A_{11} + 8\alpha^2\beta^2 A_{12} + 16\beta^4 A_{22}\right)}$$

$$+ \frac{\left(\alpha^2 + \frac{A_{13}}{A_{11}}\beta^2\right)^2\left(f_0^2 + \frac{3}{4}g_0^2\right)}{6\bar{m}_2\left(A_{22} - \frac{A_{13}^2}{A_{11}}\right)} - \frac{A_{13}\left(\alpha^2 + \frac{A_{13}}{A_{11}}\beta^2\right) g_0}{3 A_{11} R\bar{m}_2\left(A_{22} - \frac{A_{13}^2}{A_{11}}\right)}$$

$$+ \frac{\beta^4\left(f_0^2 + \frac{3}{4}g_0^2\right)}{6 A_{11}\bar{m}_2} - \frac{\beta^2 g_0}{3 A_{11} R\bar{m}_2} - \frac{4A_{13}^2}{9 A_{11}^2 R^2\bar{m}_2\left(A_{22} - \frac{A_{13}^2}{A_{11}}\right)}$$

(A-15)

$$C_2 = -\frac{16\alpha^2\beta^2 f_0(\alpha^4 S_{11} - 2\alpha^2\beta^2 S_{12} + \beta^4 S_{22} + \frac{\alpha^2}{R}}{9\bar{m}_2(\alpha^4 A_{11} + 2\alpha^2\beta^2 A_{12} + \beta^4 A_{22})} + \frac{16\alpha^4\beta^4 f_0 g_0}{9\bar{m}_2(\alpha^4 A_{11} + 2\alpha^2\beta^2 A_{12} + \beta^4 A_{22})}$$

$$\frac{4\alpha^4\beta^4 f_0 g_0}{\bar{m}_2(81\alpha^4 A_{11} + 18\alpha^2\beta^2 A_{12} + \beta^4 A_{22})} + \frac{4\alpha^4\beta^4 f_0 g_0}{\bar{m}_2(\alpha^4 A_{11} + 18\alpha^2\beta^2 A_{12} + 81\beta^4 A_{22})}$$

(A-16)

$$C_3 = \frac{4\beta^2(\alpha^2 S_{11} + \frac{1}{4R})}{3A_{11}\bar{m}_2} + \frac{4\alpha^2\beta^2(\alpha^4 S_{11} - 2\alpha^2\beta^2 S_{12} + \beta^4 S_{22} + \frac{\alpha^2}{4R})}{3\bar{m}_2(\alpha^4 A_{11} + 2\alpha^2\beta^2 A_{12} + \beta^4 A_{22})}$$

$$+ \frac{4\alpha^2\beta^2 S_{22}}{3A_{22}\bar{m}_2} + \frac{A_{13}(\alpha^2 + \frac{A_{13}}{A_{11}}\beta^2)}{2A_{11}R\bar{m}_2(A_{22} - \frac{A_{13}^2}{A_{11}})} + \frac{\beta^2}{2A_{11}R\bar{m}_2}$$

(A-17)

$$C_4 = \frac{4\alpha^2\beta^2 S_{22}}{9A_{22}\bar{m}_2} + \frac{16\alpha^2\beta^2(\alpha^4 S_{11} - 2\alpha^2\beta^2 S_{12} + \beta^4 S_{22} + \frac{\alpha^2}{R})}{9\bar{m}_2(\alpha^4 A_{11} + 2\alpha^2\beta^2 A_{12} + \beta^4 A_{22})}$$

$$+ \frac{2\beta^2}{9A_{11}R\bar{m}_2} + \frac{2A_{13}(\alpha^2 + \frac{A_{13}^2}{A_{11}}\beta^2)}{9A_{11}R\bar{m}_2(A_{22} - \frac{A_{13}^2}{A_{11}})} + \frac{4\beta^2(\alpha^2 S_{11} + \frac{1}{4R})}{9A_{11}\bar{m}_2}$$

(A-18)

$$C_5 = -\frac{16\alpha^4\beta^4}{9\bar{m}_2(\alpha^4 A_{11} + 2\alpha^2\beta^2 A_{12} + \beta^4 A_{22})} - \frac{4\alpha^4\beta^4}{\bar{m}_2(81\alpha^4 A_{11} + 18\alpha^2\beta^2 A_{12} + \beta^4 A_{22})}$$

$$- \frac{4\alpha^4\beta^4}{\bar{m}_2(\alpha^4 A_{11} + 18\alpha^2\beta^2 A_{12} + 81\beta^4 A_{22})} - \frac{\beta^4}{9A_{11}\bar{m}_2} - \frac{\alpha^4}{9A_{22}\bar{m}_2}$$

$$- \frac{(\alpha^2 + \frac{A_{13}}{A_{11}}\beta^2)^2}{6\bar{m}_2(A_{22} - \frac{A_{13}^2}{A_{11}})} - \frac{\beta^4}{6A_{11}\bar{m}_2}$$

(A-19)

$$C_6 = -\frac{35\beta^4}{144 A_{11}\bar{m}_2} - \frac{17\alpha^4}{144 A_{22}\bar{m}_2} - \frac{2\alpha^4\beta^4}{9\bar{m}_2(\alpha^4 A_{11} + 2\alpha^2\beta^2 A_{12} + \beta^4 A_{22})}$$

$$- \frac{\alpha^4\beta^4}{18\bar{m}_2(16\alpha^4 A_{11} + 8\alpha^2\beta^2 A_{12} + \beta^4 A_{22})} - \frac{\alpha^4\beta^4}{18\bar{m}_2(\alpha^4 A_{11} + 8\alpha^2\beta^2 A_{12} + 16\beta^4 A_{22})}$$

$$- \frac{(\alpha^2 + \frac{A_{13}}{A_{11}}\beta^2)^2}{8\bar{m}_2(A_{22} - \frac{A_{13}^2}{A_{11}})} \qquad \text{(A-20)}$$

$$C_7 = \frac{4(\alpha^2 + \frac{A_{13}}{A_{11}}\beta^2)V_0}{3\bar{m}_2 L(A_{22} - \frac{A_{13}^2}{A_{11}})} \qquad \text{(A-21)}$$

$$C_8 = -\frac{16 A_{13} V_0}{9 A_{11} R \bar{m}_2 L(A_{22} - \frac{A_{13}^2}{A_{11}})} \qquad \text{(A-22)}$$

$$C_9 = \frac{16 g_0}{9\bar{m}_2}(3\alpha^4 D_{11} + 2\alpha^2\beta^2 D_{12} + 3\beta^4 D_{22} + \frac{1}{4A_{11}R^2})$$

$$+ \frac{32 g_0(\alpha^2 S_{11} + \frac{1}{4R})^2}{9 A_{11}\bar{m}_2} - \frac{4\beta^2(f_0^2 + g_0^2)(\alpha^2 S_{11} + \frac{1}{4R})}{9 A_{11}\bar{m}_2}$$

$$+ \frac{16 g_0(\alpha^4 S_{11} - 2\alpha^2\beta^2 S_{12} + \beta^4 S_{22} + \frac{\alpha^2}{4R})^2}{9\bar{m}_2(\alpha^4 A_{11} + 2\alpha^2\beta^2 A_{12} + \beta^4 A_{22})} - \frac{4\alpha^2\beta^2 g_0^2(\alpha^4 S_{11} - 2\alpha^2\beta^2 S_{12} + \beta^4 S_{22} + \frac{\alpha^2}{4R})}{9\bar{m}_2(\alpha^4 A_{11} + 2\alpha^2\beta^2 A_{12} + \beta^4 A_{22})}$$

$$- \frac{4\alpha^2\beta^2 S_{22}(f_0^2 + g_0^2)}{9 A_{22}\bar{m}_2} + \frac{32\beta^4 g_0 S_{22}^2}{9 A_{22}\bar{m}_2} - \frac{2\beta^2(f_0^2 + \frac{3}{4}g_0^2)}{9 A_{11} R \bar{m}_2}$$

$$- \frac{2 A_{13}(\alpha^2 + \frac{A_{13}}{A_{11}}\beta^2)(f_0^2 + \frac{3}{4}g_0^2)}{9 A_{11} R \bar{m}_2 (A_{22} - \frac{A_{13}^2}{A_{11}})} + \frac{4 A_{13}^2 g_0}{9 A_{11}^2 R^2 \bar{m}_2 (A_{22} - \frac{A_{13}^2}{A_{11}})}$$

(A-23)

APPENDIX B : THE COMPUTER PROGRAM OF THE COMBINED METHOD

1. A Summary of Composite Shell Parameters.

$$K = \frac{Eh}{1-\nu^2}$$

$$K_\nu = \frac{\nu Eh}{1-\nu^2}$$

$$K_G = \frac{Eh}{2(1+\nu)} = Gh$$

$$K_P = K_\nu + K_G = \frac{Eh}{2(1-\nu)}$$

$$K_S = \frac{E_S A_S}{d}$$

$$K_R = \frac{E_R A_R}{\ell}$$

$$K_{MS} = K + K_S = \frac{Eh}{1-\nu^2} + \frac{E_S A_S}{d}$$

$$K_{MR} = K + K_R = \frac{Eh}{1-\nu^2} + \frac{E_R A_R}{\ell}$$

$$\bar{m} = \rho h + \rho_S \frac{A_S}{d} + \rho_R \frac{A_R}{\ell}$$

$$I_{\bar{m}} = \rho \frac{h^3}{12} + \rho_S \frac{I_{SC} + A_S \bar{z}_S^2}{d} + \rho_R \frac{I_{RC} + A_R \bar{z}_R^2}{\ell}$$

$$\bar{m}_1 = \bar{m} + (\alpha^2 + \beta^2) I_{\bar{m}}$$

$$\bar{m}_2 = \bar{m} + \frac{4}{3}(\alpha^2 + \beta^2) I_{\bar{m}}$$

$$F_{Sb} = \frac{E_S A_S}{d} \bar{z}_S$$

$$F_{Rb} = \frac{E_R A_R}{\ell} \bar{z}_R$$

$$S_H = \frac{K_\nu F_{Sb}}{K_{MS} K_{MR} - K_\nu^2}$$

$$S_{12} = \frac{1}{2} \frac{K_{MR} F_{Sb} + K_{MS} F_{Rb}}{K_{MS} K_{MR} - K_\nu^2}$$

$$S_{13} = \frac{K_{MS} F_{Rb}}{K_{MS} K_{MR} - K_\nu^2}$$

$$S_{14} = \frac{K_{MR} F_{Sb}}{K_{MS} K_{MR} - K_\nu^2}$$

$$S_{22} = \frac{K_\nu F_{Rb}}{K_{MS} K_{MR} - K_\nu^2}$$

$$A_{11} = \frac{K_{MS}}{K_{MS} K_{MR} - K_\nu^2}$$

$$A_{12} = \frac{1}{2K_G} - \frac{K_\nu}{K_{MS} K_{MR} - K_\nu^2}$$

$$A_{13} = \frac{K_\nu}{K_{MS} K_{MR} - K_\nu^2}$$

$$A_{22} = \frac{K_{MR}}{K_{MS} K_{MR} - K_\nu^2}$$

$$D = \frac{Eh^3}{12(1-\nu^2)} \qquad D_\nu = \frac{\nu E h^3}{12(1-\nu^2)} \qquad D_G = \frac{Eh^3}{12(1+\nu)} = \frac{Gh^3}{6} = (1-\nu)D$$

$$D_S = \frac{E_S I_{SO}}{d} = \frac{E_S}{d}\left[I_{SC} + \bar{z}_S^2 A_S\right] \qquad D_R = \frac{E_R I_{RO}}{\ell} = \frac{E_R}{\ell}\left[I_{RC} + \bar{z}_R^2 A_R\right]$$

$$D_{GS} = \frac{G_S J_S}{d} \qquad D_{GR} = \frac{G_R J_R}{\ell}$$

$$D_{MS} = D + D_S = \frac{Eh^3}{12(1-\nu^2)} + \frac{E_S}{d}\left[I_{SC} + \bar{z}_S^2 A_S\right]$$

$$D_{MR} = D + D_R = \frac{Eh^3}{12(1-\nu^2)} + \frac{E_R}{\ell}\left[I_{RC} + \bar{z}_R^2 A_R\right]$$

$$D_{MGS} = D_G + D_{GS} = \frac{Gh^3}{6} + \frac{G_S J_S}{d} \qquad D_{MGR} = D_G + D_{GR} = \frac{Gh^3}{6} + \frac{G_R J_R}{\ell}$$

$$D_1 = D_G + \tfrac{1}{2}\left(D_{GS} + D_{GR}\right) \qquad D_2 = D_\nu + \tfrac{1}{2}\left(D_{MGS} + D_{MGR}\right)$$

$$D_{11} = D_{MS} - \frac{K_{MR} F_{Sb}^2}{K_{MS} K_{MR} - K_\nu^2} \qquad D_{12} = D_2 + \frac{K_\nu F_{Sb} F_{Rb}}{K_{MS} K_{MR} - K_\nu^2}$$

$$D_{22} = D_{MR} - \frac{K_{MS} F_{Rb}^2}{K_{MS} K_{MR} - K_\nu^2}$$

$$\mu_1 = A_{11} D_{11} + S_{11}^2 \qquad \mu_2 = 2\left(A_{11} D_{12} + A_{12} D_{11} - 2 S_{11} S_{12}\right)$$

$$\mu_3 = A_{22} D_{11} + 4 A_{12} D_{12} + A_{11} D_{22} + 2\left(S_{11} S_{22} + 2 S_{12}^2\right)$$

$$\mu_4 = 2\left(A_{22} D_{12} + A_{12} D_{22} - 2 S_{12} S_{22}\right) \qquad \mu_5 = A_{22} D_{22} + S_{22}^2$$

2. The Annotated Fortran-Pitt Program

The computer program presented below is written in Fortran-Pitt Code Language (Pitt:University of Pittsburgh). A few comments about its structure seem necessary. The coded quantities follow generally the abbreviations used in the main text of this dissertation, except that capital letters are used, including the subscripts of these abbreviations. Whenever the beginning letter of the abbreviated quantity starts with I,J, K,L,M or N, the letters A, B etc.,are used as the first letter of the coded quantity, preceding the letters of the usual symbol; thus, for example, ν is coded as ANU, which also shows how the Greek letters are translated.

The program begins with the generic calculation of FUNCTION SRNX which is the expression for $\bar{N}_{ox}$ (V-9). Both, constant and exponentially decaying rates of endshortening, are incorporated.

The SUBROUTINE DRYZ computes the quantities R_1 and R_2, which are identical with $F_1(x,y,z)$ and $F_2(x,y,z)$ of (VI-2). The FUNCTION and SUBROUTINE procedures are used in the main program.

Two nested DO loops follow. They execute the program several times. For the given input data of this particular program, all computations are executes first for n=6, for m-values starting from 2 up to 1o, in steps of 2. The same computation cycles then follow for n=8 and n=10.

The statement NPROB=1 initiates the calculation for the internally stiffened shell first, followed by that for the externally reinforced shell, which is controlled by statement 799 near the

end of the program.

There follow the geometry and material input parameters for Card's shell, in this particular case, including the values for γ, f_o, g_o, and V_o.

XS and XE are the values of t at the beginning (here zero) and the end of the anticipated time period for which the computation is desired. INT is the number of steps into which this period is devided.

The calculation of the composite shell parameters follows their definitions, as can be seen from the summary of these parameters of this Appendix.

The computation of the B's and C's traces their definitions in Appendix A, except that AMBAR=$\bar{m}$ replaces $\bar{m}_1$ and $\bar{m}_2$. We conclude from (A-3) and (A-13) that rotatory inertia is therefore not included. The TEMP terms signify temporary storage of the individual terms that make up the B and C expressions.

The RAT1 and RAT2 ratios measure the influence of rotatory inertia. They are numerically smaller than one. The smaller quantity, RAT2, is utilized in a control statement that offers the choice of doing the calculations again with the rotatory inertia included. This is shown by statement 250 later in the program.

The P-values are computed for use in the FUNCTION SRNX.

HT is the step size as opposed to H, which represents the monocoque shell thickness.

The Runge-Kutta method is initialized with 790 and the subse-

quent statements.

The expressions involving ICAL are print control statements. In this case, only every tenth calculation is printed-out.

The DO 233 stores the four initial "Runge-Kutta" values in the appropriate locations.

The expressions following statement 180 are the Runge-Kutta formulas (VI-3).

After statement 233, the computation is continued with the Predictor (VI-5) and the Corrector formulas (VI-6). CALL DRYZ involves the computation of the second derivatives of the predicted y and z, each time. Two more iterations are performed. ERY and ERZ are the errors between the last predicted and corrected values and they are printed out.

The DO 237 and the following statements relocate the appropriate values for the next step in the computation.

The actual program is shown on the following pages.

```
   DIETZ, W. SHELL DYNAMIC RESPONSE

   COMPILE FORTRAN, EXECUTE FORTRAN, DUMP

   FUNCTION SRNX (T,Y,Z,G,P)
   DIMENSION P(4)
   IF (G) 2,1,2
 1 S=P(1)*T
   GO TO 3
 2 S=P(1)*(1.-EXPEF(-1.*G*T))/G
 3 SRNX=S-P(2)*Y*Y-0.75*P(2)*Z*Z+P(3)*Z+P(4)
   RETURN
   END

   SUBROUTINE DRYZ (XT,Y,Z,B,C,G,R1,R2)
   DIMENSION B(7),C(9)
   R1T=Y*(B(1)+B(5)*Y**2)+Z*(B(2)+(B(3)+B(4)*Z)*Y)+B(7)
   R2T=Z*(C(1)+Z*(C(3)+C(6)*Z))+Y*(C(2)+Y*(C(4)+C(5)*Z))+C(9)
   IF (G) 10,9,10
 9 R1=R1T+B(6)*Y*XT
   R2=R2T+C(7)*Z*XT+C(8)*XT
   GO TO 11
10 P=-1.*G*XT
   PE=(1.-EXPEF(P))/G
   R1=R1T+B(6)*Y*PE
   R2=R2T+C(7)*Z*PE+C(8)*PE
11 RETURN
   END

   NN=6
701 MM=0
699 MM=MM+2
   PRINT 177
177 FORMAT (39X,1HM,39X,1HN,40X//)
   PRINT 178, MM,NN
178 FORMAT (38X,I2, 38X,I2///)
   NPROB=1
   ZS=0.165
   PRINT 60
 60 FORMAT (45X,10HINTERNALLY,11X,9HSTIFFENED,45X///)
 40 ANU=0.3
   GAMA=0.
   E=10.5*10.**6
   ES=10.5*10.**6
   GS=4.038*10.**6
   GR=0.
   ER=0.
   RHO=2.59/10.0**4
   RHOS=2.59/10.0**4
   RHOR=0.
   H=0.0283
   AS=0.02926
```

```
AR=0.
DDSTR=1.
DLRIN=1000.
SISC=2.2160/10.**4
RIRC=0.
SJS=7.242/10.**5
RJR=0.
ZR=0.
AM=MM
AN=NN
R=9.55
CL=38.
FO=0.014
GO=0.014
VO=100.
XS=0.
XE=0.010
INT=1000
DIMENSION B(7),C(9),P(4)
DIMENSION X(5),Y(5),Z(5),D2Y(5),D2Z(5)
EQUIVALENCE (FO,F0)
EQUIVALENCE (GO,G0)
EQUIVALENCE (VO,V0)
ANUD=1.-ANU**2
AK=E*H/ANUD
AKNU=ANU*AK
ANUG=1.+ANU
AKG=E*H/(2.*ANUG)
AKP=AKNU+AKG
AKS=ES*AS/DDSTR
AKR=ER*AR/DLRIN
AKMS=AK+AKS
AKMR=AK+AKR
AMBAR=RHO*H+RHOS*AS/DDSTR+RHOR*AR/DLRIN
D=E*H**3/(12.*ANUD)
DNU=ANU*D
DG=(1.-ANU)*D
DS=ES/DDSTR*(SISC+ZS**2*AS)
DR=ER/DLRIN*(RIRC+ZR**2*AR)
DGS=GS*SJS/DDSTR
DGR=GR*RJR/DLRIN
DMS=D+DS
DMR=D+DR
DMGS=DG+DGS
DMGR=DG+DGR
D1=DG+(DGS+DGR)/2.
D2=DNU+(DMGR+DMGS)/2.
FSB=ES*AS*ZS/DDSTR
FRB=ER*AR*ZR/DLRIN
DENOM=AKMR*AKMS-AKNU**2
D11=DMS-AKMR*FSB**2/DENOM
D12=D2+AKNU*FSB*FRB/DENOM
D22=DMR-AKMS*FRB**2/DENOM
S11=AKNU*FSB/DENOM
S12=(AKMR*FSB+AKMS*FRB)/(2.*DENOM)
```

```
S22=AKNU*FRB/DENOM
A11=AKMS/DENOM
A12=1./(2.*AKG)-AKNU/DENOM
A22=AKMR/DENOM
A13=AKNU/DENOM
ALPH1=AM*3.14159/CL
BETA1=AN/R
ALPH2=ALPH1**2
ALPH4=ALPH2**2
BETA2=BETA1**2
BETA4=BETA2**2
TEMP1=-(ALPH4*D11+2.*ALPH2*BETA2*D12+BETA4*D22)/AMBAR
SUM1=ALPH4*S11-2.*ALPH2*BETA2*S12+BETA4*S22+ALPH2/R
DEN1=ALPH4*A11+2.*ALPH2*BETA2*A12+BETA4*A22
DEN2=81.*ALPH4*A11+18.*ALPH2*BETA2*A12+BETA4*A22
DEN3=ALPH4*A11+18.*ALPH2*BETA2*A12+81.*BETA4*A22
DEN4=A22-A13**2/A11
DEN5=16.*ALPH4*A11+8.*ALPH2*BETA2*A12+BETA4*A22
DEN6=ALPH4*A11+8.*ALPH2*BETA2*A12+16.*BETA4*A22
SUM2=ALPH2+BETA2*A13/A11
SUM3=ALPH2*S11+1./(4.*R)
SUM4=ALPH4*S11-2.*ALPH2*BETA2*S12+BETA4*S22+ALPH2/(4.*R)
TEMP2=-SUM1**2/(AMBAR*DEN1)
TEMP3=ALPH4*(F0**2+G0**2)/(16.*A22*AMBAR)
TEMP4=BETA4*(3.*F0**2+5.*G0**2/2.)/(16.*A11*AMBAR)
TEMP5=-ALPH2*BETA2*S22*G0/(2.*A22*AMBAR)
TEMP6=SUM2**2*(F0**2+3.*G0**2/4.)/(8.*AMBAR*DEN4)
TEMP7=-A13*SUM2*G0/(4.*A11*R*AMBAR*DEN4)
TEMP8=-BETA2*G0/(4.*A11*R*AMBAR)
TEMP9=-BETA2*G0*SUM3/(2.*A11*AMBAR)
B(1)=TEMP1+TEMP2+TEMP3+TEMP4+TEMP5+TEMP6+TEMP7+TEMP8+TEMP9
B10=TEMP1+TEMP2
TEMP1=-ALPH2*BETA2*F0*SUM1/(AMBAR*DEN1)
TEMP2=ALPH4*BETA4*F0*G0/(AMBAR*DEN1)
TEMP3=9.*ALPH4*BETA4*F0*G0/(4.*AMBAR*DEN2)
TEMP4=9.*ALPH4*BETA4*F0*G0/(4.*AMBAR*DEN3)
B(2)=TEMP1+TEMP2+TEMP3+TEMP4
TEMP1=2.*ALPH2*BETA2*SUM1/(AMBAR*DEN1)
TEMP2=BETA2*SUM3/(2.*A11*AMBAR)
TEMP3=ALPH2*BETA2*S22/(2.*A22*AMBAR)
TEMP4=BETA2/(4.*A11*R*AMBAR)
TEMP5=A13*SUM2/(4.*A11*R*AMBAR*DEN4)
B(3)=TEMP1+TEMP2+TEMP3+TEMP4+TEMP5
TEMP1=-ALPH4*BETA4/(AMBAR*DEN1)
TEMP2=-9.*ALPH4*BETA4/(4.*AMBAR*DEN2)
TEMP3=-9.*ALPH4*BETA4/(4.*AMBAR*DEN3)
TEMP4=-5.*BETA4/(32.*A11*AMBAR)
TEMP5=-ALPH4/(16.*A22*AMBAR)
TEMP6=-3.*SUM2**2/(32.*AMBAR*DEN4)
B(4)=TEMP1+TEMP2+TEMP3+TEMP4+TEMP5+TEMP6
TEMP1=-ALPH4/(16.*A22*AMBAR)
TEMP2=-3.*BETA4/(16.*A11*AMBAR)
TEMP3=-SUM2**2/(8.*AMBAR*DEN4)
B(5)=TEMP1+TEMP2+TEMP3
```

```
      B(6)=SUM2*VO/(AMBAR*CL*DEN4)
      TEMP1=FO*(ALPH4*D11+2.*ALPH2*BETA2*D12+BETA4*D22)/AMBAR
      TEMP2=FO*SUM1**2/(AMBAR*DEN1)
      TEMP3=-FO*GO*ALPH2*BETA2*SUM1/(AMBAR*DEN1)
      B(7)=TEMP1+TEMP2+TEMP3
      TEMP1=-16.*(3.*ALPH4*D11+2.*ALPH2*BETA2*D12+3.*BETA4*D22
     1+1./(4.*A11*R**2))/(9.*AMBAR)
      TEMP2=-32.*SUM3**2/(9.*A11*AMBAR)
      TEMP3=-16.*SUM4**2/(9.*AMBAR*DEN1)
      TEMP4=-32.*BETA4*S22**2/(9.*A22*AMBAR)
      TEMP5=-8.*BETA2*GO*SUM3/(9.*A11*AMBAR)
      TEMP6=BETA4*(FO**2+GO**2)/(9.*A11*AMBAR)
      TEMP7=-8.*ALPH2*BETA2*S22*GO/(9.*A22*AMBAR)
      TEMP8=ALPH4*(FO**2+GO**2)/(9.*A22*AMBAR)
      TEMP9=-8.*ALPH2*BETA2*GO*SUM4/(9.*AMBAR*DEN1)
      TEM10=2.*ALPH4*BETA4*GO**2/(9.*AMBAR*DEN1)
      TEM11=ALPH4*GO**2/(144.*A22*AMBAR)
      TEM12=BETA4*GO**2/(144.*A11*AMBAR)
      TEM13=ALPH4*BETA4*GO**2/(18.*AMBAR*DEN5)
      TEM14=ALPH4*BETA4*GO**2/(18.*AMBAR*DEN6)
      TEM15=SUM2**2*(FO**2+3.*GO**2/4.)/(6.*AMBAR*DEN4)
      TEM16=-A13*GO*SUM2/(3.*A11*R*AMBAR*DEN4)
      TEM17=BETA4*(FO**2+3.*GO**2/4.)/(6.*A11*AMBAR)
      TEM18=-BETA2+GO/(3.*A11*R*AMBAR)
      TEM19=-4.*A13**2/(9.*A11**2*R**2*AMBAR*DEN4)
      C(1)=TEMP1+TEMP2+TEMP3+TEMP4+TEMP5+TEMP6+TEMP7+TEMP8+TEMP9+TEM10+
     1TEM11+TEM12+TEM13+TEM14+TEM15+TEM16+TEM17+TEM18+TEM19
      C10=TEMP1+TEMP2+TEMP3+TEMP4+TEM19
      TEMP1=-16.*ALPH2*BETA2*FO*SUM1/(9.*AMBAR*DEN1)
      TEMP2=16.*ALPH4*BETA4*FO*GO/(9.*AMBAR*DEN1)
      TEMP3=4.*ALPH4*BETA4*FO*GO/(AMBAR*DEN2)
      TEMP4=4.*ALPH4*BETA4*FO*GO/(AMBAR*DEN3)
      C(2)=TEMP1+TEMP2+TEMP3+TEMP4
      TEMP1=4.*BETA2*SUM3/(3.*A11*AMBAR)
      TEMP2=4.*ALPH2*BETA2*SUM4/(3.*AMBAR*DEN1)
      TEMP3=4.*ALPH2*BETA2*S22/(3.*A22*AMBAR)
      TEMP4=A13*SUM2/(2.*A11*R*AMBAR*DEN4)
      TEMP5=BETA2/(2.*A11*R*AMBAR)
      C(3)=TEMP1+TEMP2+TEMP3+TEMP4+TEMP5
      TEMP1=4.*ALPH2*BETA2*S22/(9.*A22*AMBAR)
      TEMP2=16.*ALPH2*BETA2*SUM1/(9.*AMBAR*DEN1)
      TEMP3=2.*BETA2/(9.*A11*R*AMBAR)
      TEMP4=2.*A13*SUM2/(9.*A11*R*AMBAR*DEN4)
      TEMP5=4.*BETA2*SUM3/(9.*A11*AMBAR)
      C(4)=TEMP1+TEMP2+TEMP3+TEMP4+TEMP5
      TEMP1=-16.*ALPH4*BETA4/(9.*AMBAR*DEN1)
      TEMP2=-4.*ALPH4*BETA4/(AMBAR*DEN2)
      TEMP3=-4.*ALPH4*BETA4/(AMBAR*DEN3)
      TEMP4=-BETA4/(9.*A11*AMBAR)
      TEMP5=-ALPH4/(9.*A22*AMBAR)
      TEMP6=-SUM2**2/(6.*AMBAR*DEN4)
      TEMP7=-BETA4/(6.*A11*AMBAR)
      C(5)=TEMP1+TEMP2+TEMP3+TEMP4+TEMP5+TEMP6+TEMP7
```

```
      TEMP1=-35.*BETA4/(144.*A11*AMBAR)
      TEMP2=-17.*ALPH4/(144.*A22*AMBAR)
      TEMP3=-2.*ALPH4*BETA4/(9.*AMBAR*DEN1)
      TEMP4=-ALPH4*BETA4/(18.*AMBAR*DEN5)
      TEMP5=-ALPH4*BETA4/(18.*AMBAR*DEN6)
      TEMP6=-SUM2**2/(8.*AMBAR*DEN4)
      C(6)=TEMP1+TEMP2+TEMP3+TEMP4+TEMP5+TEMP6
      C(7)=4.*SUM2*V0/(3.*AMBAR*CL*DEN4)
      C(8)=-16.*A13*V0/(9.*A11*R*AMBAR*CL*DEN4)
      TEMP1=16.*G0*(3.*ALPH4*D11+2.*ALPH2*BETA2*D12+3.*BETA4*D22
     1+1./(4.*A11*R**2))/(9.*AMBAR)
      TEMP2=32.*G0*SUM3**2/(9.*A11*AMBAR)
      TEMP3=-4.*BETA2*(F0**2+G0**2)*SUM3/(9.*A11*AMBAR)
      TEMP4=16.*G0*SUM4**2/(9.*AMBAR*DEN1)
      TEMP5=-4.*ALPH2*BETA2*G0**2*SUM4/(9.*AMBAR*DEN1)
      TEMP6=-4.*ALPH2*BETA2*S22*(F0**2+G0**2)/(9.*A22*AMBAR)
      TEMP7=32.*BETA4*G0*S22**2/(9.*A22*AMBAR)
      TEMP8=-2.*BETA2*(F0**2+3.*G0**2/4.)/(9.*A11*R*AMBAR)
      TEMP9=-2.*A13*SUM2*(F0**2+3.*G0**2/4.)/(9.*A11*R*AMBAR*DEN4)
      TEM10=4.*A13**2*G0/(9.*A11**2*R**2*AMBAR*DEN4)
      C(9)=TEMP1+TEMP2+TEMP3+TEMP4+TEMP5+TEMP6+TEMP7+TEMP8
     1+TEMP9+TEM10
      B61=SUM2*V0/(AMBAR*CL*DEN4)
      AIMBA=RH0*H**3/12.+RHOS*(SISC+AS*ZS**2)/DDSTR+RHOR*(RIRC
     1+AR*ZR**2)/DLRIN
      AMBA1=AMBAR+AIMBA*(ALPH2+BETA2)
      AMBA2=AMBAR+AIMBA*4.*(ALPH2+BETA2)/3.
      RAT1=AMBAR/AMBA1
      RAT2=AMBAR/AMBA2

C     FINDING THE VALUES OF P
      P(1)=V0/(DEN4*CL)
      P(2)=SUM2/(8.*DEN4)
      P(3)=A13/(4.*A11*R*DEN4)
      P(4)=P(2)*F0*F0+0.75*P(2)*G0*G0-P(3)*G0
      SINT=INT
      HT=(XE-XS)/SINT
  790 X(1)=-HT
      Y(1)=F0
      DELY=0.
      Z(1)=G0
      DELZ=0.
      DY=0.
      DDY=0.
      DZ=0.
      DDZ=0.
      Y2=F0
      Z2=G0
      Y3=F0
      Z3=G0
      PRINT 80
   80 FORMAT (43X,35HB'S    IN    SEQUENTIAL    ORDER,42X//)
      PRINT 41,B
```

```
 41 FORMAT (//6E20.8/3E20.8///)
    PRINT 90
 90 FORMAT (43X,35HC'S    IN    SEQUENTIAL    ORDER,42X//)
    PRINT 41,C
    PRINT 100
100 FORMAT (33X,57HB'S    WITH    ZERO    IMPERFECTIONS    (B(2)=B(
   17)=0),30X//)
    PRINT 121,B10,B(3),B(4),B(5),B(6)
121 FORMAT (E20.8,20X,4E20.8////)
    PRINT 110
110 FORMAT (33X,57HC'S    WITH    ZERO    IMPERFECTIONS    (C(2)=C
   1(9)=0),30X//)
    PRINT 122, C10,C(3),C(4),C(5),C(6),C(7),C(8)
122 FORMAT (E20.8,20X,4E20.8/2E20.8///)
    TB1=2.*3.14159/SQRTF(ABSF(B(1)))
    TC1=2.*3.14159/SQRTF(ABSF(C(1)))
    PRINT 366
366 FORMAT (17X,4HP(1),20X,4HP(2),20X,4HP(3),21X,3HTB1,21X,3HTC1,3X//)
    PRINT 367, P(1),P(2),P(3),TB1,TC1
367 FORMAT (5E24.8//)
    PRINT 77
 77 FORMAT (//10X,4HTIME,13X,3HNOX,15X,2HF1,13X,7HF1-RES.,12X,2HG1,
   113X,7HG1-RES.,11X,4HZETA,4X///)
    ICAL=10
    DO 233 I=2,5
    X(I)=X(I-1)+HT
    Y(I)=Y(I-1)+DELY
    Z(I)=Z(I-1)+DELZ
    ICAL=ICAL+1
    ENX=SRNX(X(I),Y(I),Z(I),GAMA,P)
    ZETA=(Y(I)+Z(I))/H
179 IF (ICAL-10) 180,61,61
 61 PRINT 150,X(I),ENX,Y(I),Z(I),ZETA
150 FORMAT (1X,3E17.8,17X,E17.8,17X,E17.8)
    ICAL=0
180 CALL DRYZ (X(I),Y(I),Z(I),B,C,GAMA,D2Y(I),D2Z(I))
    AK1=HT*D2Y(I)
    AL1=HT*D2Z(I)
    X2=X(I)+HT/2.
    DY=DY+DDY
    DZ=DZ+DDZ
    Y2=Y2+HT*DY/2.+HT*AK1/8.
    Z2=Z2+HT*DZ/2.+HT*AL1/8.
    CALL DRYZ (X2,Y2,Z2,B,C,GAMA,F1,F2)
    AK2=HT*F1
    AL2=HT*F2
    X3=X(I)+HT
    Y3=Y3+HT*DY+HT*AK2/2.
    Z3=Z3+HT*DZ+HT*AL2/2.
    CALL DRYZ (X3,Y3,Z3,B,C,GAMA,F1,F2)
    AK3=HT*F1
    AL3=HT*F2
    DELY=HT*(DY+(AK1+2.*AK2)/6.)
```

```
      DELZ=HT*(DZ+(AL1+2.*AL2)/6.)
      DDY=(AK1+4.*AK2+AK3)/6.
      DDZ=(AL1+4.*AL2+AL3)/6.
  233 CONTINUE
      XU=X(5)
  235 XU=XU+HT
      ICAL=ICAL +1
      YP=2.*Y(4)-Y(2)+4./3.*HT**2*(D2Y(5)+D2Y(4)+D2Y(3))
      ZP=2.*Z(4)-Z(2)+4./3.*HT**2*(D2Z(5)+D2Z(4)+D2Z(3))
      CALL DRYZ (XU,YP,ZP,B,C,GAMA,D2YP,D2ZP)
      YC=2.*Y(5)-Y(4)+HT**2/12.*(D2YP+10.*D2Y(5)+D2Y(4))
      ZC=2.*Z(5)-Z(4)+HT**2/12.*(D2ZP+10.*D2Z(5)+D2Z(4))
      CALL DRYZ (XU,YC,ZC,B,C,GAMA,D2CY,D2CZ)
      YCC=2.*Y(5)-Y(4)+HT**2/12.*(D2CY+10.*D2Y(5)+D2Y(4))
      ZCC=2.*Z(5)-Z(4)+HT**2/12.*(D2CZ+10.*D2Z(5)+D2Z(4))
      CALL DRYZ (XU,YCC,ZCC,B,C,GAMA,D2CCY,D2CCZ)
      YU=2.*Y(5)-Y(4)+HT**2/12.*(D2CCY+10.*D2Y(5)+D2Y(4))
      ZU=2.*Z(5)-Z(4)+HT**2/12.*(D2CCZ+10.*D2Z(5)+D2Z(4))
      IF (ICAL-10) 239,240,240
  240 ZETA=(YU+ZU)/H
      ENX=SRNX (XU,YU,ZU,GAMA,P)
      ERY=ABSF (YU-YCC)
      ERZ=ABSF (ZU-ZCC)
      ICAL =0
      PRINT 236,XU,ENX,YU,ERY,ZU,ERZ,ZETA
  236 FORMAT (1X,7E17.8)
      IF (ABSF(ZETA)-200.) 238,250.250
  238 IF (XU-XE) 239,250,250
  239 DO 237 K=3,5
      X(K-1)=X(K)
      Y(K-1)=Y(K)
      Z(K-1)=Z(K)
      D2Y(K-1)=D2Y(K)
  237 D2Z(K-1)=D2Z(K)
      X(5)=XU
      Y(5)=YU
      Z(5)=ZU
      D2Y(5)=D2CCY
      D2Z(5)=D2CCZ
      GO TO 235
  250 IF (RAT2-0.99) 73,799,799
   73 IF (ABSF(B(6)-B61)-1.0E-6) 65,65,799
   65 DO 51 J=1,7
   51 B(J)=B(J)*RAT1
      DO 52 J=1,9
   52 C(J)=C(J)*RAT2
      B10=B10*RAT1
      C10=C10*RAT2
      GO TO 790
  799 NPROB=NPROB+1
      ZS=-0.165
```

```
      IF (NPROB-2) 50,50,199
   50 PRINT 70
   70 FORMAT (//45X,10HEXTERNALLY,11X,9HSTIFFENED,45X///)
      GO TO 40
  199 MM=AM
      NN=AN
      IF (MM-10) 699,700,700
  700 IF (NN-10) 702,999,999
  702 NN=NN+2
      GO TO 701
  999 STOP
      END
```

BIBLIOGRAPHY

[1] Hoff, N.J."Buckling and Stability", Forty-first Wilbur Wright Memorial Lecture, J.Roy.Aeron.Soc.Vol.58, January,1954.

[2] Ziegler, H. "On the Concept of Elastic Stability", Advances in Applied Mechanics, Vol.IV, Academic Press, 1956.

[3] Fung, Y.C. and Sechler, E.E."Instability of Thin Elastic Shells", in "Structural Mechanics", ed. by J.N. Goodier and N.J. Hoff, Pergamon Press, 1960.

[4] Hoff, N.J. "Buckling of Thin Shells", Aerospace Symposium in honor of Th. von Kármán on his 80th Anniversary, The Institute of the Aerospace Sciences, 1962.

[5] NASA TN D-1510, "Collected Papers on Instability of Shell Structures", many individual authors contributing, 1962.

[6] Evan-Iwanowski, R.M. "Parametric (Dynamic) Stability of Elastic Systems", Developments in Theoretical and Applied Mechanics, Vol.1, Plenum Press, 1963.

[7] Evan-Iwanowski, R.M. "On the Parametric Response of Structures", Applied Mechanics Revs., Vol.18, No.9, September, 1965.

[8] Nash, W.A. "Recent Advances in the Buckling of Thin Shells", Applied Mechanics Revs., Vol.13, No.3, March, 1960.

[9] Kalnins, A. "Dynamic Problems of Elastic Shells", Applied Mechanics Revs., Vol.18, No.11, November, 1965.

[10] Naghdi, P.M. "A Survey of Recent Progress in the Theory of Elastic Shells", Applied Mechanics Revue, Vol.9, No.9, September, 1956.

[11] Thielemann, W.F. "New Developments in the Nonlinear Theories of the Buckling of Thin Cylindrical Shells", Proceedings of the Durand Centennial Conference on Aeronautics and Astronautics, Vol.9, Div.IX, Pergamon Press, 1960.

[12] Nash, W.A. "Bibliography on Shell and Shell-Like Structures" Report 863, David Taylor Model Basin, November, 1954.

[13] Nash, W.A. "Bibliography on Shell and Shell-Like Structures 1954-1956", Dept.Engineering Mechanics, University of Florida.

[14] Delano, W.B. "Investigation of Strength and Buckling Characteristics-Bibliography", MIT, March, 1954, AD-40826.

[15] Goldman, J.B. and McCormick, H. "Dynamic Loading and Structure Analysis: An Annotated Bibliography", Lockheed Special Bibliography SB-63-43, July, 1963, AD-438182.

[16] Donnell, L.H. "A New Theory for the Buckling of Thin Cylinders under Axial Compression and Bending", Transactions ASME, Vol56, 1934.

[17] von Kármán, Th. and Tsien, H.S. "The Buckling of Thin Cylindrical Shells under Axial Compression", J. Aeronautical Science, Vol.8, No.8, June, 1941.

[18] Donnell, L.H. and Wan, C.C. "Effects of Imperfections on Buckling of Thin Cylinders and Columns under Axial Compression", J. Applied Mechanics, Vol.17, No.1, 1950.

[19] Kempner, J. "Postbuckling Behaviour of Axially Compressed Circular Cylindrical Shells", J. Aeronautical Science, Vol.21, No.5, 1954.

[20] Almroth, B.O. "Postbuckling Behavior of Axially Compressed Circular Cylindrical Shells", AIAA-Journal, Vol.1, 1963.

[21] Fischer, G. "Ueber den Einfluss der gelenkigen Lagerung auf die Stabilität dünnwandiger Kreiszylinderschalen unter Axiallast und Innendruck", Zeitschrift der Flugwissenschaften, No.3, March, 1963.

[22] Stein, M. "The Influence of Prebuckling Deformation and Stresses on the Buckling of Perfect Cylinders", NASA TR R-190, February, 1964.

[23] Flügge, W. "Die Stabilität der Kreiszylinderschale", Ingenieurarchiv, III. Band, December, 1932.

[24] Anonymous, "Some Investigation of the General Instability of Stiffened Metal Cylinders", CAL. TECH, NACA TN 905 to 911, 1943.

[25] Gerard, G. and Becker, H. "Handbook of Structural Stability", Parts I to V, NACA TN 3781 to 3785, and Supplement TN D-163, 1959.

[26] Lekhnitskii, S.G. "Theory of Elasticity on an Anisotropic Elastic Body", Holden-Day, 1963.

[27] Hearmon, R.F.S. "Applied Anisotropic Elasticity", Oxford University Press, 1961.

[28] Ambartsumyan, S.A. "Theory of Anisotropic Shells", State Publishing House for Phys. and Math. Lit., Moscow, 1961, NASA TT F-118.

[29] Bodner, S.R. "General Instability of a Ring-Stiffened Circular Cylindrical Shell under Hydrostatic Pressure" J. Applied Mechanics, June, 1957.

[30] Hedgepeth, J.M. and Hall, D.B. "Stability of Stiffened Cylinders" AIAA-Paper No.65-79, January, 1965.

[31] Czerwenka, C. "Untersuchungen von dünnen Zylindern, die durch Ring-Kleinstprofile enger und mitlerer Teilung verstärkt sind und unter Manteldruck stehen", Zeitschrift für Flugwissenschaften, June, 1961.

[32] Van der Neut, A. "The General Instability of Stiffened Cylindrical Shells under Axial Compression", Rept. S.314, Natl. Aeron. Res. Inst. Amsterdam, 1947.

[33] Baruch, M. and Singer, J. "Effects of Eccentricity of Stiffeners on the General Instability of Stiffened Cylindrical Shells under Hydrostatic Pressure", Journal Mech. Engr. Science, Vol.5, No.1, 1963.

[34] Card, M.F. "Preliminary Results of Compression Tests on Cylinders with Eccentric Longitudinal Stiffeners" NASA TM X-1004, 1964.

[35] McElman, J.A., Mikulas, M.M. and Stein, M. "Static and Dynamic Effects of Eccentric Stiffening", AIAA-Meeting Presentation, San Francisco, July, 1965.

[36] Mikulas, M.M. and McElman, J.A. "On Free Vibrations of Eccentrically Stiffened Cylindrical Shells and Flat Plates", NASA TN D-3010, September, 1965.

[37] Block, D.L., Card, M.F. and Mikulas, M.M. "Buckling of Eccentrically Stiffened Orthotropic Cylinders", NASA TN D-2960, August, 1965.

[38] Arnold, R.N. and Warburton, G.B. "Flexural Vibrations of the Walls of Thin Cylindrical Shells Having Freely Supported Ends", Proc. Roy. Soc. Ser. A, No.1049, Vol.197, June, 1949.

[39] Arnold, R.N. and Warburton, G.B. "The Flexural Vibrations of Thin Cylinders", The Institution of Mech.Engrs., Proc. (A), Vol.167, No.1, 1953.

[40] Reissner, E. "On the Transverse Vibrations of Thin, Shallow Elastic Shells", Quarterly Applied Math., Vol.XIII, No.2, July, 1955.

[41] Schnell, W. "Eigenschwingungen versteifer Kreiszylinderschalen", Deutsche Versuchsanstalt für Luftfahrt (DVL), Munich, 1963, N64 10823,

[42] Bolotin, V.V. "Dynamic Stability of Elastic Systems", Translation from the Russian, Holden-Day, 1964.

[43] Wenzke, W. "Die dynamische Stabilität der Axialpulsierend belasteten Kreiszylinderschale", Wissenschaftl. Zeitschr. der T.H. Otto von Guericke, Magdeburg, VII, 1, March,1963.

[44] Vijayaraghavan, A. "Parametric Instability of Cylindrical Shells", M.S. Thesis, Dept. of Mechanical and Aerospace Engineering, Syracuse University, June, 1966.

[45] Wood, J.D. and Koval, L.R. "Buckling of Cylindrical Shells under Dynamic Loads", AIAA-Journal, Vol.1, No.11,Nov.,1963.

[46] Agamirov, V.L. and Volmir, A.S. "Behavior of Cylindrical Shells under Dynamic Loading by Hydrostatic Pressure or Axial Compression", Translation from the Russian (1959) in J. American Rocket Soc., January, 1961.

[47] Hoff, N.J. "The Dynamics of the Buckling of Elastic Columns", J. Applied Mechanics, March, 1951.

[48] Hoff, N.J., Nardo, S.V. and Erickson, B. "The Maximum Load Supported by an Elastic Column in a Rapid Compression Test", Proc. of the First U.S. Nat. Congress of Appl. Mechs., 1952.

[49] Volmir (Wolmir) A.S. "Biegsame Platten und Schalen", German Translation from the Russian, Verlag VEB für Bauwesen, Berlin, 1962.

[50] Yao, J.C. "The Dynamics of the Elastic Buckling of Cylindrical Shells", Aerospace Corporation Rep., April, 1962, AD-285327.

[51] Coppa, A.P. and Nash, W.A. "Dynamic Buckling of Shell Structures Subjected to Longitudinal Impact", General Electric (Philadelphia) Rept. ASD-TDR 62-774, December, 1962, AD-295491.

[52] Nowinski, J.L. "Nonlinear Transverse Vibrations of Orthotropic Cylindrical Shells", AIAA-Journal, Vol.1, No.3, March,1963.

[53] Roth, R.S. and Klosner, J.M. "Nonlinear Response of Cylindrical Shells Subjected to Dynamic Axial Loads", AIAA-Journal, Vol.2, No.10, October, 1964.

[54] Evan-Iwanowski, R.M., Loo, T.C. and Tierney, D.W. "Local Buckling of Shells", Developments in Theoretical and Applied Mechanics, Vol.2, Pergamon Press, 1965, pp.221-251.

[55] Nixon, F.E. "Handbook of Laplace Transformation", Prentice-Hall, 1960.

[56] Abramovitz, M. and Stegun, I.A., Editors, "Handbook of Mathematical Functions", Dover, 1965.

[57] Luke, Y.L. "Integrals of Bessel Functions", McGraw Hill, 1962.

[58] Timoshenko, S. and Goodier, J.N. "Theory of Elasticity", McGraw Hill, 1951.

[59] McCracken, D.D. and Dorn, W.S. "Numerical Methods and Fortran Programming", Wiley, 1964.

[60] Scarborough, J.B. "Numerical Mathematical Analysis", The Johns Hopkins Press, Fifth Edition, 1962.

[61] Hamming, R.W. "Numerical Methods for Scientists and Engineers", McGraw Hill, 1962.

[62] Gorman, D. "Stability of Cylindrical Shells- An Analytical and Experimental Investigation of the Effects of Large Prebuckling Deformation on the Buckling of Clamped Thin-Walled Cylindrical Shells Subjected to Axial Loading and Internal Pressure", Ph.D. Dissertation, Dept. of Mechanical and Aerospace Engineering, Syracuse University, June, 1965.